Investigating Early-Stage Process Flow and Reactor Sequencing to Maximise Gold Extraction ln the Thiosulphate Leaching of Waste Printed Circuit Boards

Melissa Gugulethu Gonte

Supervisors: Dr. Thandazile Moyo and Prof. Jochen Petersen

February 2023

A thesis submitted to the Faculty of Engineering and the Built Environment, University of Cape Town, in fulfilment of the requirements for the degree of Master of Science in in Chemical Engineering.

Plagiarism declaration

I know the meaning of plagiarism and declare that all the work in the document, save for that which is properly acknowledged, is my own. This thesis has been submitted to the Turnitin module and I confirm that my supervisor has seen my report and any concerns revealed by such have been resolved with my supervisor.

Name: Melissa Gugulethu Gonte

Date: 11 February 2023

Signature: Signed by candidate

Acknowledgements

I want to start by thanking my primary supervisor, Doctor Thandazile Moyo, for accepting me as a student. I appreciate her continued patience and unwavering belief in me. I also appreciate her wisdom, encouragement, and the freedom she gave me to undertake this research on my own while continually supporting me. I gained a lot from her that aided in my own development. I appreciate her efforts toward constantly guiding me in the right direction when I thought I was getting lost.

Furthermore, I would like to convey my sincere gratitude to my co-supervisor, Professor Jochen Petersen, who was always approachable and never hesitated to help, advise, and guide me throughout the duration of this study. Being under his supervision was an honour.

I also want to thank the National Research Foundation and the SARChI for their financial support of this project.

I would like to show my appreciation to the Minerals to Metals team for also providing the funding necessary for me to complete my M.Sc. degree. I also value the way the Hydromet Group helped me to evolve, encouraged me to think creatively, and helped me become more sociable. Thanks, in particular to Kathija who assisted me in the laboratory throughout this research. The following individuals deserve special recognition: Nicole, Wilson, Archippe, Jordy, Bavisha, Fernando, Sage, Emmanuel, Ariana, Aysha, and Eddy.

I also appreciate the work of Sibongile and Sandeeran Govender from the University of Cape Town's Analytical Lab, Charney Anderson-Small and Mareli Grobbelaar-Moolman from CAF, Stellenbosch University, and Stellenbosch University in analysing my samples.

I would especially like to thank my friends and family for supporting me as I worked toward my degree. The following people deserve a special note of appreciation: Dorothy, Temba, Kelvin, Lilly, Ndaba, Anene, Enhle, Inami, Lwazi, Tanae, Patie, Yebo, Meki, and Pepe. I do not think I could have thrived without them. Meki, I cannot thank you enough for what you have continually done for me; there are not enough words in the world that can express my gratitude.

Finally, and most importantly, I want to express my sincere gratitude to my personal saviour and friend Jesus, The Great I Am, for giving me the confidence and fortitude to complete my master's thesis.

Abstract

Fast growing volumes of waste electronic and electrical equipment (WEEE) present a rising environmental challenge while offering opportunities for creating a circular economy. Once dismantled and sorted, waste printed circuit boards (PCBs) are one of the value-bearing fractions of WEEE. Waste PCBs contain valuable metals like copper (Cu) and gold (Au) that can be profitably recovered using metallurgical methods like hydrometallurgy, pyrometallurgy, or a combination of the two. Successful implementation of pyrometallurgical technologies have been demonstrated in large-scale integrated recycling operations. These require high capital investment, large volumes of waste, and advanced scrubber/filter equipment to combat toxic flue gas pollution.

Hydrometallurgical technologies present a viable processing route for the African context, where waste volumes are relatively low and energy supply is uncertain and expensive. Many lixiviants, such as cyanide, halides and aqua regia can be used to extract Au from waste PCBs. Due to its great selectivity and relatively low toxicity, this research focuses on the ammonium thiosulphate chemistry for the extraction of Au from waste PCBs.

While ammonium thiosulphate solutions are effective in dissolving Au, there are challenges regarding reagent consumption when the system is used on materials that contain significant quantities of Cu. This is because Cu dissolves preferentially and plays a role in catalysing the breakdown of the thiosulphate ion. The method of pre-treatment and the sequence in which metals are leached in a multi-stage leach process determine the presence of co-existing metals, especially Cu for dissolution from waste PCBs in an ammonia thiosulphate system. In this work we hypothesized that the extraction of Au prior to delamination and size reduction will reduce the loss of Au, owing to Au being situated on the topmost layer of discarded PCBs. It would also result in less exposure of Cu to the leaching system which would ultimately limit reagent consuming side reactions. Four potential leaching sequences were examined to evaluate Au extraction, Au loss and base metal (BM) (Cu and Ni) co-extraction. Sequences A and B involved Au leaching of cut (A) and shredded (B) PCBs using a 0.5M ammonium thiosulphate ($(NH_4)_2S_2O_3$) in the presence of 0.04M copper sulphate ($CuSO_4$) and 1M ammonia (NH_3), at a solid/liquid ratio of 100g/L. Sequences C and D involved BM extraction from cut (C) and shredded (D) PCBs prior to Au leaching, under the same conditions.

The results showed that sequence A had the highest Au extraction of 97% Au. However, the co-extraction of Cu and Ni, was also high at 21% Cu and 96% Ni, respectively. Nevertheless, in this study, this was preferable due to the considerable Au loss that other sequences experienced. Sequence D, B, and C, each suffered an overall Au loss of 53% , 26% and 20%, respectively.

Leaching of Au leaf (93.1% Au) in the presence of predetermined amounts of Cu and Ni in 0.5M $(NH_4)_2S_2O_3$ and 0.5M sodium cyanide (NaCN) was used to simulate the leaching of Au from waste PCBs. Within the first hour of leaching, a high Au extraction of 99% and 88% was achieved in $(NH_4)_2S_2O_3$ and NaCN solutions, respectively, in the absence of background Cu and Ni. Addition of predetermined quantities of Cu (11500 mg) and Ni (519 mg) in both lixiviants resulted in a decline in Au extraction to 42% and 37%, respectively. The actual leaching of PCB in the same concentrations of $(NH_4)_2S_2O_3$ and NaCN gave 97% and 38% Au extraction, respectively.

The optimisation tests (of sequence A) showed that a $0.5M(NH_4)_2S_2O_3$ and 1M NH_3 lixiviant concentration and a solid to liquid (S/L) ratio of 100g/L was optimal for leaching. Under these conditions 99% Au was extracted within 7.5 hours. In comparison, 36% Au extraction was achieved when NaCN was used for leaching under the same conditions. This showed that it is difficult to implement the optimal sequence, obtained for $(NH_4)_2S_2O_3$ leaching, in the leaching of waste PCBs using NaCN. NaCN suffers from the interference of foreign ions as side reactions compete for the reagent. Other than NaCN's level of toxicity, the results suggest that this system also requires implementation of the prior removal of BMs before leaching of Au.
In conclusion, the highest Au extraction occurs when Au is extracted from PCBs using sequence A (before delamination, aggressive size reduction, and BMs extraction). Sequence A's low co-extraction of Cu demonstrates that most of the Cu remains interlocked within the boards during Au extraction.

Table of Contents

List of Figures

List of Tables

Nomenclature

Abbreviations

WEEE	Waste Electronic And Electrical Equipment
EEE	Electric And Electronic Equipment
PCBs	Printed Circuit Boards
BM	Base Metal
PM	Precious Metal
E-waste	Electronic Waste
PLS	Pregnant Leach Solution
MP-AES	Microwave Plasma Atomic Emission Spectroscopy

Chemical Formula

Au	Gold
Cu	Copper
Ni	Nickel
Fe	Iron
Sn	Tin
$(NH_4)_2S_2O_3$	Ammonium Thiosulphate
$(NH_4)_2SO_4$	Ammonium Sulphate
NH_3	Ammonia
NH_4OH	Ammonium Hydroxide
$CuSO_4.5H_2O$	Copper(II) Sulphate Pentahydrate
$CuSO_4$	Copper Sulphate
NaCN	Sodium Cyanide
CN^-	Cyanide ion
$S_2O_3^{2-}$	Thiosulphate ion
$[Cu(NH_3)_4]^{2+}$	Copper Tetramine Complex
Cu^{2+}	Cupric ions
$(Au(S_2O_3)_2^{3-}$ and $Au(S_2O_3)^-$	Aurothio-Sulphate Complexes

1. INTRODUCTION

1.1 Motivation

According to the UN's Global (Electronic waste) E-waste Monitor 2020, a record 53.6 million metric tonnes (Mt) of waste electronic and electrical equipment (WEEE) was generated worldwide in 2019, an increase of 21% in just five years (Forti et al., 2020). The analysis also projects that by 2030, the amount of e-waste will globally reach 74 Mt, nearly doubling in just 16 years (Baldé et al., 2017). This makes e-waste the fastest-growing home waste stream in the world, driven mostly by rising rates of electric and electronic equipment consumption, short life cycles, and limited repair options. Only 17.4% of the e-waste generated in 2019 was collected and recycled (Forti et al., 2020). This means that instead of being collected for processing and reuse, high-value, recoverable materials with a conservative worth of US $57 billion including gold (Au) silver (Ag), copper (Cu), platinum (Pt), and others were primarily burned or discarded (Forti et al., 2020).

This rising environmental challenge offers opportunities for creating a circular economy since e-waste is a rich secondary metal source (EPA, 2015). In developed countries the more successful gainful recycling of these metals uses integrated pyrometallurgical and hydrometallurgical technologies.

These hybrid technologies require a huge capital injection for the installation of state-of-the-art gas scrubbers which prevent the emission of toxic flue gases. Additionally, their operational costs are high. Unfortunately, developing countries such as South Africa have insufficient e-waste volumes, poor energy supply and limited access to capital to implement advanced recycling facilities and models (Lydall et al., 2017; Moyo et al., 2020). There is therefore a need to explore recycling options that can be used to economically process and recover valuable metals from components of the waste such as waste printed circuit boards (PCBs). The extraction of gold through the hydrometallurgical route emerges as the more viable route due to its high selectivity and high potential for the optimization of Au recovery from waste PCBs (Kasper et al., 2018). Amongst a variety of lixiviants including traditional cyanide, ammonium thiosulphate shows potential because it is less toxic, highly selective, and cheaper (Akcil et al., 2015).

A conventional leaching sequence when using the thiosulphate system to leach gold from waste PCBs involves physical pre-treatment, followed by base metal (BM) leaching ending with Au leaching (Albertyn, 2017; Ficeriová et al., 2011; Gámez et al., 2019; Petter et al., 2013; Tanisali et al., 2021).

The physical pre-treatment is done to increase the leaching surface area and enhance BM extraction. However, it has been ascertained that it leads to the loss of a significant proportion of Au (between 50% and 90%) through the formation of fine flakes of Au during copper leaching (Kaya, 2019; Prestele, 2020). This contributes to an overall significant Au loss. Additionally, due to their dominance (particularly Cu) and dispersion on waste PCBs, Cu and nickel (Ni) are more likely to compete with Au for the lixiviant, which thereby hampers the extraction of Au. Therefore, it appears that the extraction of Au is affected by the order in which the leaching processes are performed.

The aim of this study is to investigate four potential reactor sequences (order/flow of the leaching processes) to evaluate the extent of Au extraction, Cu and Ni co-extraction as well as associated Au losses in the ammonium thiosulphate leaching of waste PCBs. The specific objectives are given in the following section.

1.2 Objectives

1. To investigate the effect of background Cu and Ni in the dissolution of Au from waste PCBs within an ammonium thiosulphate leaching system.
    i. Use Au leaf as a proxy to simulate Au dissolution from waste PCBs, in the presence of background metallic Cu and Ni.
2. To investigate and select the reactor sequencing in an ammonium thiosulphate leaching system that maximizes the amount of Au extracted from waste PCBs.
3. Use the best reactor sequencing obtained from (2) to optimize Au extraction from waste PCBs over a selected range of parameters.
4. To benchmark the optimal leaching of waste PCBs in ammonium thiosulphate obtained in (3) with the leaching of Au from waste PCBs using cyanide.

1.3 Hypothesis

Since Au mainly exists on the surface layer of waste PCB, its extraction before the process of aggressive size reduction and BM extraction will minimize Au loss whilst exposing less Cu and Ni to the lixiviant. This will in turn effectively minimize BM exposure in the thiosulphate leaching medium and limit side reactions.

1.4 Key questions

1. To what extent do Cu and Ni affect the rate and extent of Au dissolution in an ammonium thiosulphate leaching system?
2. What is the best reactor sequence that maximises Au extraction from waste PCBs, in an ammonium thiosulphate leaching system?
3. Using the selected sequence from (2), what is the optimal process for Au leaching from waste PCBs over the proposed range of parameters?
4. How does the leaching of Au from waste PCBs, selected in 3, compare to the cyanide leaching of Au from waste PCBs.

1.5 Research approach

The first step in the experimental work was to characterise the PCBs to determine the head grade of the Au, Cu, Sn, and Ni present. This was achieved via two methods;

1. acid digestion using aqua regia
2. microwave assisted acid digestion

In the tests that used gold leaf (23 carat Au), the concentration of Cu and Ni introduced as background metals was informed by the results of the head grade analysis. This was done in effort to keep the concentrations used in the simulated leaching of gold from waste PCBs as close as possible to that of the PCB samples used in the rest of the tests. The simulation experiments were conducted to obtain baseline studies and eliminate the uncontrolled interference that would come from co-dissolving metals from waste PCBs. Instead, these metals (Ni and Cu) were introduced at set/controlled concentrations and their effect Au dissolution was monitored. In all experiments, $(NH_4)_2S_2O_3$, with NH_3 as a buffer, was used as the lixiviant and cyanide (CN^-) was then used to evaluate this process. Four potential reactor sequences A through D were then examined with the goal of choosing one that yields the maximum Au extraction, result in less Au loss and Cu and Ni co-extraction during the thiosulphate leaching stage. The sequences are described as follows;

A. Sequence A- the PCBs are cut (3 cm x 2 cm) and then immediately move on to the Au leaching stage.
B. Sequence B- Similar to sequence (A) except in this instance the PCBs are shredded (in 6 passes) instead of being cut.

C. Sequence C- the PCBs are cut (3 cm x 2 cm) and undergo BM (Cu and Ni) extraction prior to the Au leaching stage.
D. Sequence D- Similar to sequence (C) except in this instance the PCBs are shredded (in 6 passes) instead of being cut.

In all sequences the leaching of Au leaching was achieved under the following conditions; 0.5M ammonium thiosulphate ($(NH_4)_2S_2O_3$) in the presence of 0.04M copper sulphate ($CuSO_4$) and 1M ammonia (NH_3), under a S/L ratio of 100g/L. In Sequences C and D, the prior leaching from PCBs was carried out using ammonium sulphate ($(NH_4)_2SO_4$). The leached residues from (C) and (D) were then used as the feed for the Au leaching step using $(NH_4)_2S_2O_3$. Using the full factorial approach, 8 trials combinations were then tested to optimize the thiosulphate leaching of PCBs while employing the optimal reactor sequence obtained from the previous tests. The parameters optimized were solid to liquid ration (S/L) ratio, NH_3 and $(NH_4)_2S_2O_3$ concentration. Similar PCB samples were leached in NaCN in an effort to benchmark the ammonia-ammonium thiosulphate leaching step.

Residue from the leaching step was digested and solutions analysed to determine residual metals and allow for a closed mass balance of the tests that involved the use of PCBs. A microwave plasma atomic emission spectroscopy (MP-AES) was used to quantify the Au, Ni, and Cu content of all liquid samples, and the percentage extraction was then calculated using the head grade as a basis.

1.6 Scope and limitations

In this study, only custom-made boards were used to ensure that the same design, composition, and quality of the PCBs was maintained throughout the leaching experiments. Leaching of actual waste PCBs sourced from e-waste was outside the scope of this study. This is due to the inhomogeneity and compositional variation of waste PCBs, which may have caused the results to be incomparable across different sets of experiments. This study only focused on the investigation of Au extraction via ammonium thiosulphate leaching of PCBs; the investigation of the downstream processes of Au recovery from the pregnant leach solution (PLS) was out of scope. Au samples (Au leaves) were used primarily to investigate how background Ni and Cu affect Au's ability to dissolve in the presence of cyanide and ammonium thiosulphate.

The other set of experiments evaluated how Ni and Cu impacted the extent to which ammonium thiosulphate extracted Au from custom made PCBs. During this step, only four proposed reactor sequences were investigated to determine which sequence resulted in the highest overall extraction

while also considering the effects of background metals namely Cu and Ni, in the leaching process. Only the specified set of parameters were used in the optimization process using ammonium thiosulphate. The best performing tests were benchmarked against the cyanide gold leaching process. The co-extraction of other valuable metals other than, Cu and Ni during thiosulphate leaching was not investigated.

1.7 Correlation to Sustainable Development Goals (SDGs)

Goals 3 (Good health and well-being), 6 (Clean water and sanitation), 11 (Sustainable Cities and Communities), 12 (Responsible Consumption and Production) and Goal 8 (Decent Work and Economic Growth), are all strongly related to this project.

Achieving these SGDs is being significantly hampered by rising volumes of e-waste, improper and unsafe treatment, and disposal in landfills or through incineration.

Target 3.9 of goal 3 seeks to reduce the number of deaths and illnesses brought on by hazardous substances, as well as by pollution and poisoning of the air, water, and soil. Target 6.3 of goal 6 also seeks to lessen pollution, stop dumping, and limit the release of dangerous chemicals and materials. Whereas Target 6.1 aims to provide everyone with equitable access to safe and inexpensive drinking water.

Goal 11 -Since cities are where more than half of the world's population resides, rapid urbanization necessitates innovative approaches to deal with escalating environmental and health problems, particularly in densely populated areas. The majority of e-waste will be produced in metropolitan areas; thus, it is crucial to effectively manage e-waste there, increase collection and recycling rates, and lessen the quantity of e-waste that ends up in landfills.

Similar to Goal 11, Target 12.4 aims to achieve environmentally sound management of chemicals and all waste throughout the life cycle, in accordance with recognized international frameworks, and to drastically reduce their release into the air, water, and soil in order to reduce their negative effects on human health and the environment. Through prevention, reduction, repair, recycling, and reuse, Target 12.5 seeks to significantly lower waste generation.

SDG Target 8.3 strives to foster the formalization and expansion of micro, small, and medium-sized firms as well as development-oriented policies that support productive activities, the creation of decent jobs, entrepreneurship, creativity, and innovation.

Through this project, the optimised sustainable Au extraction via thiosulphate leaching, provides an option for the proper handling and processing of smaller volumes of PCBs from e-waste. This can be set up at low cost and utilize less energy as opposed to traditional e-waste recycling methods. This will be essential in making production and consumption of commodities more sustainable as the world's population grows.

1.8 Document outline

A literature overview is presented in chapter 2 of this thesis, and the materials and methods are presented in chapter 3. The literature review examines the chemistry involved in the leaching of BMs (with a special focus on Cu), and on Au . Also included are the findings from earlier studies that served as the basis for choosing the leaching parameters. The experimental strategy for each leaching stage, tools, reagents, and methods are described in the experimental approach. Chapter 4 covers the experimental results and discussion of the findings, whereas Chapter 5 covers the recommendations and conclusions.

2. LITERATURE REVIEW

2.1 Background

E-waste generation has been a subject of great discussion around the world due to the continuous technological advancements and innovation. This rapid development in the; functions, consumer designs and marketing and compatibility of electric and electronic equipment (EEE) have reduced life spans of these products, which end up in landfills (Mishra et al., 2021). According to literature, about 54 Mt of e-waste is produced each year globally, and this value is expected to increase by 3-5% per annum, as shown in Figure 2-1 (Forti et al., 2020; Gámez et al., 2019; Gertjegerdes et al., 2022; Panda et al., 2020). Even with the escalated efforts to try and improve its recycling and reuse, a substantial proportion of WEEE, such as waste PCBs, is still being disposed in the environment.

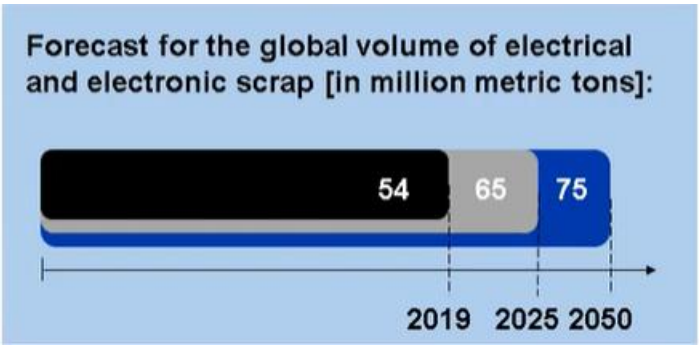

Figure 2-1: Past, current, and projected global volumes of WEEE in million metric tonnes (Gertjegerdes et al., 2022)

Even though e-waste is generated everywhere, high-income nations like the US, the EU, East-Asia, especially Japan, Korea, and China, etc, are the primary e-waste producers as illustrated in Figure 2-2. E-waste makes up 8% of the total solid waste produced in these nations, on average (Gertjegerdes et al., 2022; Hossain et al., 2015). On the other hand, low-income countries, generally generate lower volumes. However, several developing and transitional nations import a considerable portion of e-waste (Hossain et al., 2015; Widmer et al., 2005). Some of these importations are in the guise of donations intended to aid the underprivileged. Under this condition, many developing nations in Asia and Africa are the most often used dumping sites and end up accumulating relatively large volumes of e-waste (Widmer et al., 2005).

Furthermore, Baldé et al., (2017) and Forti et al., (2020) showed that the volumes of WEEE being transferred and or exchanged between states and countries (specifically to developing countries) is causing significant social and economic complications (Widmer et al., 2005). The rapid transition to

technologically progress without the corresponding procedures for managing the resultant waste stream, policies, and infrastructure, rapidly impacts the developing and transitional countries (Hossain et al., 2015). This lack of policies allows for an e-waste recycling economy that thrives on unregulated and risky low-cost practices, together with the existence of a very inventive and low-income informal sector (Hossain et al., 2015; Widmer et al., 2005). Most industry participants are unaware of the threats to the environment and public health, and they either lack knowledge of best practices or lack access to resources to fund even profitable upgrades or adopt safety measures (Widmer et al., 2005).

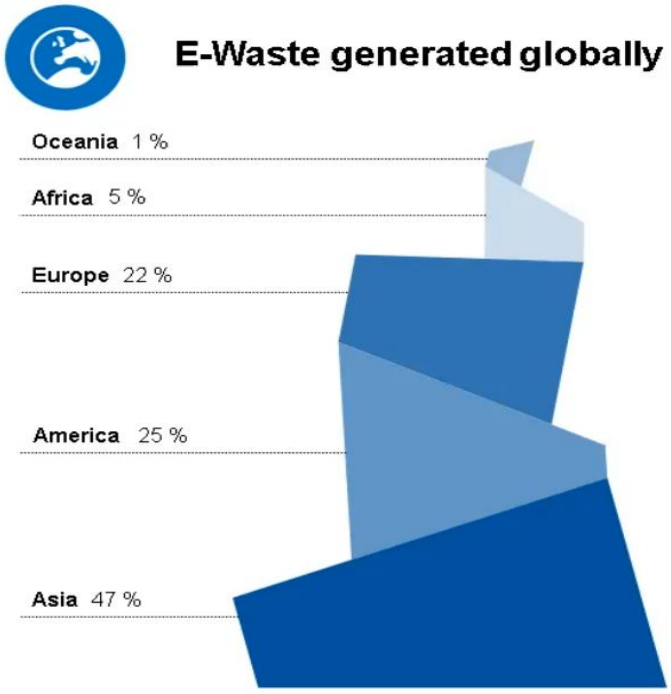

Figure 2-2: WEEE generated globally (Gertjegerdes et al., 2022).

The increasing volume and high content of both hazardous and valuable materials contained within e-waste, represents an ongoing environmental challenge as well as a business opportunity (Widmer et al., 2005). Examples of harmful material include heavy metals and plastics for instance the brominated organic flame retardants (BFRs) (Hossain et al., 2015).

It is a global perception that e-waste can be considered as a secondary metallic resource as illustrated in Figure 2-3 (Baldé et al., 2017; Cerchier et al., 2017; Forti et al., 2020; Işıldar et al., 2017; Kaya, 2019; Widmer et al., 2005). The recycling of these metals can recompense for the demand for mining since, it is projected that in the long run, conventional ores will be insufficient to account for the consumption of metals (Ha et al., 2014; Kaya, 2019). The efficient recovery of these metals is of grave importance not only because of their high economic potential and the need for the conservation of

primary natural sources and but also the potential environmental and human health risks (Tanisali et al., 2021).

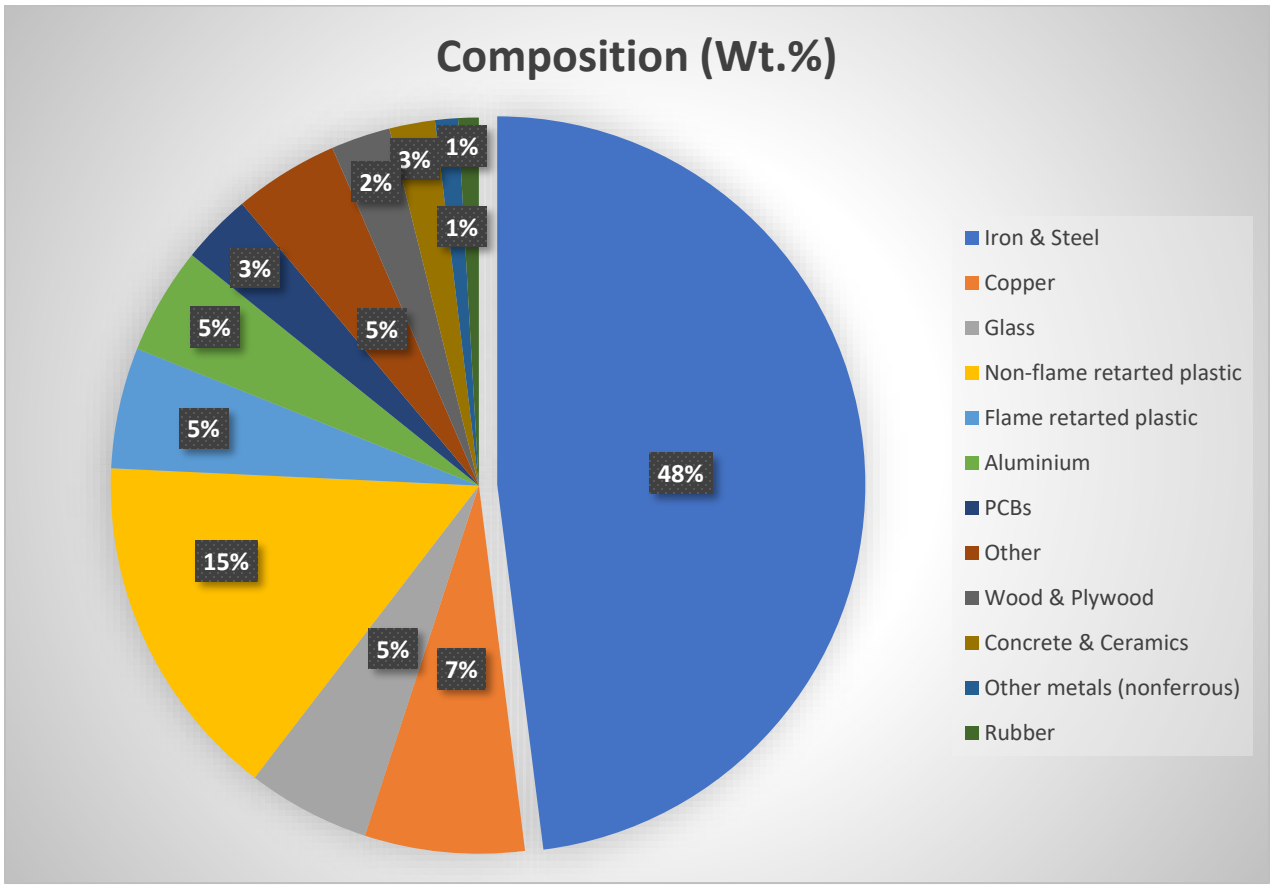

Figure 2-3: Material contained in e-waste adapted from Widmer et al., (2005).

2.2 PCB materials composition and value

E-waste contains 3–5% waste PCBs (Chirume, 2019; Cui et al., 2016; Kaya, 2019; Prestele, 2020). These are essential structures in the electronic components and the key component of the WEEE recycling process. PCBs are solid structures that contain electrical circuitry. These are made up of embedded metal surfaces known as traces and larger metal sections known as planes (Cadence®, 2023). Metal pads on the board are soldered with components to connect them to the circuitry of the board. This makes it possible to link components. Circuitry may be spread across one, two, or more layers of a board. To ensure efficient circuitry transmission, circuit boards are constructed using a dielectric core material with limited electrical conductivity, which is spaced with additional metal and dielectric layers necessary (Cadence®, 2023). While the metal traces and planes for the circuitry are

often made of Cu, the common dielectric material used for PCBs is a flame-resistant mixture of woven fiberglass fabric and epoxy resin known as FR-4 (Cadence®, 2023; Chirume, 2019).

Waste PCBs also constitute other metallic elements such as Au, palladium (Pd), etc. Au, is typically found as the final layer (Jeon et al., 2020b; Moyo et al., 2020; Petter et al., 2013). The other metallic elements present in waste PCBs include, hazardous elements like lead (Pb) and arsenic (As) as well as other valuable metals such as aluminium (Al), iron (Fe), Ni, and zinc (Zn). Akcil et al., (2015), Jeon et al., (2020b), Mishra et al., (2021), and Kaya, (2019), further elaborate that the concentrations of PMs, especially Au, Ag and Pd, is much higher than their respective primary resources. Therefore, the principal driving force for developing metal recovery methodologies is the high content of both base and precious metals in waste PCBs.

Table 2-1 shows that the content of waste PCBs varies as reported in literature. In this study, only custom-made boards were used, While this is a limitation to the study as no “real" waste PCBs were used, this approach overcame challenges of lack of homogeneity, allowing for results to be comparable across different sets of experiments. This means that, the same design, composition, and quality was maintained for each board. Section 3.1.1 of this study's methodology includes a description of the PCBs that were used.

Table 2-1:Chemical analysis of metallic elements presents in PCBs.

Metallic Element w/w%	**[1]**	**[2]**	**[3]**	**[4]**	**[5]**	**[6]**	**[7]**	**[8]**	**[9]**	**[10]**	**Average**
Cu	56.68	30.57	20.19	25.06	19.19	20	20	23.5	60.67	21.5	29,74
Al	1.42	11.69	5.7	4.56	4.01	5	2	1.3	4.94	-	4,51
Fe	0.24	15.21	7.33	0.66	1.13	7	8	1.2	0	4.53	4,53
Sn	1.4 0	7.36	8.83	1.86	0.69	2.9	4	1.5	7.38	4.09	4,00
Ni	-	1.58	0.43	0.0024	0.17	1	2	2.4	-	0.85	1,05
Zn	0.22	1.86	4.48	0.04	0.84	-	1	1.5	2.27	1.34	1,51
Pb	-	6.70	5.53	0.8	0.39	1.5	2	1.0	5.06	2.77	2,86
Pd	0.01	-	-	-	-	-	0.0050	0.029	0	0.0124	0,01
Mn	0.005	-	-	-	0.04	-	-	-	-	-	0,02
Sb	-	-	-	-	0.37	-	-	-	-	-	
Au	0.021	0.0238	0.13	-	0.0130	0.025	0.1	0.057	0.00005	0.0191	0,04
Ag	0.1	0.0688	0.16	-	0.0704	0.1	0.2	0.33	0.00018	0.0618	0,12
Other (mainly resins & glass fibres)	39.9	24.94	47.22	67.02	73.09	62.48	60.70	67.184	19.68	64.827	52,70

Sources: [1] (Tripathi et al., 2012), [2] (Birloaga et al., 2013), [3] (Li et al., 2012; Wu et al., 2017), [4](Yang et al., 2009), [5] (Behnamfard et al., 2013), [6] (Tuncuk et al., 2012), [7] (Hageluken, 2006), [8] (Ogunniyi et al., 2009); [9] (Guo et al., 2015) and[10] (Cui et al., 2020)

As shown in Figure 2-4, the metal connectors within the waste PCBs contain a significant amount of Au coating, which is the most essential component considering its value (Peng et al., 2020a). However, several sources listed in Table 2-1 show that, in terms of quantity, Cu is the most dominant metal. During the manufacturing process Peng et al., (2020b) and Birich, (2020), reported that Ni and Au are electroplated separately, not as an alloy, while Kasper et al., (2018), Chirume, (2019) and Moyo et al., (2020) show that Au exists as an alloy on the surface of waste PCBs. Birich, (2020) reported that Pd can be also used as an intermediate layer between Ni and Au thereby reducing the required amount of Au. However, these sources all agree that Au is not covered by other components and distributed across the surface of PCBs, as shown on Figure 2-4. The interlayer made of Ni or a Ni compound (found on the outer layers) is essential to avoid the diffusion of Au into Cu or vice versa (Birich, 2020).

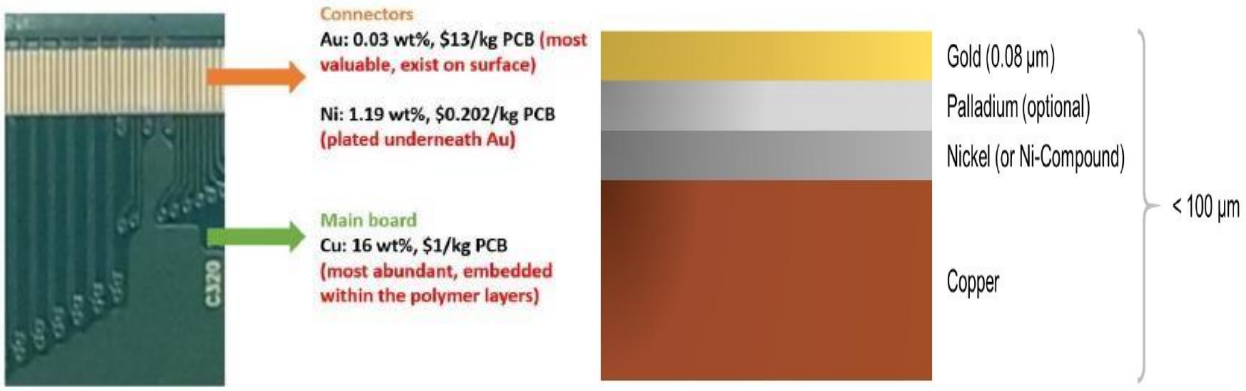

Figure 2-4: Average concentrations and values of main metals in multi-layered PCBs as well as their locations (Birich, 2020; Peng et al., 2020)

An estimation of the market value of the metals present on waste PCBs has shown that at least 80% of the overall market value is from precious metals (Au, Ag and Pd). Table 2-2 shows the market value of metals found in waste PCBs per tonne. Cui et al., (2020) identified that Au alone has an approximate market value of USD 7927 per tonne of waste PCBs from a total of USD 15,231 (total market value per tonne of waste PCBs), despite the much greater concentrations of BMs (Cu, Zn, Ni and Sn) present in waste PCBs. Yu et al., (2009) showed that Au in waste PCBs had an approximate value of USD 5620 per tonne. The difference in prices is largely because the type and concentration of materials (specifically Au) used in electronics change frequently and so did the price of Au between 2009 and 2020 (Macrotrends©, 2023). This is due to rapid and steady technological development as previously stated. Additionally, the use of various PCB types and/or the year the PCBs were manufactured can both account for the discrepancy in the numbers provided in the literature (Hageluken, 2006; Kasper et al., 2018).

Table 2-2: Market value (USD) per tonne of waste PCBs

Metal	Au	Ag	Pd	Cu	Sn	Fe	Pb	Zn	Ni	total
Potential Value [1]	7927	334	4030	1505	818	429	55	40	94	15231
Potential Value [2]	5620	189	610	349.2	279	36.8	27	-	72.5	7283.5

Sources: [1](Cui et al., 2020) and [2] (Yu et al., 2009).

2.3 Processing routes for the recycle of waste PCBs

The two prime processing routes for the extraction of valuable metals from waste PCBs, are via pyrometallurgy and hydrometallurgy. Each route has its own advantages and drawbacks which are summarised in Table 2-3. As illustrated in Figure 2-5, the first step that comes before extraction, is the collection of e-waste which is then followed by pre-treatment of the waste PCBs. The pre-treatment consists of disassembling, dismantling, shredding/grinding and other different separation, and size reduction processes to upgrade the desirable material content (Akcil et al., 2015; Kaya, 2019; Yu et al., 2009).

The second step is the further separation and processing of the metal streams. This step is the most essential from an economic and environmental perspective. This step, consisting of different processing pathways, is presented in Figure 2-5. The red dotted lines denote optional pathways.

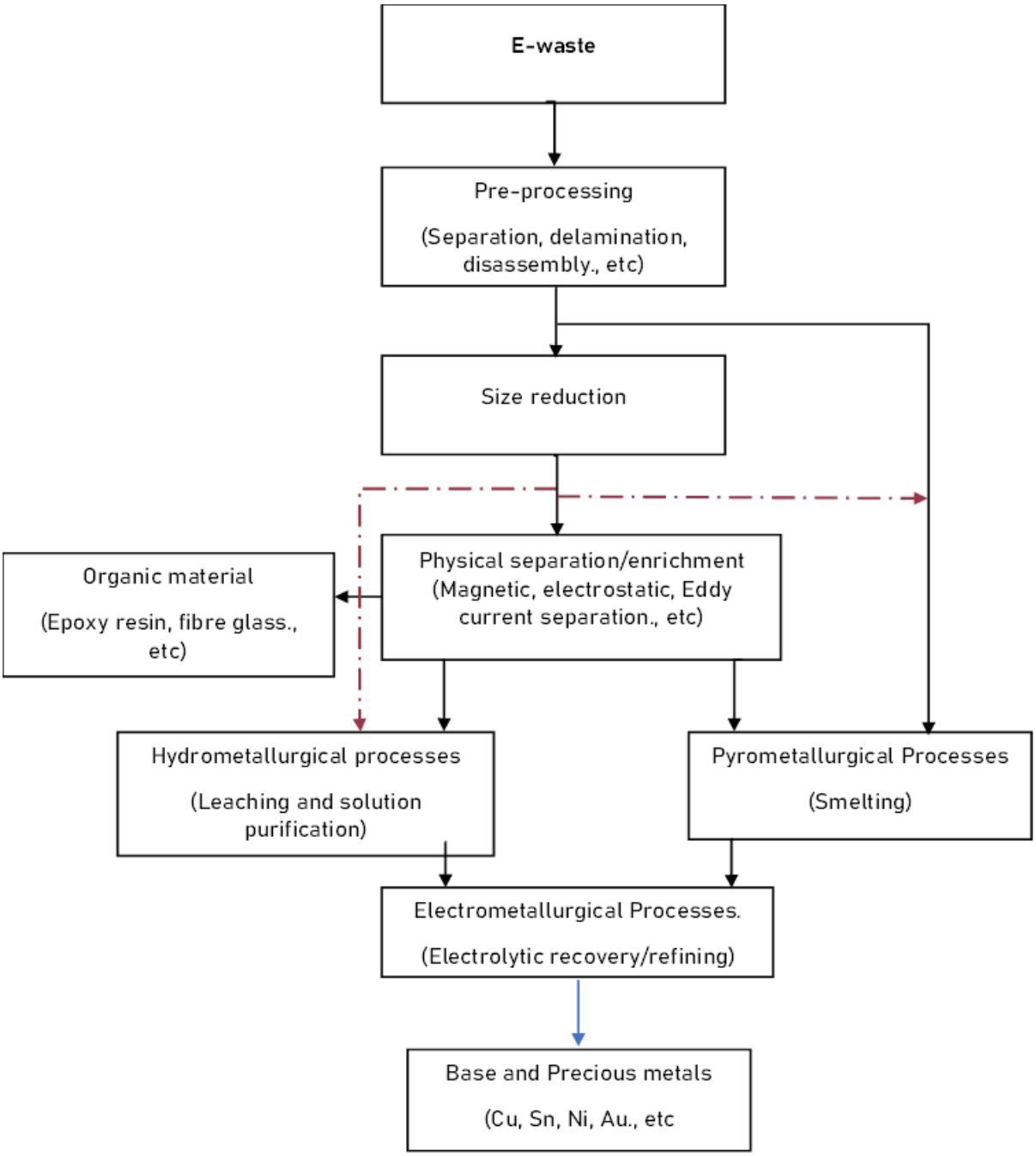

Figure 2-5: Overview of metallurgical process routes for the recycling of e-waste adapted from Tuncuk et al., (2012) and Akcil et al., (2015).

Pyrometallurgy

Pyrometallurgy refers to processes that employ high temperature and take advantage of the metallurgical/chemical properties of the mineral substance. One example is the widely applied smelting process. During this process, high temperatures between 500-2000℃ are required to reduce the metals from their compound form to elemental form. This results in their liquefaction with goal of

simultaneously concentrating wanted metals and separating unwanted materials into a slag phase (Yu et al., 2009; Zhukov et al., 2013). Other examples include calcining, roasting, all which require application of elevated temperatures (Cui et al., 2008b). Pyrometallurgical processes are relatively simple. They are also applicable for heterogeneous material feeds and are suited for large scale production (Shuey et al., 2006). The largest drawback to using this route is the impact it has on the environment (Kaya, 2019). The advantages and disadvantages of the two routes are summarised in Table 2-3.

Table 2-3: Summary of advantages and disadvantages of Pyrometallurgical and hydrometallurgical route in Au recovery from e-waste (Birich, 2020)

Pyrometallurgy	**Hydrometallurgy**
Requires mechanical and physical pre-treatment.	Only manual pre-treatment required.
Required equipment is very expensive.	Low-cost equipment required.
Complex process operation and control.	Simpler techniques and equipment.
Involves numerous purifying and separation stages.	Fewer stages are required in the process, e.g., leaching, precipitation and solvent treatment
A thorough exhaust gas treatment is required.	Lesser need for gas treatment in closed leaching tanks.
High capital injection results from a lengthy process.	High selectivity permits a rapid and cost-effective Au recovery.
Typically, a single furnace is used to handle several WEEE fractions.	High value e-waste component fractions can be processed separately.
Centralized in large-scale companies, fewer prospects for small scale recycling.	Small-scale and decentralized processing units are a possibility.

Hydrometallurgy

For the hydrometallurgical route, two main stages are involved in the extraction of PMs from waste PCBs. The first step comprises of the extraction of BMs (for instance Cu) via leaching. The most common lixiviants are acids and these include sulphuric acid (H_2SO_4), nitric acid (HNO_3), aqua regia (HNO_3: Hydrochloric acid (HCl), chlorides with a combination of H_2O_2 in some reactions (Behnamfard et al., 2013; Cui et al., 2016; Ficeriová et al., 2011; Nesakumar et al., 2014; Tuncuk et al., 2012; Wang et al., 2020; Yang et al., 2011). Other less corrosive lixiviants include ammonia (NH_3)

leaching which is combined with carbonates, chlorides, and sulphates (Bari et al., 2009; Chirume, 2019; Koyama et al., 2006; Moyo et al., 2020; Radmehr et al., 2013; Rudnik et al., 2016).

The product from the first step (solid residue) is then fed to the second stage, and subjected to further leaching, where PM, such as Au, are extracted. The traditional lixiviant used for Au leaching is cyanide. Although it is highly effective, it is an environmental risk and a human toxin. It is a challenge to process the produced wastewater which can contaminate water bodies (Akcil et al., 2015; Kasper et al., 2018). Other common and less hazardous lixiviants include thiourea, halides and thiosulphates. For a hydrometallurgical route, pre-treatment is an essential primary step for BM extraction/removal that governs the rate and extent of Au dissolution during leaching. The desired effect of pre-treatment is to expose and extract as many BMs (e.g., Cu) as possible during the first stage of leaching to eliminate their presence in the successive PM recovery aqueous systems. This step is explored further in section 2.5.

Recovery

Metal products from both the pyrometallurgical and hydrometallurgical processes are then recovered in downstream processes. Different methods have been established for the purification of PLS to then recover the pure metals, for instance Au in this project/case. Au follows Cu via the pyrometallurgical pathway and is recovered during Cu electrorefining. It reports to the anode slimes that are subsequently treated by hydrometallurgical procedures (Akcil et al., 2015; Jeon et al., 2020b; Kasper et al., 2018). The Au from the CN leach step of the primary hydrometallurgical process for PCBs is recovered using the conventional activated carbon method used in primary Au production, followed by electrowinning (Akcil et al., 2015; Jeon et al., 2020b; Kasper et al., 2018).

2.4 Criteria for lixiviant selection for leaching

Leaching is an essential primary extraction operation in hydrometallurgy. It is a process by which a metal of interest is transferred from its ore into aqueous solutions which results in the production of a pure metal-rich solution (Aylmore et al., 2001; Kholmogorov et al., 2002). It is therefore, of great importance to select the most suitable leaching agent. That said, an ideal leaching agent is one that meets the following criteria:

i. fast leaching kinetics
ii. selective

iii. not hazardous to both human health and the environment

iv. cost effective

2.5 Cu leaching lixiviants

Several studies, most at laboratory scale, have been done on Cu extraction and other BMs through leaching from waste PCBs. The popular ones include the previously mentioned acids, chlorides and ammoniacal lixiviants. A few studies based on the work that has been done on the prior leaching of BMs including Cu (using different lixiviants) before PM leaching from waste PCBs is shown in Table 2-4.

From the Table 2-4, it is evident that acid leaching gives high BM extraction particularly Cu, even with shorter residence times (Behnamfard et al., 2013; Ficeriová et al., 2011; Long et al., 2011; Mecucci et al., 2002; Vijayaram et al., 2013; Yang et al., 2011). However; this is with the exception of Bari et al., (2009) and Nesakumar et al., (2014) who obtained the overall lowest extraction after 48 hours. This was most likely because HCl is a non-oxidizing acid which exhibits weak reducing properties during digestion. It requires the assistance of an oxidant, for example HNO_3 or H_2O_2 (Mecucci et al., 2002). In contrast, Mecucci et al., (2002) and Long et al., (2011) obtained the highest extraction (above 99%) with HNO_3 which has far greater oxidising properties. However, their study showed that high temperatures are very necessary for effective leaching regardless of its oxidising capabilities. This is also emphasized in the study by Vijayaram et al., (2013), which shows that aqua regia requires system temperatures of about 60℃ for effective leaching.

Behnamfard et al., (2013) and Yang et al., (2011) also obtained high extraction with the use of H_2SO_4, although aided by H_2O_2 as the oxidant. The study done by Yang et al., (2011) showed that concentration of H_2SO_4 has insignificant effect on the Cu recovery. While, Ficeriová et al., (2011) also reported slightly lower recoveries after introducing heat to their system. However, despite the high recoveries, acidic lixiviants have several shortcomings.

Alkaline lixiviants, specifically, ammoniacal systems, have many advantages over acidic leaching despite having the longest residence times displayed in Table 2-4. For one, the problems associated with equipment corrosion are eliminated (Radmehr et al., 2013; Rudnik et al., 2016). Ammonia also has a suitably selective capacity for metals such as Cu relative to other metals like Fe, Ni and Al, which are highly soluble in acidic conditions (Chirume, 2019; Ficeriová et al., 2011; Koyama et al., 2006; Vijayaram et al., 2013).

Table 2-4: Summary of experimental work carried out on different PCBs for BM recovery from PCBs.

Source	**Lixiviant**	**Particle size (mm)**	**T ℃**	**Residence Time (hrs)**	**% Extraction**
(Bari et al., 2009)	1M HCl	0.06	25	48	Cu: 37, Zn: 28, Fe: 10 & Ni: 17
(Behnamfard et al., 2013)	2M H_2SO_4, 25 mL H_2O_2 (35 wt.%)	≤ 0.3	25	3	Cu: 99.75
(Yang et al., 2011)	5M – 35 wt.% H_2SO_4, 5 - 25 mL (30 wt.%) H_2O_2	0.5 - 8	25- 50	0.5 – 4	Cu :93
(Ficeriová et al., 2011)	2M H_2SO_4, 0.2M H_2O_2	≤ 0.8	80	8	Cu: 85, Zn: 76, Fe:82, Al: 77, Ni:70
(Vijayaram et al., 2013)	3M HCl + 1M HNO_3	≤ 0.2	60	2	Cu: 92.7
(Nesakumar et al., 2014)	3N HCl	-	60	2	Cu :20
	1N HNO_3				Cu :96
	2.18N H_2SO_4,				Cu:<10
(Long et al., 2011)	(1.25 – 7)M HNO_3	≤ 1	30 - 60	1	Cu :99.99
(Mecucci et al., 2002)	6M HNO_3	≤ 2.5	80	6	Cu: >99
(Bari et al., 2009)	5M NH_3, 1M $(NH_4)_2SO_4$	0.06	25	48	Cu: 64, Zn: 48, Fe:0 & Ni: 2.2
(Bari et al., 2009)	5M NH_3, 1M $(NH_4)_2CO_3$,	0.06	25	48	Cu: 93, Zn: 68 Fe:0 & Ni: 19
(Chirume, 2019)	4M NH_3, 2M $(NH_4)_2SO_4$, ~100ppm $CuSO_4$	20×15	25	120+	Cu: 49.
(Koyama et al., 2006)	0.3M $CuSO_4$, 5M NH_3, 1M $(NH_4)_2SO_4$:	≤ 1 .5	25	2.5	Cu :93
(Chirume, 2019)	4M NH_3, 2M $(NH_4)_2CO_3$, ~100ppm $CuSO_4$	20×15	25	120+	Cu: 28
(Rudnik et al., 2016)	0.5M NH_3, 1M $(NH_4)_2CO_3$, 50mM Cu^{2+}	25×25×7 (Alloy ingots)	-	24	Cu: ~95, Zn: ~90 &Ni: ~10, Fe:13
	0.5M NH_3, 1M $(NH_4)_2SO_4$, 50mM Cu^{2+}				Cu: ~95, Zn: ~90, Fe~2.5 & Ni: ~80
	0.5MNH_3, 1M $(NH_4)_2S_2O_3$, 50mM Cu^{2+}				Cu:0, Zn: 100 Fe: & Ni:100

This is one of the reasons why lixiviants such as aqua regia are commonly used for characterization purposes due to their poor selectivity. Owing to this, it was selected for the characterisation experiments outlined in chapter 3 of this study. To add to that, characteristics such as low toxicity, low cost, easy recyclability are some of the factors for increased use of ammonia in leaching over acidic leaching (Koyama et al., 2006; Radmehr et al., 2013). The major challenge that comes with the use of ammonia is its high evaporation capacity (Radmehr et al., 2013). Previous studies on ammoniacal leaching shall be explored in the next section.

2.5.1 Ammoniacal leaching of Cu

Numerous studies have also been conducted on the alkaline ammonia-ammonium salt leaching of Cu and other BMs. To assist with the selection of optimum Cu leaching conditions employed in this study, a few studies and their leaching conditions will be briefly discussed.

Rudnik et al., (2016) showed that alkaline ammonia–ammonium salt solutions exhibit some advantages in the leaching of polymetallic materials such as PCBs, especially since dissolution of Cu is specific (autocatalytic). This is demonstrated by the following equations,

$$Cu(NH_3)_4^{2+} + Cu \rightarrow 2Cu(NH_3)_2^{+} \quad (1)$$

$$2Cu(NH_3)_2^{+} + 4NH_4^{+} + 2OH^{-} + \frac{1}{2}O_2 \rightarrow 2Cu(NH_3)_4^{2+} + 3H_2O \quad (2)$$

This characteristic enhances separation from co-extracted metals Rudnik et al., (2016). Other metals (e.g., Ni) are also transferred into solution (electrolyte) as soluble ammine complexes, but the rate of their dissolution is determined by oxygen transport to the metal surface (Rudnik et al., 2016). In addition, ammonium systems give the possibility of Fe removal by precipitation of Fe(III) hydrated oxides, and this is shown by the following equations.

$$Fe + 4NH_3 + H_2O + \frac{1}{2}O_2 \rightarrow Fe(NH_3)_4^{2+} + 2OH^{-} \quad (3)$$

$$2Fe(NH_3)_4^{2+} + 5H_2O + \frac{1}{2}O_2 \rightarrow 2Fe(OH)_3 + 4NH_4^{+} + 4NH_3 \quad (4)$$

$$2Fe(OH)_3 \rightarrow Fe_2O_3.3H_2O \quad (5)$$

Unlike other BMs, it is extremely challenging to dissolve Sn in alkali solutions at room temperature. In an alkaline environment, the stability region for the soluble Sn specie SnO_3^{2-} only increases as the temperature rises (Yang et al., 2017)
Referring to Table 2-4, and other sources, ammonia-based lixiviants, display higher specific BM selectivity, especially towards Cu (Bari et al., 2009; Koyama et al., 2006; Rudnik et al., 2016).

The influence of ammonium salts on the Cu recovery from waste PCBs was reported by Oishi et al., (2007); Moyo et al., (2020) and Bari et al., (2009). Oishi et al., (2007) revealed that Cu leaching was more selective in chloride than sulphate systems. On the other hand, in the study by Bari et al., (2009) on various ammonium salts for Cu recovery from waste PCBs, highest recoveries of 90% Cu, 60% Zn, and 9% Ni were achieved for an ammonia–ammonium persulphate solution. For $(NH_4)_2SO_4$ and ammonium carbonate ($(NH_4)_2CO_3$) salts, they reported a recovery of 64% and 92.6% respectively under the same conditions. However, Moyo et al., (2020), and Chirume, (2019) reported contradictory recoveries of 49% and 28% for $(NH_4)_2SO_4$ and $(NH_4)_2CO_3$ salts respectively.
These recoveries were lower due to the particle size that that they used of 20 ×15 mm compared to a particle size of < 0.06mm which was used by Bari et al., (2009). Moreover, of the size of waste PCBs that were used by Chirume, (2019), the outer Cu layers and the Cu electroplated in connectors both contribute only about 31% of the total Cu in each PCB. Given that 31% of the Cu was the only leachable Cu, it follows that some of the inner Cu layers were also leached. This demonstrates that a 49% extraction was very high. With a PCB size of <1.5mm, Koyama et al., (2006) was able to obtain Cu recoveries of 93% within 2.5 hours under the same conditions, which clearly shows that particle size plays a major role during leaching. However, Tuncuk et al., (2012) showed that size reduction techniques can result in losses up to about 35%. This was confirmed by Chirume, (2019) who recorded a loss of 39% of the PCB, which meant that only 61% of the PCB was available for leaching.

Rudnik et al., (2016)'s study on different ammonium salt solutions, $(NH_4)_2SO_4$, $(NH_4)_2CO_3$ and $(NH_4)_2S_2O_3$, showed that $(NH_4)_2S_2O_3$ is not applicable for leaching of the Cu alloy ingots. This is due to secondary reactions of the formation of copper(I) thiosulphate complexes and precipitation of copper(I) sulphide, thus inhibiting dissolution process. Although they did not specify the leaching temperature, they concluded that the most favourable conditions for the alloy dissolution can be

achieved in the ammonia–ammonium carbonate system (summarised in Table 2-4). This system favoured the leaching of Cu and Zn effectively, without uncontrolled alloy degradation. The same observation was made in the case of $(NH_4)_2SO_4$ where the same recoveries of 95% and 90% were obtained for Cu and Zn respectively. However, unlike $(NH_4)_2CO_3$, the same concentration of $(NH_4)_2SO_4$ was able to leach Ni under the same conditions, and this was shown by a recovery of 80%. This would be a good attribute if the goal is to remove BMs prior to PM leaching to minimise their interference. Chirume, (2019)'s results agree with Rudnik et al., (2016), as they concluded that the system with ammonium sulphate had the highest Cu recovery although carbonate salts proved to be a better buffer than sulphate as it had less fluctuations in pH.

The common observation on most of these studies is that the extraction of other BMs, save for Cu, was not disclosed. To minimise the precipitation of copper, the pH was kept between 8 and 11 by adding ammonia.

From literature summarised in Table 2-4, ammoniacal solutions, are the preferable lixiviants for Cu leaching. Ammonium sulphate fits the criteria outlined in section 2.4. Leaching is favoured by the following conditions: room temperature to avoid evaporation of NH_3, and a pH that ranges from 8-11, to reduce precipitation of Cu.

2.6 Gold leaching lixiviants

In Au hydrometallurgy, the first stage involves the extraction of Au by dissolution using suitable lixiviants (leaching). This is followed by the recovery of extracted Au ions from pregnant leach solutions (Jeon et al., 2018; Jeon et al., 2020b). Most hydrometallurgical based processes suffer from slow reaction kinetics because of low temperature applications. To improve the leaching of the metal, it is imperative to optimize process variables including particle size, lixiviant type, temperature, concentration of the lixiviant, solid to liquids ratio (S/L), and agitation rate. (Cui et al., 2008b; Li et al., 2012). For PMs such as Au, which have a low likelihood to form complexes, the chemical leaching reaction is still slow despite optimization of leaching conditions. Au requires the action of catalysts to facilitate the rate of dissolution through the formation of intermediate complexes or acting as an electron donor or recipient (Gámez et al., 2019; Kasper et al., 2018; Xiu et al., 2015).

2.6.1 Hydrometallurgical recycling techniques for gold recovery from waste PCBs

The thermodynamic stability of metallic Au in aqueous solutions requires addition of oxidants and complexing agents. A conventional method, and the leading choice for the recovery of Au from Au ores, is cyanide leaching. Cyanidation has been the dominant process for a century because of its simplicity, robustness, and cost efficiency. It also allows application of alkaline, non-corrosive solutions and the use of efficient downstream Au separation processes. Equation 6 gives the Au dissolution reaction in cyanide systems, that is facilitated by atmospheric redox potential (Akcil et al., 2015; Kasper et al., 2018).

$$4Au + 8CN^- + O_2 + 2H_2O \rightarrow 4Au(CN)_2^- + 4OH^- \quad (6)$$

The cyanide anion can be found as complexes (weak to strong complexes), as simple compounds in cyanidation solutions or as free cyanide depending on the pH of the system. Free cyanide can be in the form of either cyanide anion (CN^{-1}) or hydrocyanic acid (sometimes called hydrogen cyanide, HCN). Flynn et al., (1995) showed that HCN is a relatively weak acid that is predominantly found in a system with a pH of approximately 8.5. Under these conditions volatilisation of cyanide takes place. Optimal Au extraction takes place at a pH of 10.5 or greater where most of the free cyanide in the solution is in the form of the cyanide anion and its loss by volatilisation is limited, else cyanidation process would neither be feasible, safe nor economically and environmentally feasible (Akcil et al., 2015).

In a study, Kasper et al., (2018) achieved an average 88% extraction of the Au from waste PCBs over the course of two hours using cyanide. Two hours was a reasonably good residence time, at room temperature and a pH of 12.5. However, the concentration of CN and PCB size were not specified and therefore it is unclear which parameter influenced the efficiency.

Petter et al., (2013) also managed to reach close to 70% extraction using 6-8% potassium cyanide at 25°C for 2-4 hours in a pH of 12.5. However, the co-extraction of other metals was not specified.

Nevertheless, cyanide application in e-waste has serious drawbacks that render it unmanageable despite the high extraction capacity, especially in the context of extracting Au from waste PCBs with a high Cu concentration. Leaver et al., (1931) demonstrated that metallic Cu is readily and practically soluble in CN at ambient temperature and typical Au cyanidation conditions. In a study, they were

able to extract 90% and 100% from pure metallic Cu, at 23℃ and 45℃, respectively, using a 0.099% NaCN solution and a 24-hour retention time.

In an investigation of column leaching of waste PCBs, Montero et al., (2012) observed that even at a high CN concentration of 0.15M, very modest Au extraction of 48% can be achieved, while the level of Cu coextraction was quite high (77%).

Akcil et al., (2015), Kasper et al., (2018) and Tripathi et al., (2012) reported that, cyanide is not only toxic, and an environmental risk, but its wastewater is also difficult to process. Moreover Birich, (2020) reported that cyanide is less selective as it can leach both Cu and Au from waste PCBs. The increasing environmental pressure on the use of cyanide and it limited selectivity is what motivated the ongoing research into non-cyanide alternatives.

Aqua regia (HNO_3+ HCl) is one of the alternative lixiviants for Au recovery, however Akcil et al., (2015) and Cui et al., (2008a) reported that other than being highly corrosive and least selective, it shares the same disadvantages with cyanide which include environmental and public health concerns, volatility, toxic emissions, and low selectivity. As previously mentioned in section 2.5 this characteristic of aqua regia is an advantage for digestion/characterisation purposes.

Halides are also commonly used to extract Au from both natural ores and e-wastes because of their high extraction efficiency. As an alternative to cyanide, He et al., (2015) studied a chlorination process to recycle Au from waste PCBs, after an optimal supercritical pre-treatment which resulted in a 99% Au recovery. Compared to conventional Au leaching methods, their method gave high Au and Cu recoveries respectively with high purities. Xiu et al., (2015) also studied the possibility of using iodine-iodide system for leaching Au from pre-treated WPCBs (by supercritical water + HCl). They were able to recover 100% Cu and 98.5% Au. This method and other halides, provide an efficient way for recycling Au and Cu and from waste PCBs. However, even with excellent Au leaching properties, the high cost of bromine and iodine and their potential health risks limit their application in e-waste leaching (He et al., 2015; Xiu et al., 2015; Xu et al., 2017). Birich, (2020) and Cui et al., (2020) added that after factoring in the high reagent consumption, the cumulative costs for bromine would be even higher than the profit of recovered Au. The advantage with iodine use is that it can be regenerated (Lucheva et al., 2017).

(Li, et al., 2012) studied the thiourea $CS(NH_2)_2$ leaching process as an alternative for cyanide and they obtained 90% Au recovery. In this research, solution chemistry had more influence on the leaching of Au and Ag from the waste PCBs. Birloaga et al., (2013) investigated a double step oxidative leaching pre-treatment method, for the removal of Cu and other BMs. This was followed by thioureation which gave 69% Au recovery. The study showed that thiourea can give a good extraction. However, operating at a higher temperature leads to the decomposition of thiourea which led to a lower Au recovery. Moreso, review studies show that it has an overall poor stability and high consumption which make it more expensive than cyanide (Akcil et al., 2015; Wu et al., 2017).

In the case of thiosulphate, Abbruzzese et al., (1995), Akcil et al., (2015), Tripathi et al., (2012) and Jeon et al., (2018) reported that it is relatively greener, cheaper, less toxic, and selective. Despite its challenges with stability, it is the most favourable alternative Au lixiviant as it has the advantage of a thermodynamically stable Au complex, which other non-cyanide lixiviants do not have. The Au thiosulphate complex is the closest in stability to the Au cyanide complex (Aylmore et al., 2001).

To facilitate Au dissolution, strong oxidizing conditions are required, however this results in the consumption of reagent which is the case for both thiosulphate and thiourea systems. On the other hand, lower oxidizing systems results in a lower Au dissolution rate (Birich, 2020). Among other factors, the stability of the Au complexes is practically significant in the design of efficient leaching processes (Cui et al., 2008a; Zhang et al., 2004).

However, there exists little information on full scale operation with thiosulphate leaching of Au (Akcil et al., 2015). If further research is done to develop an efficient processing pathway, thiosulphate leaching may be considered as a viable lixiviant that can maximize Au extraction . Table 2-5 gives a summarized comparison of the potential lixiviants for Au to assist with the choice of a non-cyanide lixiviant for the Au leaching stage from waste PCBs.

Table 2-5: Comparison of different kinds of Au leaching solvents

SOLVENT	PROS	CONS
Cyanide	Well researched and reliable method. Highly effective. Low reagent dosage. Not corrosive.	Highly toxic and environmental impact. Difficult to process wastewater. Slow kinetics. Interference from foreign ions
Thiourea	Fast reaction rates. Less toxic. Well established method.	Poor stability & decomposes rapidly. High consumption. Downstream metal recovery. More expensive than cyanide.
Thiosulphate	Good leaching performance nontoxic. Non-corrosive. Non-toxic and less environmental impact. Lesser interference from foreign cations.	Higher reagent consumption. Downstream metal recovery. Low research level and reliability.
Halide	High leaching rate, High selectivity. Relatively low environmental impact and toxicity safe except for bromine.	Highly corrosive for chlorine High consumption for iodine High reagent cost. Relatively less researched and less reliable except for chlorine.
Aqua Regia	Fast kinetics. Low reagent dosage. Relatively low reagent cost. Well researched and reliable method.	Strongly oxidative and corrosive. Difficult to deal with downstream. Poor selectivity

2.7 Ammonium thiosulphate leaching of gold

The dissolution of Au occurs through a formation of soluble aurothio-sulphate complexes that include $(Au(S_2O_3)_2^{3-}$ and $Au(S_2O_3)^-$ (Kasper et al., 2018). The ammonia-thiosulphate system chemistry is very complex because of the simultaneous presence of complexing ligands such as ammonia and thiosulphate, the Cu(II)-Cu(I) redox pair and the oxidative decomposition reactions of thiosulphate involving the formation of additional sulphur compounds such as tetrathionate (Aylmore et al., 2001; Zipperian et al., 1988).

Thiosulphate is a metastable anion which has a tendency of decomposing in aqueous solutions (Zipperian et al., 1988). It has therefore been established that neutral and alkaline media are conducive for the stability and solubility of the complexes (Aylmore et al., 2001; Zipperian et al., 1988). Moreso, adequate concentrations of ammonium thiosulphate, Cu and gaseous O_2 are what enable efficient extraction of the Au (Kasper et al., 2018; Tripathi et al., 2012). As mentioned earlier, the presence of Cu in the form of cupric ions (Cu^{2+}) ions alongside ammonia form a copper tetramine complex $[Cu(NH_3)_4]^{2+}$, a beneficial catalyst for Au dissolution (Aylmore et al., 2001; Breuer et al., 2002; Senanayake et al., 2003; Sitando et al., 2018; Zhang et al., 2004). There is however a need to pay special attention to the copper concentration because an excess of this metal ion is preferentially dissolved and thereby competes with Au to complex thiosulphate resulting in the depletion of the lixiviant (Abbruzzese et al., 1995; Senanayake, 2005; Zhang et al., 2004).

2.7.1 Thiosulphate reaction mechanism

The redox equilibrium that exists between the cuprous-cupric pair in an ammoniacal system is represented by the following reaction (Abbruzzese et al., 1995):

$$Cu(NH_3)_4^{2+} + 3S_2O_3^{2-} + e \rightarrow Cu(S_2O_3)_3^{5-} + 4NH_3 \quad (7)$$

Abbruzzese et al., (1995) stated that during the thiosulphate leaching of Au, chemical reactions involving dissolution, oxidation and complexation occur. Their research also revealed that oxidising agents, such as Cu ions, are adequate in ammoniacal solutions and that gaseous O_2 seems inefficient for metallic Au oxidation. The following reaction shows the role of Cu^{2+} ions, present in the form of the tetra-amine complex, in the Au oxidation from its metallic state to aurous Au^{+} ion. In other words, the equation shows the actual dissolution of Au in ammonium thiosulphate) (Aylmore et al., 2001; Chu et al., 2003; Ha et al., 2014).

$$Au + 5S_2O_3^{2-} + Cu(NH_3)_4^{2+} \rightarrow Au(S_2O_3)_2^{3-} + 4NH_3 + Cu(S_2O_3)_3^{5-} \quad (8)$$

The ammonia/ammonium alkaline buffer maintains the solution pH between 8.5 and 10.5 to prevent the decomposition of thiosulphate ions. In this system Au is oxidized by $Cu(NH_3)_4^{2+}$ and extracted as thiosulphate complex, $Au(S_2O_3)_2^{3-}$. The thiosulphate complex of Cu(I), $Cu(S_2O_3)_3^{5-}$generated by

equation (8) is then oxidised by dissolved O_2. This then leads to the regeneration of Cu (II) ammonia complex ($Cu(NH_3)_4^{2+}$) shown by the following equation:

$$4Cu(S_2O_3)_3^{5-} + 16NH_3 + O_2 + 2H_2O \rightarrow 4Cu(NH_3)_4^{2+} + 4OH^- + 12S_2O_3^{2-} \quad (9)$$

The Cu (II) ammonia complex is a strong oxidant that catalyses the dissolution rate of Au by about 18-20 fold (Aylmore et al., 2001). According to Abbruzzese et al., (1995), effective Au dissolution will only take place if an oxidation potential of 150 to 200 mV, with reference to standard hydrogen electrode (SHE), is achieved. As mentioned earlier, in section 2.6.1, the aurou-thiosulphate complex is the most stable Au-bearing soluble species in the leaching system. This is only possible between the pH range 8.5-10.5, according to ammonia concentration (Aylmore et al., 2001). Above this value, in strongly alkaline systems, Zipperian et al., (1988) explains that the predominant Au compound is represented by the Au(I) di-ammine complex demonstrated in the equations below:

$$Au(S_2O_3)_2^{3-} + 2NH_3 \rightarrow Au(NH_3)_2^{+} + 2S_2O_3^{2-} \quad (10)$$

A summary of the ammonium thiosulphate reaction mechanism is demonstrated in Figure 2-6 as an adaptation of Aylmore et al., (2001).

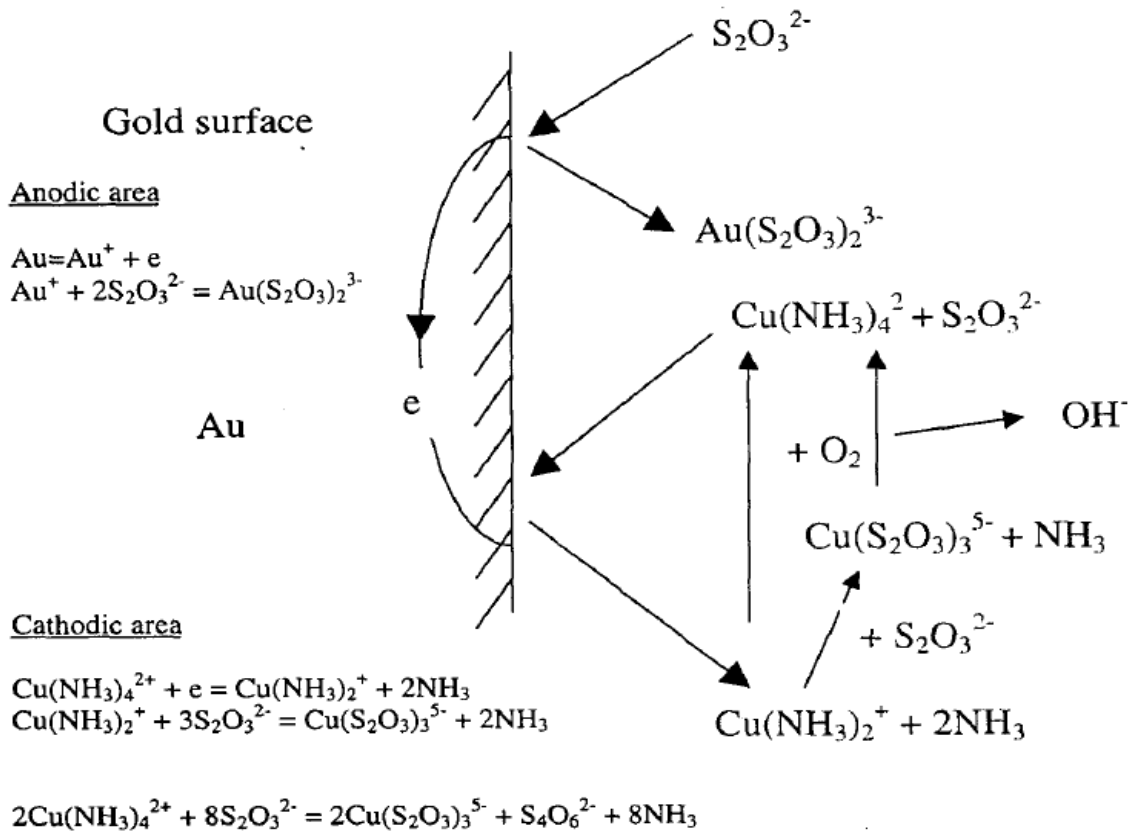

Figure 2-6: The electrochemical-catalytic mechanism model of ammoniacal thiosulphate leaching of Au adapted from Aylmore et al. (2001)

In summary, Au is oxidised to form Au^+ ions which react with ammonium thiosulphate ions on the anodic area of Au and thereby enter the solution to form $Au(S_2O_3)_2^{3-}$ as shown in Figure 2-6. The $Cu(NH_3)_4^{2+}$ present in solution accepts the released electrons on the cathodic area of the Au and thereby gets reduced to $Cu(NH_3)_2^{+}$. $Cu(NH_3)_2^{+}$ ions are converted to $Cu(S_2O_3)_3^{5-}$ species in the presence of $S_2O_3^{2-}$ ions (Aylmore et al., 2001). The $Cu(S_2O_3)_3^{5-}$ species (and $Cu(NH_3)_2^{+}$ species if present) in solution is converted back to the catalyst, $Cu(NH_3)_4^{2+}$ either through an intermediate oxidation reaction with $S_2O_3^{2-}$ ions or O_2 (Wan et al., 1997). The relative concentrations of the species in solution are what dictates the predominancy of the cathodic reaction (Aylmore et al., 2001; Wan et al., 1997).

2.7.2 Thermodynamics

The Au-Cu-NH_3-S_2O_3 and Au-NH_3-S_2O_3, is a very complex system that is quite difficult to understand as already mentioned. This is all attributed to all main reactions that include:

i. the Cu (II)-Cu(I) redox couple,
ii. simultaneous presence of NH_3 and thiosulphate ligands previously discussed and,
iii. interim oxidative decomposition of thiosulphate and other oxidative reactions.

A series of Eh-pH (Pourbaix diagrams) diagrams can be utilised to identify the predominant species under different potentials and pH conditions of the ammoniacal thiosulphate and copper system (Zipperian et al., 1988). During assessment, the conditions of the system that must be chosen, are those that include a region where the Cu (II) ammine complex ($Cu(NH_3)_4^{2+}$) is stable and Au dissolution occurs. The Pourbaix diagrams, for high and low concentrations of ammonia, copper and thiosulphate, are shown from Figure 2-7 to Figure 2-10.

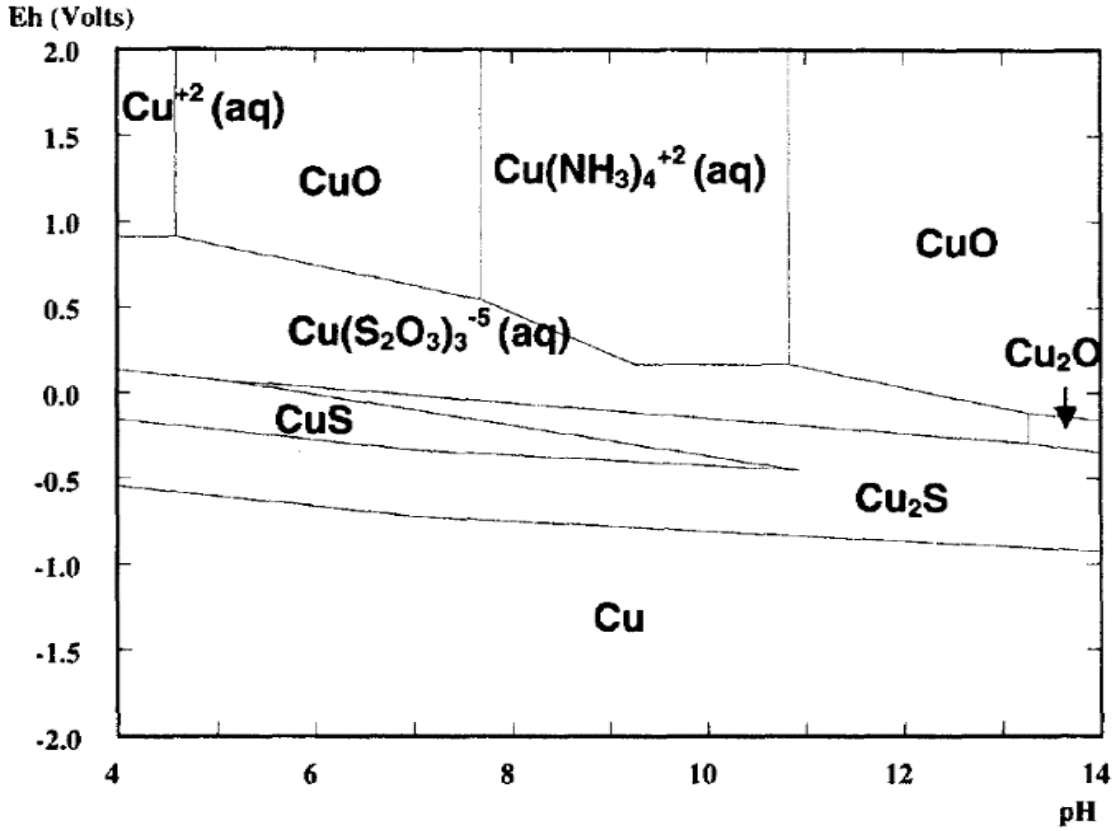

Figure 2-7: Pourbaix diagrams at 5x10^{-4}M Au; 1M$S_2O_3^{2-}$, 1M NH_3/NH_4^+ and 0.05M Cu^{2+}concentrations for a Cu-NH_3-$S_2O_3^{2-}$ system (Aylmore et al., 2001).

An increase in the dissolution of Au in copper-thiosulphate-ammonia solutions is attributed to the

stabilisation of the oxidant, Cu (II), by ammonia by forming cupric ammine complexes, as previously iterated (Aylmore et al., 2001; Zipperian et al., 1988). Figure 2-7 shows that, the pH range of stability for the catalyst ($Cu(NH_3)_4^{2+}$) is approximately between 8 and 11. Outside this range, Cu precipitates out as oxides CuO and Cu_2O or sulphides. At a high concentration, the stability region for $Cu(S_2O_3)_3^{5-}$is quite wider than of $Cu(NH_3)_4^{2+}$).

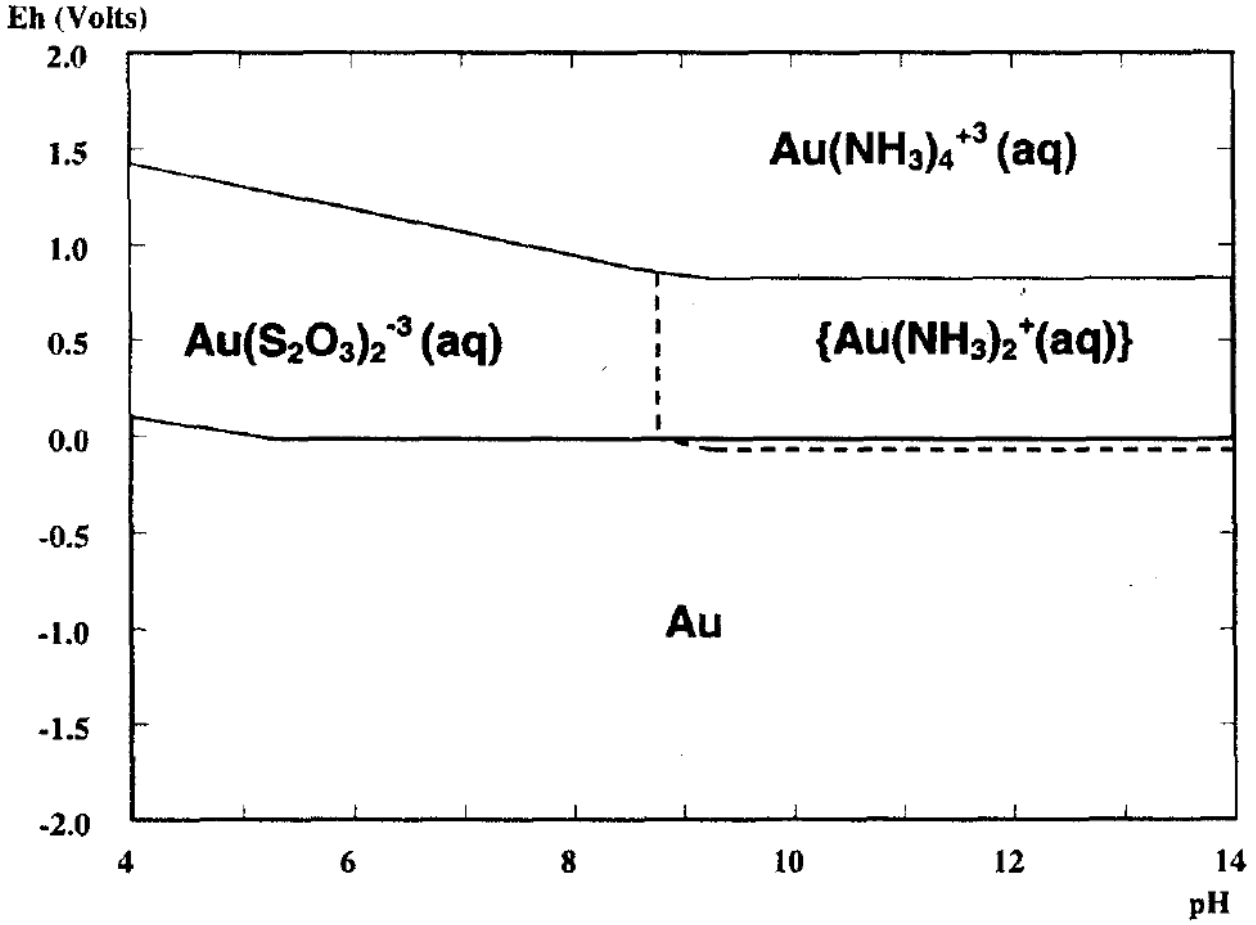

Figure 2-8: Pourbaix diagrams at 5x10^{-4}M Au; 1MS$_2O_3^{2-}$, 1M NH_3/NH_4^+ and 0.05M Cu^{2+}concentrations for a Au-NH_3-$S_2O_3^{2-}$ system (Aylmore et al., 2001).

In Figure 2-8, the stability region shown by the dotted line marks the stability region of $Au(NH_3)_2^+$, where the stability constant, log K= 26.0 (Aylmore et al., 2001; Zipperian et al., 1988).

Figure 2-9 shows that reducing the concentrations of Cu, NH_3 and $S_2O_3^{2-}$ significantly reduces the region of stability for $Cu(S_2O_3)_3^{5-}$ and $Cu(NH_3)_4^{2+}$ while simultaneously increasing the stability region of CuO, Cu_2O and Cu_2S.

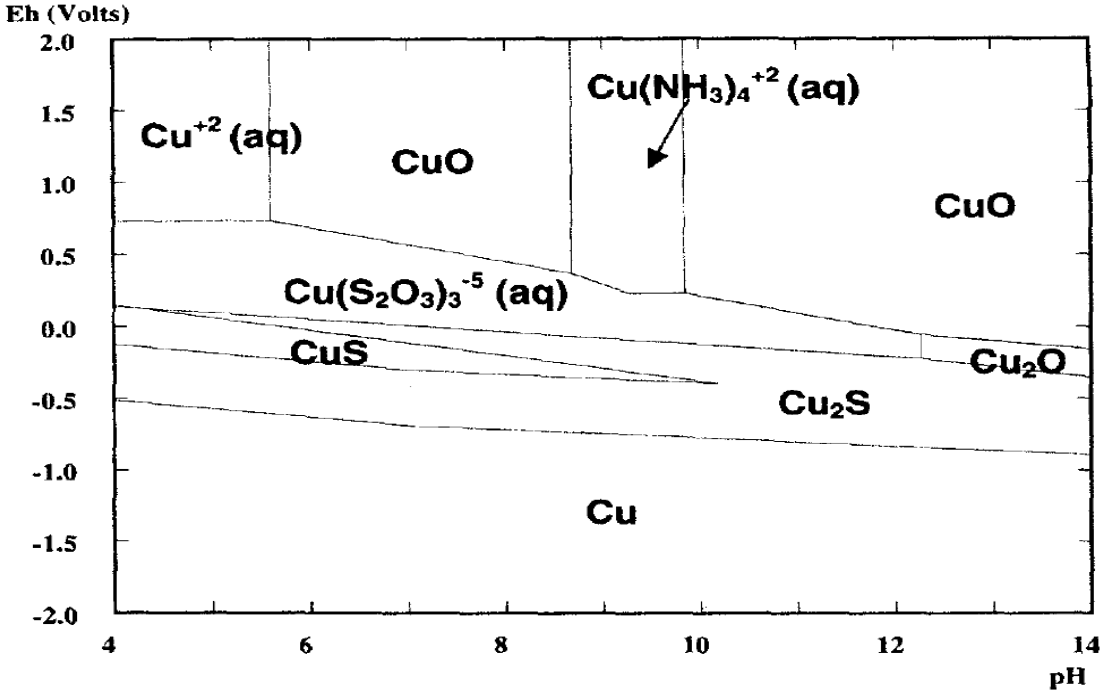

Figure 2-9: Pourbaix diagrams at $5x10^{-4}$M Au; 0.1M$S_2O_3^{2-}$,0.1M NH_3/NH_4^+ and $5x10^{-4}$ M Cu^{2+} for a Cu-NH_3-$S_2O_3^{2-}$ system (Aylmore et al., 2001; Zipperian et al., 1988)

As the concentration of the system changes, so does the stability region of the Au species. pH values also change significantly with a change in NH_3 or $S_2O_3^{2-}$ concentration. When the copper-ammoniacal thiosulphate system potential is too low, Au remains undissolved from pH 0-14 and Cu precipitates out as a sulphide. The Pourbaix diagrams in Figure 2-8 and Figure 2-10 of the Au-NH_3-$S_2O_3^{2-}$ system show that under certain conditions Au could be present in solution as $[Au(NH_3)_2]^+$ instead of $Au(S_2O_3)_2^{3-}$ (Zipperian et al., 1988). The $Au(S_2O_3)_2^{3-}$ complex is the most stable species in the leaching system up to a pH of 8.5 of below 0.01M NH_4^+. Beyond this pH when NH_4^+ converts to NH_3 and when the concentration of NH_3 exceeds 0.1M, the Au exists predominantly as $[Au(NH_3)_2]^+$(Aylmore et al., 2001; Zipperian et al., 1988).

However; above a pH 9, Au rest potential changes with thiosulphate concentration instead of ammonia concentration (Wan et al., 1997). This means that the predominant Au species is $Au(S_2O_3)_2^{3-}$ instead of $[Au(NH_3)_2]^+$. Aylmore et al., (2001) suggest that the variation in thermodynamics and electrochemical studies can be explained by the high activation energy of the formation of $[Au(NH_3)_2]^+$ species. Aylmore et al., (2001) also suggest that the Pourbaix diagrams generated, result in a stable region over the entire pH range for $Au(S_2O_3)_2^{3-}$.

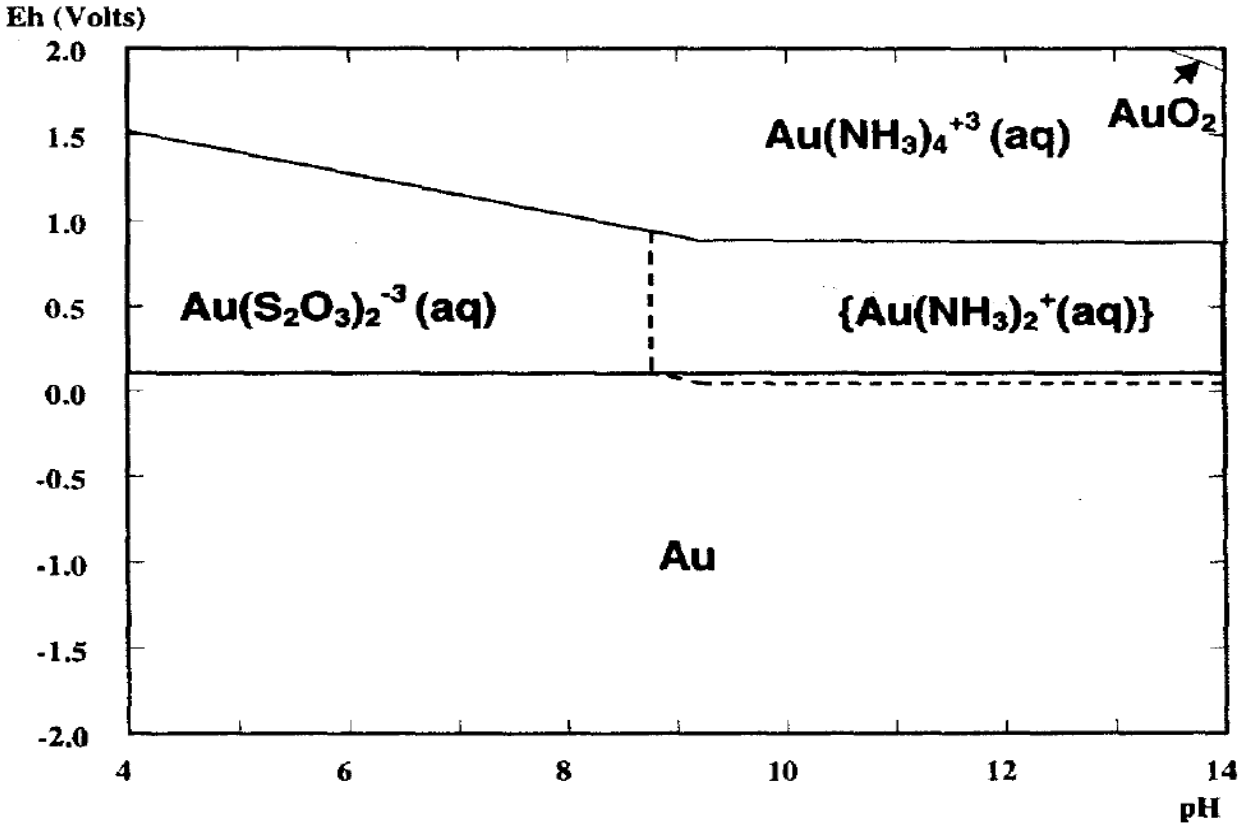

Figure 2-10:Pourbaix diagrams at $5x10^{-4}$M Au; 0.1M$S_2O_3^{2-}$,0.1M NH_3/NH_4^+ and $5x10^{-4}$ M Cu^{2+}concentrations for a Au-NH_3-$S_2O_3^{2-}$ -system (Aylmore et al., (2001) and Zipperian et al., (1988))

In Figure 2-10, the stability region shown by the dotted line, marks the stability region of $Au(NH_3)_2^+$, where the stability constant log K= 26.0 (Aylmore et al., 2001; Zipperian et al., 1988).

2.7.3 Ammonium thiosulphate stability and leaching parameters

Thiosulphate is a metastable anion that easily decomposes chemically in water-based solutions as mentioned earlier. Its stability is affected by several variables, including solution concentration and pH, temperature, the presence of certain metals, the presence of sulphur-metabolizing bacteria, and ultraviolet radiation exposure (Tykodi, 1990).

pH

Figure 2-11 demonstrates that the $S_2O_3^{2-}$, cation exists in the neutral to basic pH range. This suggests that in order to maintain thiosulphate stable in solution under ambient conditions, the solution would

need to be maintained at this range (Aylmore et al., 2001). As previously seen in Eh-pH graphs (Figure 2-7 to Figure 2-10) once produced, the metal thiosulphate complexes are stable throughout a wider pH-Eh range.

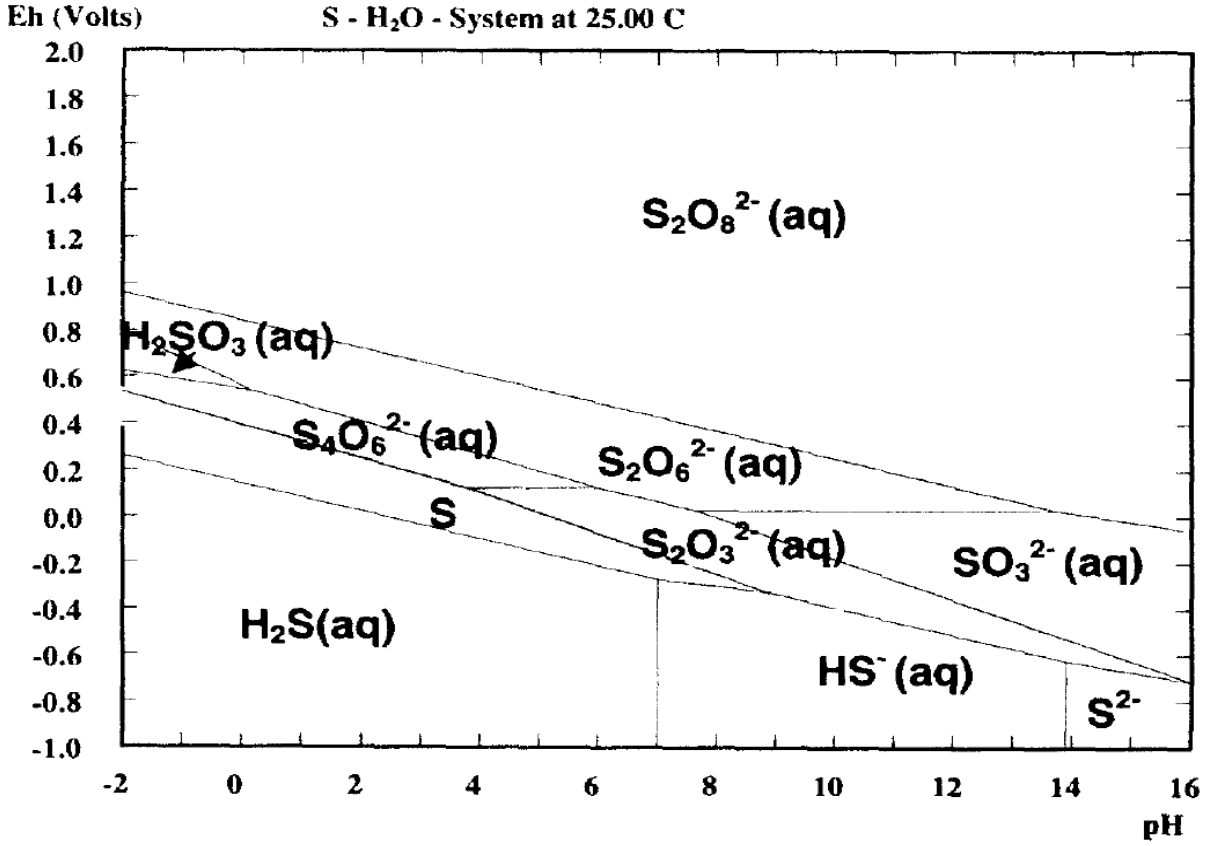

Figure 2-11: Eh-pH diagram for the metastable S-H_2O system with S = 1.0 M., The S-H_2O system without thiosulphate is superimposed to demonstrate how the tetrathionate ($S_2O_6^{2-}$) domain increases (Aylmore et al., 2001)

Thiosulphate oxidizes to tetrathionate between a pH 4 and 6, according to thermodynamics. Else, thiosulphate oxidizes to other sulphur species like $S_2O_6^{2-}$ or SO_3^{2-}. Some of thiosulphate oxidizes to tetrathionate at pH 8 to 10 in the presence of copper and ammonia. The cupric ion facilitates the oxidative decomposition of thiosulphate to tetrathionate (Byerley et al., 1973; Hemmati, 1987).

Numerous metastable sulphur compounds, including sulphite (SO_3^{2-}), thiosulphate ($S_2O_3^{2-}$), polythionates ($S_nO_6^{2-}$), (where 2<n<6) and polysulfides (S_n^{2-}), are reported to exist in alkaline systems (Aylmore et al., 2001). The sulphur-water system is more complex than the metal-water systems because sulphur is multivalent and readily forms sulphur chains and colloidal precipitates. Sulphate is more thermodynamically stable under these leaching conditions (Aylmore et al., 2001).

Effect of thiosulphate concentration

Thiosulphate solutions degrade more quickly in diluted systems (0.01M) than in concentrated ones (>0.1M). However, adding more thiosulfate to a solution will result in more thiosulphate being consumed (Cao et al., 1992). Longer leaching times (such as 24 hours) gradually lower the concentration of thiosulphate in solution, which in turn restricts consumption (Cao et al., 1992).

If there is too much thiosulphate present, it may react with copper to create the $Cu(S_2O_3)_3^{5-}$ specie, which is ineffective for recovering precious metals because copper tetramine complexes are required to dissolve Au (Senanayake, 2007). It is essential to maintain a suitable thiosulphate concentration to achieve higher PMs recoveries and fewer copper dissolutions in the leachates.

Additionally, at higher reagent concentrations, copper sulphide precipitation and accelerated thiosulphate to tetrathionate conversion were previously described when discussing the Pourbaix diagrams. If CuS and sulphur layers begin to form on top of Au particles, it is assumed that dissolving them will become more challenging. It is possible to prevent Au from passivating by adding ammonia, adjusting the Eh-pH levels, and adding oxygen, as mentioned earlier. To ensure that the Au dissolves and the greatest degree of extraction is obtained as soon as possible, it is essential to carry out the leaching procedure with the appropriate quantity of thiosulphate.

Effect of $CuSO_4$ concentration

In previous studies carried out by Abbruzzese et al., (1995), it was discovered that the presence of Cu(II) ions was crucial for accelerating the dissolution of Au in thiosulphate solutions. Under the same Eh/pH conditions, changing the Cu content from 0.03 to 0.06M $CuSO_4$ did not have a significant effect on the dominant copper species in the reaction system. Breuer et al., (2000) also demonstrated that the Au leach rate is independent of the initial copper(II) concentration; the rate at high copper(II) was the same for total copper concentrations of 5mM and 10mM.

However, Au extraction gradually increased after the first hour of leaching up to nearly 80% at high Cu(II) ions concentrations (0.1M $CuSO_4$). The species that is more thermodynamically stable was proven to be the cupric tetra-ammine complex. The stability region of this complex is however shrunk by an excessive increase in Cu(II) concentration (above 0.1M $CuSO_4$), while the stability regions of solid copper compounds like CuO, Cu_2O, CuS, and Cu_2S are widened as shown in section 2.7.2 and respective Pourbaix diagrams for high concentration (Abbruzzese et al., 1995; Breuer et al., 2000).

Effect of ammonia concentration

Abbruzzese et al., (1995) investigated the impact of NH_3 on the leaching of Au by adjusting the NH_3 concentration between 1M and 8M. The concentration of thiosulphate and $CuSO_4$ were kept constant at 2M and 0.1M, respectively. After 3 hours of leaching at a concentration of 4M NH_3, the maximum Au recovery was 78.84%. They observed that, varying the NH_3 content only affects the final Au recovery while the kinetic curve maintains the same form. However, when the ammonia concentration exceeded 4M, lower Au recoveries (less than 10%) were obtained. Raising the ammonia concentration and hence pH actually narrows the regions of thermodynamic stability of $Cu(NH_3)_4^{2+}$ and $Cu(S_2O_3)_3^{5-}$ while enlarging the stability region of precipitates of Cu (CuO and Cu_2O) (Abbruzzese et al., 1995; Aylmore et al., 2001).

Effect of O_2

For additional Au leaching, copper (I) must be converted to copper (II) using oxygen or another oxidant during the thiosulphate rection mechanism covered in section 2.7.1. Byerley et al., (1975) and Byerley et al., (1973) conducted detailed research on the function of oxygen in ammoniacal thiosulphate systems containing copper (II). They showed that rapid oxidation of Cu(I) to Cu(II) and some oxidation of thiosulphate to produce sulphate and tri-thionate depend on the amount of oxygen dispersed in solution. Thiosulphate ions in an aqueous ammonia solution are first oxidized by copper (II) ions to tetrathionate ions in the absence of oxygen and under alkaline conditions (Byerley et al., 1973; Byerley et al., 1975). They later then go through a disproportionation reaction to produce tri-thionate and thiosulphate ions. Thiosulphate ions are necessary for this reaction to be catalysed (Aylmore et al., 2001).

The breakdown of thiosulphate results in the precipitation of copper sulphides at low potentials where oxidants are insufficient, in stagnant solutions, or in solutions with high copper concentrations. As a result, the amount of oxygen in the system affects the precipitation rates and extent of copper sulphides (Byerley et al., 1975). The use of oxygen without the copper catalytic process is very slow and results in low Au dissolution due to the restricted solubility of oxygen in solutions and the sluggish reduction at the Au surface (Aylmore et al., 2001). This means bubbling gas into the lixiviant helps in dispersing it in solution which improves its solubility in the solution.

Temperature

At temperatures between 40 and 60 °C, higher rates of Au dissolution were observed by Zipperian et al., (1988) . In contrast, Abbruzzese et al., (1995) discovered that raising temperature resulted in a 23% reduction in Au extraction. They explained this outcome to be because of passivation by cupric sulphide, which is produced by the thermal interaction of Cu(II) ions with thiosulphate. The drop in extraction might have also been brought on by increased temperature-induced ammonia loss from solution, which would have made the Eh-pH leaching conditions unstable. Additionally, the loss of thiosulphate is also facilitated by the temperature increase from 25 to 60 °C. Although to a lesser extent, thiosulphate breaks down into sulphur compounds by this process (Kerley Jr, 1983). The amount of additional thiosulphate that can still be used for Au complexation is a fraction. Ammonium hydroxide is difficult to keep in solution at temperatures above 60°C (Kerley Jr, 1983).

Solid to liquid ratio

Gámez et al., (2019) revealed that the extraction of Au in the leachate decreases at greater solids content. This occurs as a result of more Au, Cu and other metals being available for the copper tetramine complex and thiosulphate to react with. To increase the solubility of valuable metals, it is therefore best to increase the thiosulphate concentration in high solids concentration during leaching. However, Jeon et al., (2020a) showed that thiosulphate should not be added in excess because doing so will result in a high Cu dissolution rate, which will hinder the dissolution of Au. Gámez et al., (2019) observed a reduction in Au extraction from 79% to 1% after increasing the percentage of solids from 5% to 25%. They also observed that raising the thiosulphate concentration at a high solids concentration only results in increased consumption and lower precious metal recoveries, which will be damaging to the process' economy. Therefore, to obtain an appropriate precious metals dissolution in the leachates, a balance between leaching period, thiosulphate and ammonia concentration, and percentage of solids must be achieved.

2.7.4 Leaching kinetics

Different leaching models can be used to describe the leaching kinetics of solids, for instance Au ores, depending on the composition and morphology of the input material. Different sources indicate that the rate of Au leaching by copper(II)–ammonia–thiosulphate systems is the chemically controlled (Breuer et al., 2000; Ha et al., 2014; Senanayake, 2007). As an example, the chemical reaction

limiting, shrinking particle model, shown on equation (11), can be used to describe the leaching processes (Levenspiel, 1973; Liddell, 2005; Senanayake, 2007).

$$1 - (1 - X)^{\frac{1}{3}} = \left(\frac{bKC}{\rho r}\right) t = \frac{t}{\tau} \quad (11)$$

where;

X = fraction of Au reacted after time, t [s]

b = Stoichiometric factor for surface reaction $A_{(s)} + bB_{aq} \rightarrow products$

K = intrinsic rate constant of surface reaction $[\frac{\mathrm{m}}{\mathrm{s}}]$

C = Reagent concentration $[\frac{\mathrm{mol}}{\mathrm{m}^3}]$

τ = The time required for reaction to reach completion $[s]$

r = Radius of the spherical particle [m]

ρ = Au molar density $[\frac{\mathrm{mol}}{\mathrm{m}^3}]$

Under optimal conditions, the reaction occurs on the particle surface. The surface dissolves gradually as the reaction zone ultimately migrates to the particle's core until it is dissolved completely. However, unlike in the case of ores, containing inert material, the dissolution of Au from PCBs ideally will not generate an unreacted shell (Birich, 2020). Therefore, no additional diffusion layer needs to be considered in the leaching model, the rate of Au leaching is chemically controlled by the reaction occurring at the solid-solution interface.

It is important to note that the shrinking sphere formulation, given by equation 11, assumes the entire particle is leached. This is hardly applicable in the leaching of waste PCBs. The present formulation is for homogeneous spherical particles which only applies for the leaching of broken mineral particles, but not for flat plates of cut or shredded PCBs. This model assumes a fixed particle size and cannot be applied for distributions. In Figure 2-12, Birich, (2020) illustrated that due to the application and structure of Au in waste PCBs, a two-dimensional dissolution reaction occurs at the surface, and the Au dissolution from the edges can be neglected.

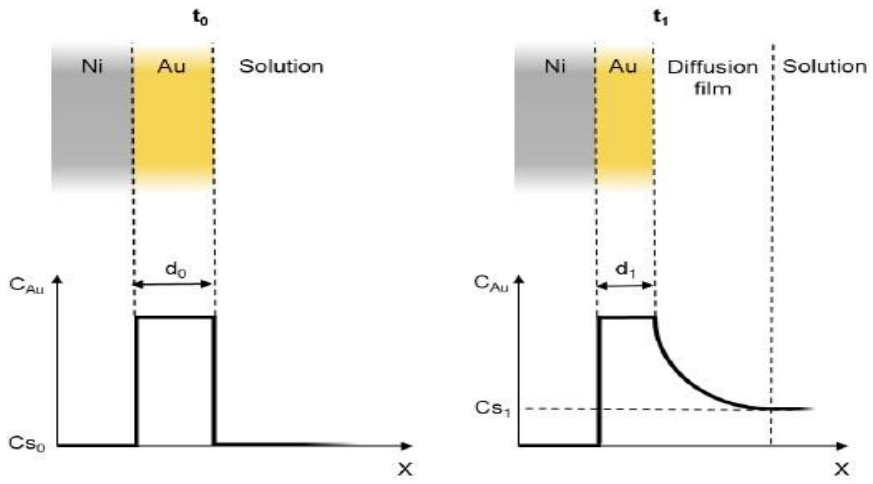

Figure 2-12: A representation of gold concentration gradient for leaching of PCBs ($d_0 > d_1$) adapted from Birich, (2020)

Figure 2-12 illustrates how the Au layer gradually becomes thinner (from t_0 to t_1), while its concentration in solution (from Cs_0 to Cs_1) increases. The products from the leaching reaction, form on the Au surface and diffuse into the solution where the thickness of the Au layer reduces from d_0 to d_1. What is expected in an ideal system is that the dissolution reaction progresses until the Au layer is completely dissolved (where final thickness of the Au layer, $d_{final} = 0$) and the solution is homogenized, however that is not the case for Au dissolution on waste PCBs. Due to its application as covering layer in PCBs, Au is produced as very thin flat plates, henceforth largely, a two-dimensional reaction takes place on the Au surface as previously stated.

Therefore, the concept of spherical particles does not apply, however, Levenspiel, (1973) provided a shrinking particle model extension for flat plates. Equation 11-A applies to a leaching reaction controlled by both film diffusion (diffusion of reactant from the bulk solution to the solid-solution interface) and chemical reaction (at the solid-solution interface). Equation 11-B applies to reactions controlled by ash diffusion (diffusion through the inert solid product) (Levenspiel, 1973).

$$\frac{t}{\tau} = X \qquad (11\text{-A})$$

$$\frac{t}{\tau} = X^2 \qquad (11\text{-B})$$

Since no additional ash layer needs to be considered in the leaching model, only equation 11-A applies.

2.7.5 Reactor sequencing in the thiosulphate leaching of waste PCBs

Most comprehensive studies on thiosulphate-based leaching, concentrate on Au ores. The extraction of Au from e-waste, however, has recently been the subject of studies. Although studies on thiosulphate-based leaching of waste PCBs, are not extensive in terms of depth, there are relevant publications on the subject.

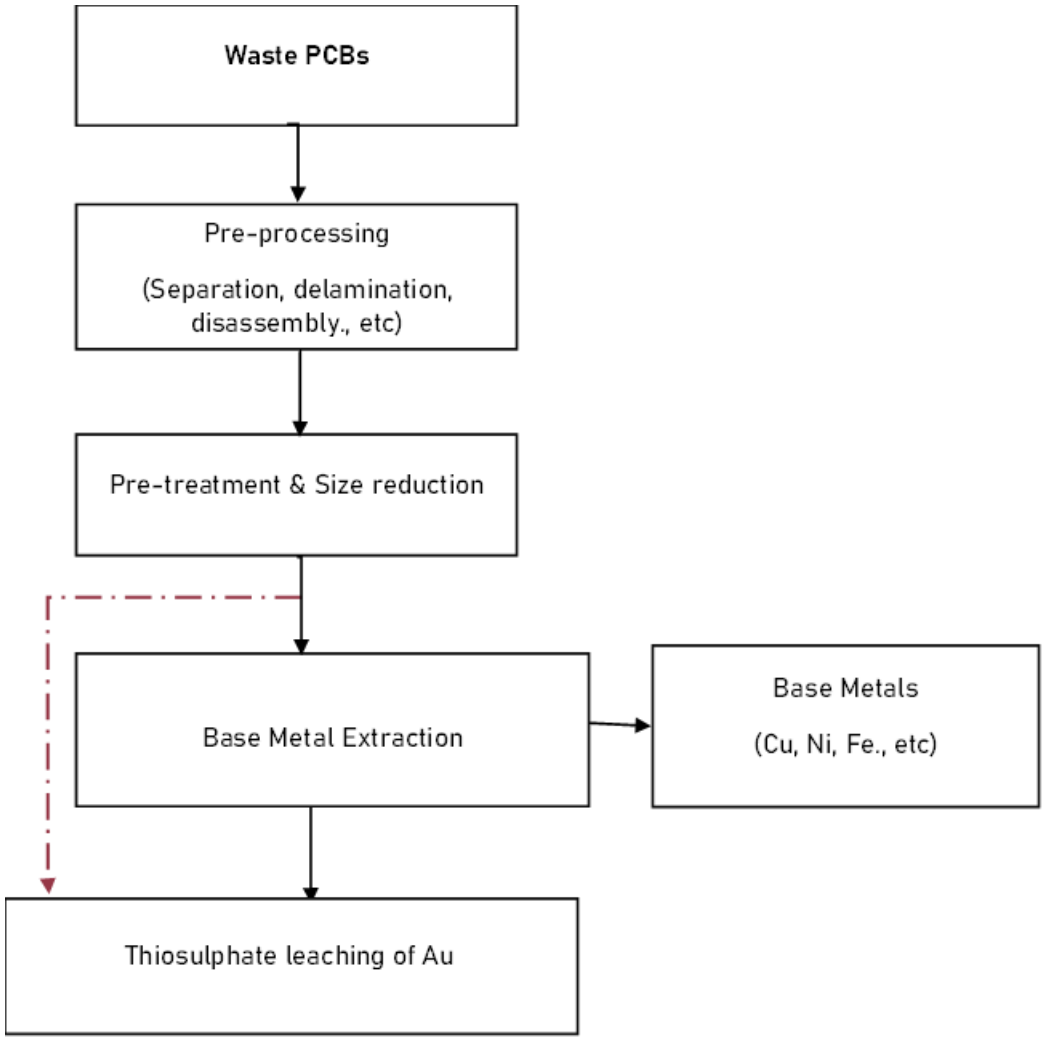

Figure 2-13:Conventional Processing sequence for extraction of Au from PCBs. (The dotted line presents the unconventional route normally applied to High Au content PCBs).

From literature survey in summary there are two research domains. The first domain and more common one, utilised low Au content PCB sources, for example waste PCBs from computers. These first undergo pre-treatment and BM leaching in a bid to extract the Cu and other BMs prior to Au leaching. It is suggested by Veit et al., (2015) that during the dissolution of Cu, the metallic Au on the surface of waste PCBs is entirely inert. The other domain of research (red doted arrow in Figure 2-13)

focused on high Au content sources for example, mobile phones which do not undergo prior leaching of Cu before Au leaching. Figure 2-13 illustrates the 2 domains of research.

This section will concentrate on the work that has been done by employing the conventional leaching sequence, which starts with the prior leaching of BMs and then moves on to the leaching of Au. It will also draw attention to the challenges associated with the sequence. A few of the studies that did not involve Cu extraction from waste PCBs prior to Au leaching will also be discussed in this section. The optimum thiosulphate leaching conditions reported in the reviewed studies are summarized in Table 2-6.

In the study by Petter et al., (2013), waste PCBs from cell phones underwent initial comminution. A 2% recovery was the maximum achieved after leaching the PCB fractions (less than 1mm) with 0.1M $(NH_4)_2S_2O_3$, 0.015M $CuSO_4$ and 0.2M NH_4OH. This, compared to 60% Au obtained by cyanide leaching. This could have resulted from the low thiosulphate concentrations they used. In addition, at the S/L ratio of 50 g/L, the small particle size of the BMs exposed in the leaching system, such as Cu, due to small particle size most likely quickly depleted the low concentration of thiosulphate used.

Using the same leaching conditions, Kasper et al., (2018) managed to extract 75% Au from whole boards that did not undergo any BM extraction (unconventional route). This demonstrates that, mechanical processing of waste PCBs results in a high rate of Au loss. Additionally, grinding exposes other metals that are present on the PCB (such Ni, Cu, etc.). Their surface area in contact with the leaching solution increases as a result, and they compete with the desired reactions of the Au leaching process.

The study done by Gámez et al., (2019) revealed that waste PCB powder with residual 1% copper can be successfully leached using ammonia-thiosulphate solutions for precious metals dissolution. The prior leaching of Cu was carried out using an acid solution of a 4M HNO_3 solution at 40 °C for 6 hours. The amount of HNO_3 consumed was extremely high because it took at least 50 ml of HNO_3 to dissolve Cu (27.2% Cu) in 10 g of waste PCBs leaving a residual of 1.6% Cu. The best thiosulphate leaching conditions were found to be: 5% solids; 0.7M $S_2O_3^{2-}$, pH of 10.5; and 6 hours of stirring at room temperature. These conditions enabled an extraction of 81% for Au in the solution and 32% for Cu. Their method had some shortcomings; when Cu was the target metal, around 5% Au was lost

during HNO_3 leaching. Additionally, during a succession of waste PCB size reductions during the pre-treatment process, more Au was lost.

Ficeriová et al., (2011) also investigated the leaching of Au using 0.5M $(NH_4)_2S_2O_3$, 0.2M $CuSO_4.5H_20$ and 1M NH_3 in a 48-hour period. They looked at how pre-treatment and time affected overall recovery. They concluded that pre-treatment and leaching time are key factors in the extraction of Au from waste PCBs. While the leaching of whole PCBs without any prior pre-treatment and BM extraction yielded only 16% after 48 hours, using the conventional leaching sequence (BM extraction parameters specified in section 2.5, Table 2-4) yielded 98% Au. This was probably caused by particle size difference. The leaching process is accelerated when the particle size is small. Additionally, they stated that the thiosulphate leaching procedure was carried out in a way that permitted the leaching of valuable metals, but they did not detail how this was done. The co-extraction of other BMs was also not specified. The passivation caused by cupric sulphide, created by the thermal interaction between Cu(II) ions and thiosulphate, may have been the cause of the reduced Au recovery at that high temperature (Abbruzzese et al., 1995).

In the investigation conducted by Ha et al., (2010), thiosulphate Au leaching from whole mobile phone waste PCBs produced promising findings. They were able to extract almost 90% of the Au at room temperature using 0.12M $S_2O_3^{2-}$, 20mM Cu(II) and 0.2M ammonia in their solution. Their implementation of the unconventional leaching sequence of Au from waste PCBs produced outcomes that were in conflict with those of Ficeriová et al., (2011). According to Ficeriová et al., (2011), higher thiosulphate concentrations resulted in less extraction. This implies that temperature and/or the S/L ratio used by Ficeriová et al., (2011), may have had an impact on the effectiveness of leaching. Since ammonia has a low vapour pressure, as was previously mentioned in section 2-5, leaching at 40 °C for a prolonged period of 48 hours enhanced the pace of evaporation. Smaller particle sizes and higher temperatures enable faster leaching rates before most of the ammonia is lost. This was confirmed in a study by Cerchier et al., (2017). In their study, higher temperatures of 60°C were used within an hour retention time. Using slightly smaller particles, they obtained an extraction of 80% Au.

On the other hand, Tripathi et al., (2012) used the unconventional sequence on shredded and whole mobile phone waste PCBs with a S/L ratio of 10g/L and achieved of 57% and 78%, Au extraction respectively. This showed a slight decline in Au extraction compared to Ha et al., (2010), on whole PCBs. The difference is that Tripathi did not add ammonia to the leaching solution except the small

amount to correct the pH. As covered in the previous section, ammonia is required as an ingredient as it prevents Au passivation by being preferentially adsorbed on Au surfaces over thiosulphate and is thereby leached as an amine complex (Ha et al., 2010).

Jeon et al., (2020b) conducted a study on crushed waste PCBs using 1M $S_2O_3^{2-}$, 10 mM $CuSO_4$,1 M NH_3 and 0.25 M $(NH_4)_2SO_4$. They showed that a higher concentration of total NH_3 enhances the extraction of Au, as it enhances formation of $Cu(NH_3)_4^{2+}$that catalyzes Au extraction. Above concentration of 1M NH_3 the extraction of Au decreased. Oxygen was also shown to be a critical parameter that affects Au extraction. Although the total oxygen introduced into the leaching system was not specified.

In another study, Albertyn, (2017) looked at the extraction of Au and Ag by leaching from waste PCBs using $(NH_4)_2S_2O_3$. This study was a continuation of the work done by Ficeriová et al., (2011); however, the extraction was slightly lower in this investigation. They stated that the low Au extraction was due to thiosulphate consumption brought on by the high Cu content in the feed material. However, the usage of low concentrations of $(NH_4)_2S_2O_3$ and NH_3 may have significantly contributed to this. At a pH of 9–9.5 and a temperature of 25°C, a maximum Au extraction of 78.5%, was achieved using 0.2M thiosulphate, 0.4M ammonia, 0.02M cupric ions on the leach residue from the first stage of BM leaching. The most important parameter affecting Au leaching was identified to be the $(NH_4)_2S_2O_3$ to NH_3 ratio.

Similarly, Tanisali et al., (2021) also extracted Cu and Au using the conventional process via a two-stage leaching process. More than 92% of the copper was successfully recovered from the base metal leaching under optimal conditions. During the precious metal leaching step, 59 % Au was extracted in 8 hours using 0.2M $S_2O_3^{2-}$, 0.02M $CuSO_4$, and 0.2M $NH_3.H_2O$. Comparably to (Albertyn, 2017), it was found that an excess of Cu ions in the solution is what led to the reduced the rate at which Au dissolved. The key parameters that influence metal extractiom were identified as particle size and leaching period.

Despite attaining substantial recoveries of Cu due to the pre-treatment processes Birich, (2020); Birloaga et al., (2013) and Kaya, (2019) found that during pre-treatment, around 50% of precious metals, including Au, are lost through the plastic and particle streams. After combining shredding and soaking, Chirume, (2019) and Prestele, (2020) reported low Cu recoveries, indicating that the remaining Cu unrecovered is likely to proceed on to the following Au leaching stage. Furthermore,

Kasper et al., (2018) demonstrated that, milling releases BMs (Ni, Cu, etc.) present on the PCB, thereby increasing their contact area with the leaching solution thus competing with the desired reactions of the Au leaching.

A trade-off must be made between pre-processing waste PCBs to unlock Cu and avoiding size reduction to improve Au extraction since Au is found in the external layers. Another solution could be to extract Au before shredding and grinding, after which Cu can be rapidly extracted from shredded and soaked waste PCB to improve Prestele, (2020)'s efficiency. That said, the present study is a continuation of the studies done by Chirume, (2019) and (Prestele, 2020), with the focus shifting to Au leaching in the next leaching sequence.

During the Au leaching stage, many studies focus on one or two target metals (for instance Au and/or Ag). Most research methods focus on improving pre-treatment to enhance the prior leaching of Cu whilst neglecting research on early-stage Au extraction prior to Cu leaching on waste PCBs.
However, most studies have neglected the investigation of different Au leaching pathways (through thiosulphate leaching) with a view to maximize Au extraction while studying the coextraction of BMs and the effects they might have on Au extraction. This is especially relevant for Cu, which, as described in the literature, has a negative effect on the leaching process by degrading thiosulphate.
Investigating the optimal reactor sequencing, that maximizes the extraction of Au from waste PCBs, is the focus of this project. Additionally, it will examine and contrast the coextraction of BMs (Cu and Ni) in the sequences under study as well as how it impacts the Au extraction efficiency.

2.7.6 Summary of previous results

The thiosulphate concentration must be kept under control in order to maintain an appropriate ratio between the concentrations of thiosulphate and ammonium for the Cu to act as a catalyst in the fluctuation between the cuprous and cupric states (Kasper et al., (2018). Additionally, Breuer et al., (2002) Breuer et al., (2000) Grosse et al., (2003) Senanayake, (2005) and Sayiner et al., (2014) all show that by maintaining the appropriate concentration for thiosulphate, ammonium, copper, and oxygen concentrations, Au can be extracted effectively under the right temperature and pH. Although most authors selected and presented in Table 2-6 do not agree on the optimal leaching conditions, there is a particular range that they obtained. The concentrations of thiosulphate, and NH_3 all range from (0.1-1)M, and (0.2-2)M. The S/L ratio ranges from 10g/L to 150g/L. However, for $CuSO_4$

concentration, temperature, and pH they all seem to agree that the optimal values are 0.02M, 25°C and 9-10.5, respectively. They also seem to agree that the optimal ratio of $NH_3/S_2O_3^{2-}$ ratio is 2. The residence time varies, but most studies agree on 8 hours. The agitation speed is not specified in most studies. Optimizing the leaching conditions is necessary to allow the recovery of Au by ammonium thiosulphate from PCBs to be economically viable. In this study, various leaching parameters, namely the impact of $(NH_4)_2S_2O_3$ and NH_3 concentrations, and S/L ratio, will be investigated while maintaining other parameters constant. The NH_3, $S_2O_3^{2-}$ and S/L ratio levels that will be optimised will be (0.5 and 1)M, (0.25 and 0.5)M, and (50 and 100) g/L , respectively. All other parameters shall be kept constant at values specified in Chapter 3.

Table 2-6: Summary of optimal leaching conditions implemented by different authors on different PCBs for Au extraction from waste PCBs.

Source	**Lixiviant**	**pH**	**Type of waste PCB and Particle size**	**T ℃**	**S/L ratio**	**Agitation**	**Residence Time (Hours)**	**% Extraction**
(Petter et al., 2013)	0.1M $S_2O_3^{2-}$, 0.015M $CuSO_4$ and 0.2M NH_4OH	9-10	(Cell phone PCBs), milled to < 1mm	25 ± 2	50g/L	Not specified	4	2% Au
(Tripathi et al., 2012)	0.1M $S_2O_3^{2-}$ and 0.4M $CuSO_4$	10-10.5	Cut PCBs	25	10g/L	250rpm	8	57% Au
			Whole PCBs					79% Au
(Gámez et al., 2019)	0.7M $S_2O_3^{2-}$ 28% NaOH	10.5	(Cell phone PCBs), Roasted and pulverized to 97 µm.	Room Temperature	50g/L	700 rpm	6	81% Au 30% Cu
(Ficeriová et al., 2011)	0.5M $S_2O_3^{2-}$ 0.02M $CuSO_4.5H_20$ and 1M NH_3	9	Crushed PCBs to 800 µm.	40	~90g/L	$8.33s^{-1}$	48	98% Au
			Whole PCBs					16% Au
(Ha et al., 2014)	0.12M $S_2O_3^{2-}$, 0.02M $CuSO_4$ and 0.2M NH_3	10-10.5	Cell phone and scrap PCBs. whole	25	67gl	200rpm	10	90% Au
(Jeon et al., 2020a)	1M $S_2O_3^{2-}$, 1M NH_3, and 10mM $CuSO_4$	-	Crushed PCBs 85 µm.	25	10g/L	10g/L	24	>99% Au
(Kasper et al., 2018)	0.12M $S_2O_3^{2-}$, 0.02M $CuSO_4$ and 0.2M NH_3	-	Cell phone and scrap PCBs. whole	25 ± 2	40g/L	Not specified	4	75% Au
(Tanisali et al., 2021)	0.2M $S_2O_3^{2-}$, 0.02M $CuSO_4$, and 0.2M $NH_3.H_2O$, .	-	Crushed PCBs	25	50g/L	Not specified	8	59% Au
(Cerchier et al., 2017)	1M $S_2O_3^{2-}$, 2M of NH_3 and 0.1mM of $CuSO_4$	>10	Cell phone crushed to <2 mm	65	150g/L	Not specified	1	80% Au
(Albertyn, 2017)	0.2M $S_2O_3^{2-}$, 0.4M NH_3 and 0.02M $CuSO_4$	9-9.5	Computer PCBs < 2mm	25	25g/L	500rpm	8	78.5 Au

3. METHODOLOGY

Outline of methodology

The structure of this chapter is in line with each objective. The set of steps followed to fulfil these objectives are provided below.

1. ***To investigate the effect of background Cu and Ni in the dissolution of Au from waste PCBs within an ammonium thiosulphate leaching system.***

Steps taken:

i. Head grade analysis performed Aqua Regia Leach and microwave assisted digestion for targeted metals, Au, Cu, Ni , and Sn.

ii. Au dissolution from PCBs was simulated using Au leaf as a proxy while background Cu and Ni concentrations were introduced in a controlled manner, as determined by the head grade analysis.

2. ***To investigate and select the reactor sequencing in an ammonium thiosulphate leaching system that maximizes the amount of Au extracted from PCBs.***

Steps taken:

Experimentally testing of the conventional Au leaching sequence.

i. Au leaching of the cut and shredded PCBs without any prior leaching of Cu and Ni, using ammonium thiosulphate.

Experimentally testing the conventional Au leaching sequence.

ii. Ammonium sulphate was used in the prior leaching of Cu and Ni from cut and shredded PCBs.

iii. Au leaching of the cut and shredded PCB residues from (i) using ammonium thiosulphate.

3. ***Use the best reactor sequencing obtained from (2) to optimize Au extraction from PCBs over a selected range of parameters.***

i. Using the full factorial design to optimize NH_3, $S_2O_3^{2-}$and S/L ratio, in the levels of (0.5 and 1)M, (0.25 and 0.5)M, and (50 and 100) g/L, respectively, while employing the optimal reactor sequence obtained from (2).

4. ***To benchmark the optimal leaching of PCBs in ammonium thiosulphate obtained in (3) with the leaching of Au from PCBs using cyanide.***

i. Au leaching of PCB's using cyanide is performed using the best reactor sequencing from (2).

3.1 Investigation of the effect of Cu and Ni in the dissolution of Au from waste PCBs within an ammonium thiosulphate leaching system

3.1.1 Materials-custom-tailored PCBs

Literature identifies extreme inhomogeneity as an essential problem with waste PCBs (Hageluken, 2006; Kasper et al., 2018). Waste PCBs vary in composition as demonstrated in Table 2-1 in the previous chapter. Although homogenisation can be improved with milling a sample to fine powder, it comes with the following previously sited drawbacks;

ii. loss of valuable metals

iii. liberation of Cu and other BM into the leaching solution.

To overcome this, the PCBs that were used throughout this research were made to order by Trax Interconnect (Pty) Ltd. This means that, the same design, composition, and quality was maintained for each board. This ensures reproducibility and precision in the comparison of the experimental data instead of waste PCBs that may have different composition. These are not populated (all components are omitted from design) since doing so would make the metal extraction process more difficult. Figure 3-1 shows the front and back faces of the sample PCB used in this study. The PCBs are a representation of the basic design that is normally requested by the company's customers.

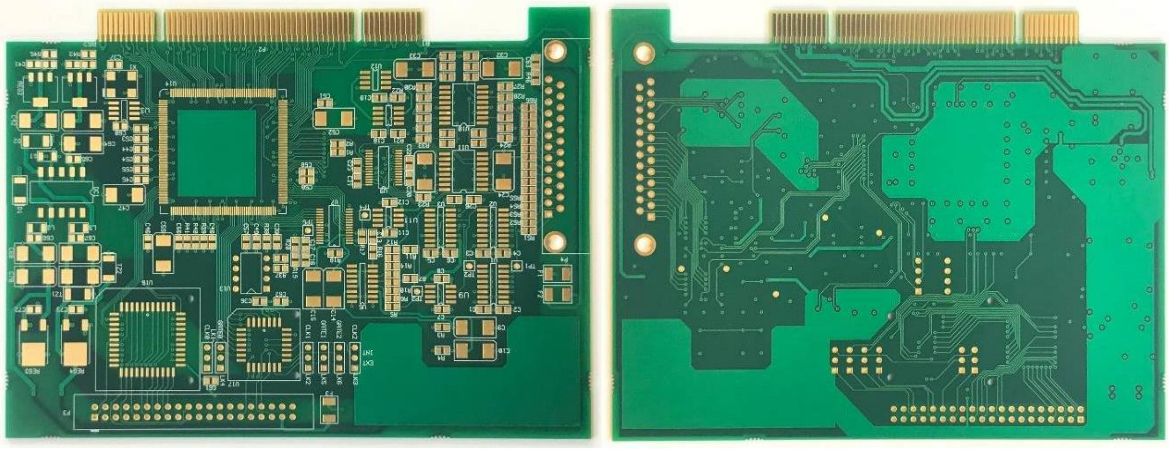

Figure 3-1: Custom made PCB Left - Top side of the PCB; Right - Bottom side of the same PCB.

Each PCB is a four-layered FR-4 (fibreglass with epoxy resin) core board, weighing approximately 52 g. Each of four layers comprise of a laminate of FR-4 inner core sandwiched by two copper foils that are 17 μm in thickness. It has the dimensions; 142×102×1,63 mm. What connects the

inner layers to the outer layers is the pre-preg (uncured FR-4 resin) which cures when the layers are combined.

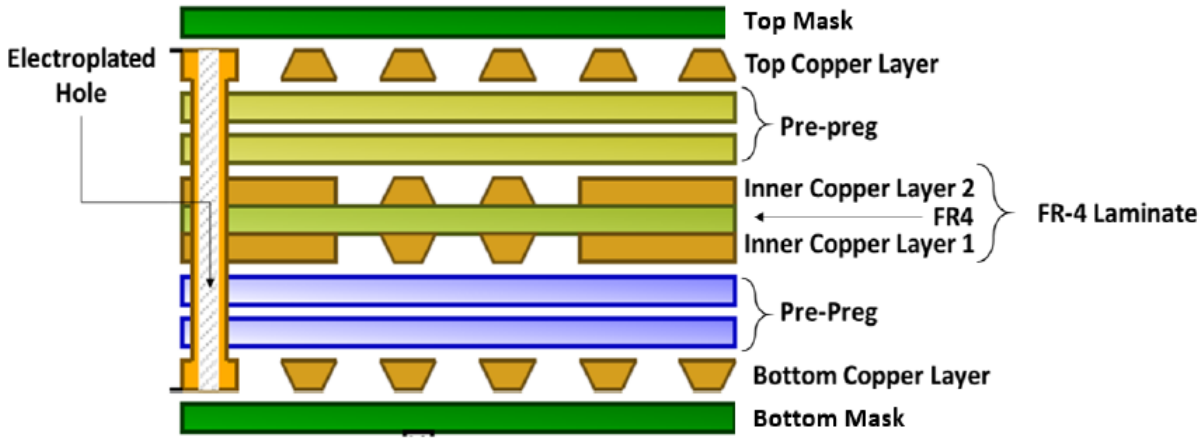

Figure 3-2:Cross-Sectional Schematic of the PCB (Moyo et al., 2020)

As briefly mentioned in section 2.2 of chapter 2, Au is solely found on the vias and upper and lower part of the board as shown in Figure 3-1, as an alloy of Au and Ni. Vias are electroplated holes, connecting the copper layers in a PCB. Furthermore, according to morphological investigations conducted by Ha et al., (2014) , the exterior layers of the Au-nickel alloy contain 90% of the Au. Through the 3D analysis of the PCBs, Chirume, (2019) revealed that about 69% of the Cu lies on the inner layers. Therefore, if the top and bottom masks are removed, only around 31% of the Cu layers are exposed, according to this assertion. The remaining Cu (69%) remains buried beneath the FR-4 and is inaccessible to the lixiviant.

During the PCB manufacturing process, Ni is electroplated onto the surface of Cu and Au is then electroplated onto the Ni, forming an Au-Ni alloy which serves to protect the Cu from oxidation and improves electrical conductivity (Chirume, 2019; Moyo et al., 2020). The percentage content of Au, Cu and Ni of the PCB was determined using the head grade analysis procedure, outlined in 3.1.2. The results are presented in chapter 4. Other than PCBs, the materials that were used include:

1 3M of 55% of HNO_3 and 1M of 32% HCl solution
2 Hot plate magnetic stirrers
3 Thermometer (20 to 110)°C
4 Customised industrial grab shredder
5 Rotary micro-riffler splitter
6 Oven

7 0.2 µm syringe-driven membrane filters

3.1.2 Head grade analysis using reverse aqua regia and aqua regia digestion

This stage's objective was to analyse and estimate the PCBs' average metal concentration using Aqua Regia digestion. The metals examined were Au, Cu, Ni, and Sn. A variety of samples collected at the following times underwent aqua regia digestions:

i. After PCB size reduction and charring method, to ascertain the initial metal content (Head grade of the PCBs).
ii. Analysing the amount of Au in the Au leaf utilized in simulated experiments.
iii. After the final Au leaching stage, to complete mass balances (on leach residues).

The proportional concentrations of elemental Cu and Ni to be introduced to elemental Au in simulation tests were likewise determined using the head grade.

PCB size reduction, charring and the leaching process

Each sample was prepared by shredding a PCB using industrial grab shredder. The shredded pieces were then pulverised in a ring mill for a total of 3 minutes to generate fine powder. Figure 3-3 (a) and (b) illustrates each process.

Figure 3-3: (a) Shredded PCB (b) PCB powder product after Pulverisation (c)Splitting process.

Each powdered PCB was then split into 8 equal portions, using a rotary micro-riffler splitter shown in Figure 3-3 (c). Each split sample weighed 5.75 ± 0.22 g. For each 8-way split of an individual

PCB, 2 samples were combined resulting in each PCB making 4 samples of 11.53 g; 11.36 g; 11.41 g and 11.42 g.

All experiments, involving the acid preparation and leaching, were set up in a fume hood. Reverse aqua regia solutions were prepared by mixing 11.7M HNO_3 and 10M HCl in the molar ratio of 5:1, respectively. The aqua regia solutions were prepared by mixing the two acids in the ratio 1:3, respectively. A solid liquid ratio of 10 g/L was used for all experiments. Leaching was done in 1L beakers, with each beaker set on a hot plate coupled with a stirrer. To regulate the temperature of the leaching system and make sure it was kept between a range of 60 ± 5 ℃, each beaker was equipped with a thermometer (Jeon et al., 2018; Kasper et al., 2018). The mixtures of the PCB powder and reverse aqua regia were mildly stirred at 300 rpm. After 4 hours the hot plate was switched off while stirring was maintained for 20 hours.

After a total of 24 hours, 10 ml aliquots were then extracted. They were then filtered through 0.2 µm syringe-driven membrane filters and taken for analysis using a MP-AES. The leached residue was washed, filtered out and air dried. After drying, the residue was then subjected to a second, similar leaching procedure except using aqua regia as the lixiviant. A second batch of aliquots were extracted and taken for analysis using an MP-AES while the solid residues were dried and taken for microwave assisted digestion.

Out of concern for incomplete acid digestion of the organics, a special charring method was used to remove combustibles without volatilization of the metals (Jeon et al., 2018). Fresh samples (pulverised and split PCBs) were charred in an oven at 250 °C, in 30ml ceramic crucibles, for 2 hours to burn of and hence reduce the organic content of the sample. The resulting ash is shown in Figure 3-4.

The resulting 4 samples each weighed 9.22 g; 9.36 g; 9.41 g and 9.95 g. The samples underwent the same leaching procedures with reverse aqua regia and aqua Regia. 10 ml aliquots were each extracted from both procedures and taken for analysis using an MP-AES while the solid samples were dried and analysed using microwave assisted digestion.

Figure 3-4: Samples of PCB ash after charring

3.1.3 Ammonium thiosulphate leaching simulation experiments; Au leaf in the presence of elemental Ni and Cu

Materials

1 23 carat Au leaf, 99.99% Ni foil and 99.99% Cu metal powder

2 ammonium hydroxide liquid (NH_4OH) (30-33% NH_3 in H_2O)

3 98% ammonium thiosulphate powder $(NH_4)_2S_2O_3$

4 99% copper(II) sulphate pentahydrate powder ($CuSO_4.5H_2O$)

5 Bottle roller and three 2 L Schott bottles used as reactors

6 Air rotameter

7 pH meter

Au dissolution from PCBs was simulated by using 23 carat Au leaf as a proxy in $(NH_4)_2S_2O_3$. These baseline studies were conducted to eliminate the uncontrolled interference that would come from co-dissolving metals from PCBs. Instead, these metals (Ni and Cu) were introduced at set/controlled concentrations and their effect on Au dissolution was monitored. In all experiments, $(NH_4)_2S_2O_3$ was used as the lixiviant and cyanide was then used to evaluate this process.

The aqua regia leaching procedure used in section 3.1.2 was used to confirm the Au content on the Au leaf. Due to the purity of the Au leaf, a one-step leaching process using aqua regia was employed in this instance. The Au content of the 23 carat Au, each leaf weighing an average of 0.015 g, was confirmed to be 93,15% (see Table 8-3 in section 8.2.1 in the APPENDICES).

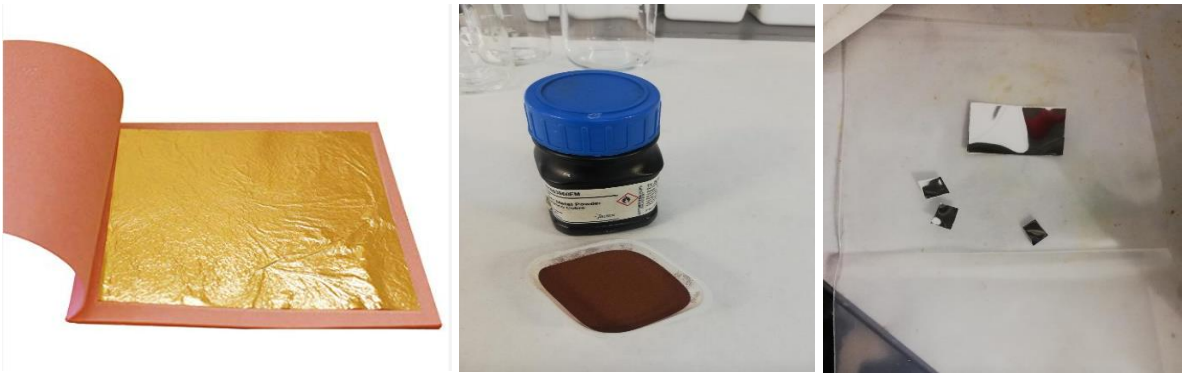

Figure 3-5: (a) 23 carat Au leaf, 93.15% Au (b) 99.99% Cu metal (c) 99.99% Ni foil

Figure 3-5 shows the proxy metals used in the simulation tests. The amount of background metallic Cu and Ni supplied into the synthetic Au leaching system was proportional to the metal content determined in section 3.1.2, as was previously mentioned.

The ammoniacal $(NH_4)_2S_2O_3$ lixiviant was prepared by mixing 1M NH_3, 0.5M $(NH_4)_2S_2O_3$ and 40mM of ($CuSO_4.5H_2O$) in a 2 L volumetric flask. The solution that resulted, was filled up to the mark of the volumetric flask with deionized water and mixed thoroughly using a magnetic stirrer until all the crystals were completely dissolved. A 500ml lixiviant was then poured into three 2 L Schott bottles. In the first run, 0.015 g Au-leaf was transferred into in each bottle. These bottles were then placed on a bottle roller with constant mixing set at 300 rpm, temperature at 25 ℃ and, the starting time was recorded. Compressed air was bubbled to provide sufficient dissolved oxygen into the reaction system. The Au leaf was leached in ammonium thiosulphate without interference from any background Ni and Cu. The reactor setup is shown in Figure 3-8 and its description in 3.2.3

In the second run, 100% and 31% of metallic Ni and Cu, respectively (proportional to the percentage of total mass of Ni and Cu in head-grade), were introduced into the leaching system alongside 0.015 g Au leaf. Per Au leaf (15.41 mg) containing 14.34 mg Au, 11501.50 mg Cu and 518.5 mg Ni were introduced (see Table 8-4 in the APPENDICES). It is essential to note that these concentrations used in the simulation are in line with what was found in literature, that unlike Au and Ni, approximately 31% Cu is leachable from the PCBs as previously stated in 3.1.1 (Chirume,

2019; Moyo et al., 2020). The experiment ran for 24 hours and was repeated three times for each set of reaction conditions. 5ml samples were taken at 0, 0.5, 1, 2, 5, 8, 9, 20, 24 and 30 hours. pH was monitored and observed to remain within the desired range of 10-10.5. Table 3-1 summarizes the leaching conditions obtained from literature in section 2.7.6. The sampled solutions were filtered through 0.2 µm syringe-driven membrane filters analysed for dissolved Au, Ni and Cu using the MP-AES.

Table 3-1: Simulation leaching parameters.

Parameter	**Roller Conditions**
30-33% NH_3 in H_2O concentration	1M
99% $(NH_4)_2S_2O_3$ powder concentration	0.5M
99% $CuSO_4.5H_2O$ concentration	40mM
Au leaf	0.015 g (14.34 mg Au)
Cu	(0 and 11501.50) mg Cu
Ni	(0 and 518.5) mg Ni
Temperature	25 ±2℃
pH	10.4
Agitation	300 rpm
Compressed air	0.1 L/min
Volume of lixiviant	500 ml
Residence time	30 hours

3.2 To Investigate and select the reactor sequencing in an ammonium thiosulphate leaching system that maximizes the amount of Au extracted from waste PCBs

As described in section 2.7.5, the following reactor sequencing strategies, summarized in Figure 3-6, were examined with the goal of choosing one that yields the maximum Au extraction during the thiosulphate leaching stage.

A. Sequence A- unconventional sequence where the PCBs are cut and then immediately move on to the Au leaching stage.
B. Sequence B- Similar to sequence (A) except in this instance the PCBs are shredded instead of being cut.

C. Sequence C- conventional sequence where the PCBs are cut and undergo BM extraction prior to the Au leaching stage.
D. Sequence D- Similar to sequence (C) except in this instance the PCBs are shredded instead of being cut.

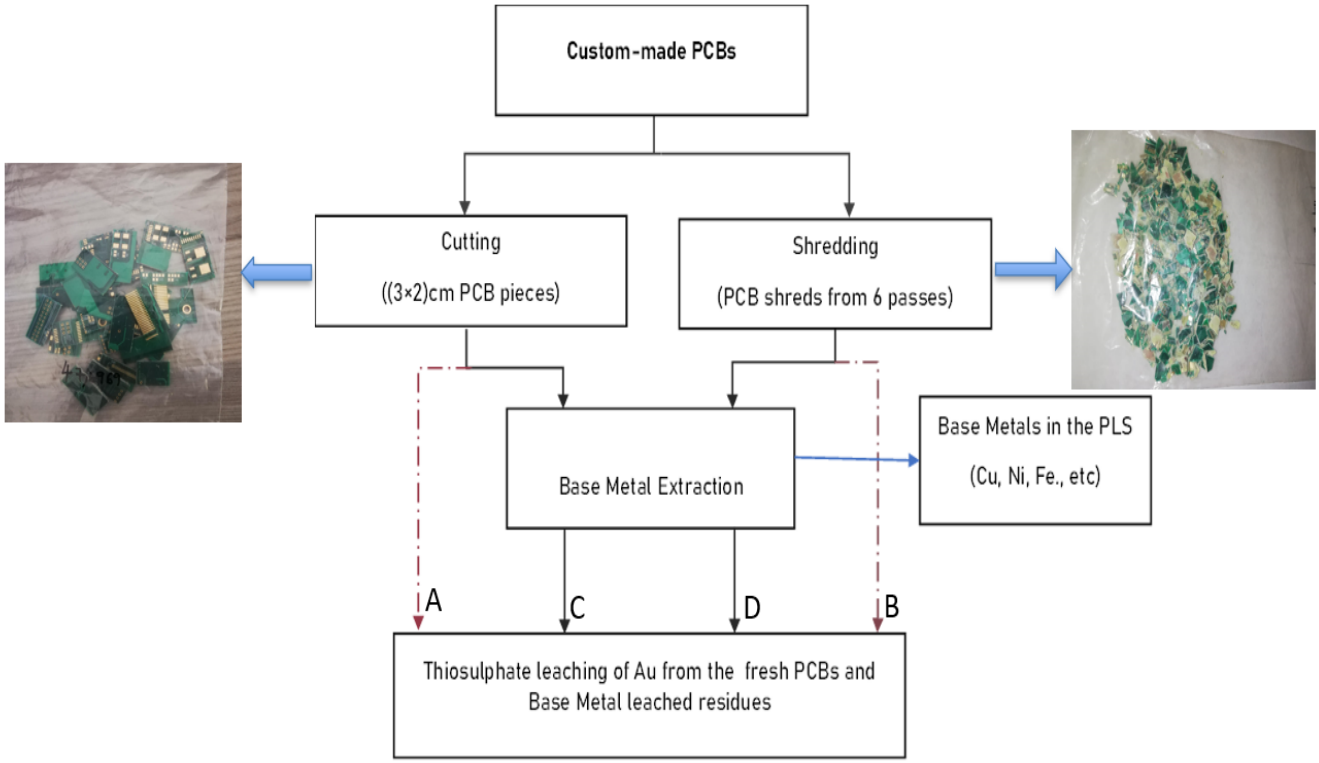

Figure 3-6:Schematic of the reactor sequencing approaches investigated in this report. The red dotted lines (from far left to far right) present the unconventional sequence (A) and (B) respectively while the other two solid lines (left to right) present sequence (C) and (D).

Figure 3-6 shows a more detailed version of Figure 2-13 which illustrates the reactor sequencing strategies investigated in this study. The red dotted lines (from far left to far right) present the unconventional sequence (A) and (B) respectively while the other two solid lines (left to right) present sequence (C) and (D).

3.2.1 Pre-treatment in the form of particle size reduction

It is important to note that the preferred size for sequence (A) and (C) were whole PCBs without any size reduction. This is because Petter et al., (2013) and Ha et al., (2010) showed that mechanical processing of waste PCBs results in a high rate of Au loss. However, for purpose of being able to fit the PCBs into reactors, each PCB was weighed and then cut using a BS-200 bandsaw. After reducing the PCBs to a 2cm x 2cm size, Chirume, (2019) was able to preserve

roughly the entire PCB mass. Even fewer losses were expected to occur with a particle size of 3 cm x 2 cm, which was ultimately adopted. Prior to being shredded by the same grab shredder as in 3.1.2, the other set of PCBs were all weighed individually. The shredding approach was informed by the work of Prestele, (2020), who explained that it produces good Cu extractions during BM leaching by ammoniacal solutions while resulting in little losses compared to other pre-treatment procedures. The two kinds of pre-treated PCBs employed in the experiments are depicted in Figure 3-7.

Figure 3-7:(a) PCBs cut into 3cm x 2cm Pieces *(b) PCBs after 6 cycles of shredding.*

3.2.2 Cu leaching tests

For sequencing (C) and (D), pre-treatment was followed by a Cu leaching stage using $(NH_4)_2SO_4$. Although the leach solution was analysed for extracted metals Au, Cu, and Ni the product of interest were the leached PCB residues. This sequence was closed off by a Au leaching stage, whereby the PCB residues were leached using ammonium thiosulphate.

Materials

1 NH_4OH liquid (30-33% NH_3 in H_2O)

2 98% $(NH_4)_2SO_4$ powder

3 99% copper(II) sulphate pentahydrate powder ($CuSO_4.5H_2O$)

4 Bottle roller and three 2 L Schott bottles used as reactors

5 Air rotameter

6 pH meter

The leaching method

Section 2.5.1 showed that an ammonia-ammonium sulphate (NH_3^+ - NH_4^+) system is effective for BMs extraction, especially for Cu extraction (Bari et al., 2009; Chirume, 2019; Rudnik et al., 2016) It was therefore selected for Cu extraction. The lixiviant was prepared by dissolving 2M $(NH_4)_2SO_4$, 4M of NH_3 solution and 100 ppm $CuSO_4{\cdot}5H_2O$ in a 2 L volumetric flask. The resulting solution was filled up to the mark of the volumetric flask with deionized water and mixed using a magnetic stirrer until all the crystals were dissolved completely.

The bottle roller temperature was set at 25°C for the first run, and each PCB (cut) was put into a 2 L Schott bottle (three Schott reactor bottles ran concurrently in each run). Each 2 L Schott bottle was then filled with 750 ml of lixiviant. The commencement time was then recorded before the bottles were put on a bottle roller with constant mixing set to 250 rpm. To ensure that the reaction system had enough dissolved oxygen, compressed air was bubbled into the reactor.

Table 3-2:Experimental parameters employed in this investigation for the dissolution of BMs from PCBs.

Parameter	**Conditions**	
30-33% NH_3 in H_2O concentration	4M	
98% $(NH_4)_2SO_4$ concentration	2M	
99% $CuSO_4.5H_2O$ concentration	1mM	
Temperature	25 ˚C ±2℃	
pH	10.5	
Compressed Air flow	0.1 L/min	
Agitation	250 rpm	
Volume of lixiviant	750 ml	
Time	72 hours	
Solid/Liquid ratio	~65 g/L (1 PCB per 0.75 L)	
PCB size	Shreds	3cm x 2cm pieces

5ml samples were taken at 0, 1.5, 3.5, 6, 9, 24, 27, 48, and 72 hours. The aliquots were filtered through 0.2 µm syringe-driven membrane filters before being taken for analysis using an MPAES. The loss in solution volume caused by sampling was accounted for by adding the initial lixiviant solution. The pH of each sample was measured and recorded. The product of interest, the leached (PCBs) residue, was filtered off the leachate using a Whatman 40 filter paper. The residues were then air dried for 24 hours before being leached for Au. The process was repeated for the PCBs that had been shredded.

3.2.3 Thiosulphate leaching of Au from the fresh PCBs and Cu leach residues

The ammoniacal, $(NH_4)_2S_2O_3$ lixiviant was prepared by mixing 1M NH_3, 0.5M $(NH_4)_2S_2O_3$ and 40mM $CuSO_4.5H_2O$ in a 2 L volumetric flask. The resulting solution was filled up to the 2 L mark of the volumetric flask with deionized water and mixed thoroughly.

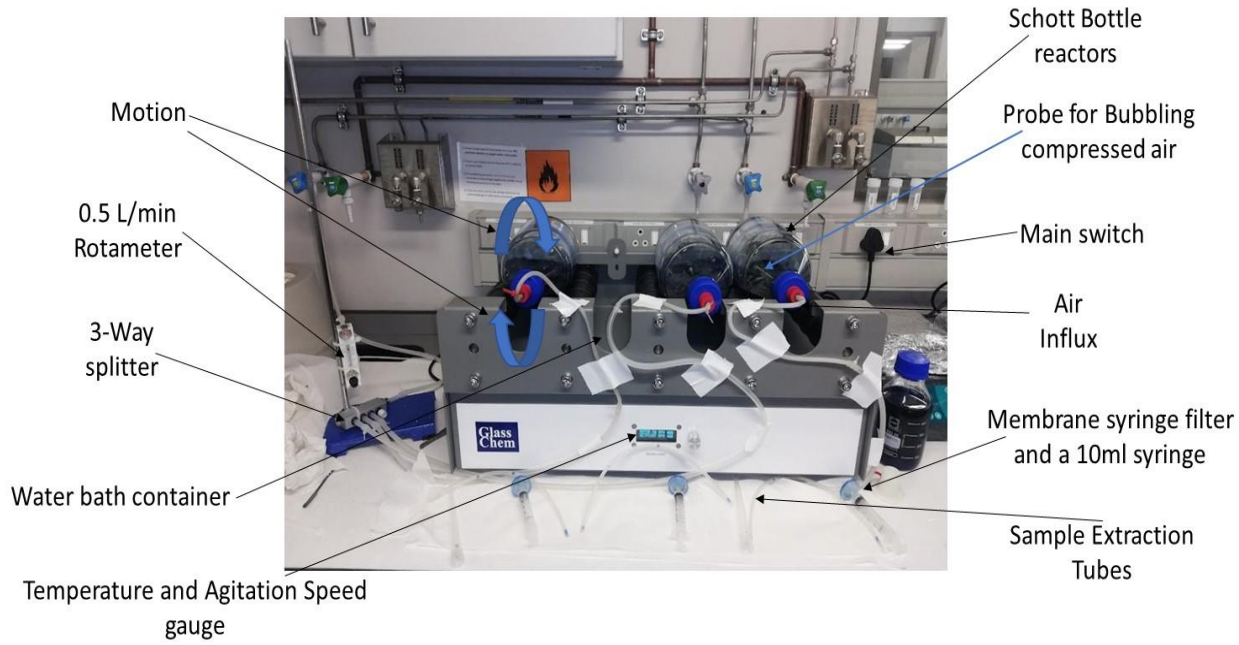

Figure 3-8: Three parallel Schott bottle reactors, with identical leaching conditions, that used in the leaching reaction involving the bottle roller.

The bottle roller temperature was set at 25°C for the first run, and each PCB (Sequence A) was put into a 2 L Schott bottle (three Schott reactor bottles ran concurrently in each run). Each 2 L Schott bottle was then filled with 500 ml of lixiviant. The commencement time was then recorded before the bottles were put on a bottle roller with constant mixing set to 300 rpm. To ensure that the reaction system had enough dissolved oxygen, compressed air was bubbled. The bottle roller set

up is shown in Figure 3-8. The type of a bottle roller is a fairly unique modification of a conventional bottle roller. A bottle roller system has been shown to produce results that are repeatable and most nearly resemble the agitation rate attained in an agitated tank at an industrial scale. On a bottle roller device, all of the material is kept in constant continuous motion, and a pulp air interface is made to allow the pulp to be aerated (Jergensen, 1999).

For sequencing (A) and (B), pre-treatment was followed by a Au leaching stage using ammonium thiosulphate. 5ml samples were taken at 0, 0.5, 1, 2, 5, 8, 9, 20, 24 and 30 hours. Due to ammonium thiosulphate metastability mentioned by Aylmore et al., (2001) and Abbruzzese et al., (1995), 5 ml aliquot samples extracted for each selected time interval were diluted with 5ml dilution solution. This dilution solution was prepared by dissolving and mixing 0.5M $(NH_4)_2S_2O_3$ and 1 M NH_4OH in a 500ml volumetric flask and the resulting solution filled to the mark. The pH of each sample was measured and recorded before dilution. Table 3-3 summarizes the leaching conditions. The sampled solutions were filtered and then analysed for dissolved Au, Ni and Cu using the MP-AES.

After a runtime of 24 hours the solution was filtered off using a Buchner funnel. After filtration, the pieces were dried in an oven and the final PCB mass was measured. These leached residues were preserved for mass balance analysis and calculations. The sampled solutions were analysed for dissolved Au, Cu and Ni using the MP-AES analysis. The process was repeated for Sequence B and for Cu leach residues obtained from Sequence C and D.

Following a comparison of the data, the sequence that produced the maximum Au extraction during the ammonium thiosulphate leaching step was chosen.

Table 3-3: Experimental parameters employed in this investigation for the dissolution of Au from PCBs for Sequence A through D.

Parameter	**Roller Conditions**
30-33% NH_3 in H_2O concentration	1M
99% $(NH_4)_2S_2O_3$ concentration	0.5M
99% $CuSO_4.5H_2O$ concentration	40mM
Compressed air	0.1 L/min
Temperature	25 ± 2℃
pH	10.4

Agitation	300 rpm
Volume of lixiviant	500 ml
Time	24 hours
Solid/Liquid ratio	100 g/L (1 PCB per 0.5 L)
Residence time	24 hours

3.3 Use the best reactor sequencing to optimize Au recovery from PCBs over a selected range of parameters

In Section 2.7.3, It was demonstrated that a balance between the leaching period, thiosulphate and ammonia concentration, and percentage of solids must be reached in order to obtain a high Au dissolution in the leachates (Abbruzzese et al., 1995; Aylmore et al., 2001; Gámez et al., 2019). For this reason, the mixing ratio of NH_3, $(NH_4)_2S_2O_3$, and S/L ratio were the parameters that were optimised. Table 3-4 gives a summary of these parameters and the levels tested. The parameters kept constant included agitation rate, temperature, oxygen concentration and the concentration of copper sulphate. The process pH was observed and recorded.

Table 3-4: List of Parameters to be optimised.

Factors	**Parameter**	**Conditions**
Variable	30-33% NH_3 in H_2O concentration	(0.5 and 1)M
	99% $((NH_4)_2S_2O_3$ concentration	(0.25; and 0.5)M
	S/L ratio	(50/ and 100) g/L (1 PCB/1000 ml and 1 PCB/500 ml
Controlled/ monitored.	Temperature	25 ±2℃
	pH	10.5
	99% $CuSO_4.5H_2O$ concentration	40mM
	Agitation	300 rpm

Using the full factorial design, 8 trial combinations were generated, and these are given in Table 3-5. It is important to note that the lower concentrations shown on the table were chosen after considering that, on average, half of the studies achieved good extractions at lower concentrations of thiosulphate and ammonia. The identical procedure described in section 3.2.3 was used for all

experiments, however in this case, only the chosen reactor sequencing selected in section 3.2.3 was applied. The co-extraction of Au, Cu and Ni was examined.

Table 3-5: Trial combinations generated by the full factorial analysis.

Trial Combination	**Ammonia (M)**	**Ammonium Thiosulphate (M)**	**Solid/Liquid ratio (g/L)**
1	0.5	0.25	100
2	0.5	0.25	50
3	0.5	0.5	100
4	0.5	0.5	50
5	1	0.25	100
6	1	0.25	50
7	1	0.5	100
8	1	0.5	50

3.4 Benchmarking the optimal leaching of PCBs in ammonium thiosulphate obtained in 3.3 with the leaching of Au from PCBs using cyanide

Materials

1 NaCN

2 sodium hydrogen carbonate ($NaHCO_3$)

3 sodium carbonate (Na_2CO_3)

4 Bottle roller and three 2 L Schott bottles used as reactors

5 Air rotameter

6 pH meter

3.4.1 Benchmarking-cyanide leaching

The next phase involved contrasting the optimised operating conditions with the cyanide leaching of Au from PCBs. The following experiments were carried out with cyanide as the leaching solvent.

i. Leaching of PCBs using the reactor sequence obtained from section 3.2

ii. Simulation tests applying the conditions identical to the method carried out in section 3.1.3

To ensure that the pH was above 10.5 before adding cyanide, 18.6 g and 2 g of Na_2CO_3 and ($NaHCO_3$), respectively, were combined with 250 ml of deionized water in a 2 L volumetric flask. The formation of HCN is inhibited at this pH, which ultimately restricts the volatilization of cyanide, as demonstrated by Akcil et al., (2015) in section 2.6.1. The solution was then combined with 0.5MNaCN and the resulting mixture was added to the volumetric flask up to the 2 L mark with deionized water. The mixture was thoroughly agitated with magnetic stirrers until all the crystals were completely dissolved.

Following the procedure described in 3.2.3, a bottle roller was used for all leaching tests. However, the optimal reactor sequencing identified in section 3.2 was employed for the leaching of PCBs, with the exception that NaCN was used in the Au extraction step and the pH was somewhat higher, as mentioned in section 2.6.2. Similar to the previous section, two sets of low and high concentrations were investigated to contrast the optimum leaching method facilitated by thiosulphate.

The frequency of sampling was the same as the one described in section 3.2.3 and the sampled solutions were analysed for dissolved Au, Cu and Ni using the MP-AES analysis. Table 3-6 gives the gives a summary of the leaching conditions used for this part of the investigation.

Table 3-6: Experimental parameters employed in this investigation for the dissolution of Au from PCBs using NaCN.

Parameter	**Conditions**
NaCN	(0.025, 0.05, 0.25 and 0.5)M
$NaHCO_3$	2 g/L
Na_2CO_3	18.6 g/L
Temperature	25℃ ±2℃
pH	10.7
Air flow O_2	0.1 L/min
Agitation	300 rpm
Volume of the lixiviant	500 ml
Residence time	24 hours
Solid/Liquid ratio	100 g/L (1 PCB per 0.5 L)

The simulations followed the procedure described in section 3.1.3 with the exception that 0.5M $NaCN$ was utilized as the lixiviant. Leaching conditions for the simulation, are summarized in Table 3-7. Figure 3-9 depicts a mixture of Au leaf, Cu powder, and Ni foil in CN-solution prior to the start of the leaching reaction.

Table 3-7: Simulation leaching conditions using CN^{-1}

Parameter	**Roller Conditions**
NaCN	0.5M
$NaHCO_3$	2 g/L
Na_2CO_3	18.6 g/L
Au leaf	0.015 g (14.34 mg Au)
Cu	(0 and 11501.50) mg Cu
Ni	(0 and 518.5) mg Ni
Temperature	25 $\pm$2℃
pH	10.7
Agitation	300 rpm
Volume	500 ml
Residence time	24 hours
Air flow O_2	0.1 I/min
Solid/Liquid ratio	100 g/L (1 PCB per 0.5 L)

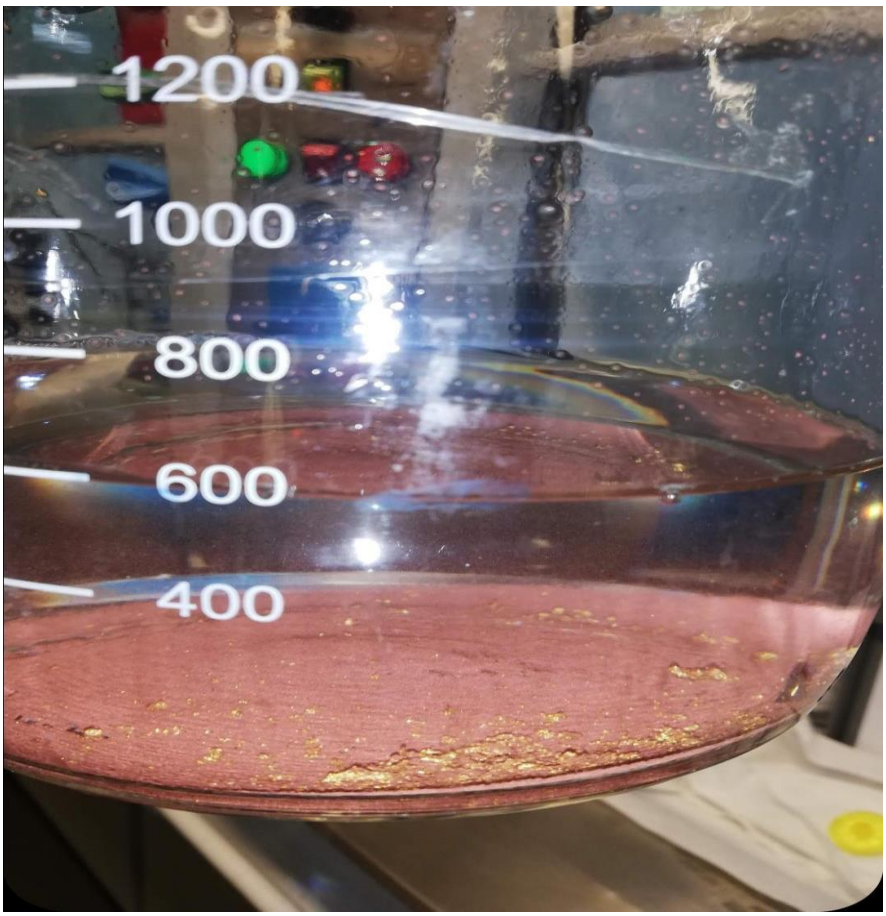

Figure 3-9:A mixture of Au leaf, Cu powder, Ni foil and CN- solution.

3.5 Mass balance

As mentioned earlier in section 3.1.2 (iii), by examining the leached residual sample, the material balance for Au leaching was verified. A satisfactory mass balance was achieved (see section 8.7 of the Appendices). To assess the amount of residual Au present in the leach residue, each PCB leach residue was dried and leached once more using aqua regia. The same conditions used in section 3.1.2 were applied.

4. RESULTS AND DISCUSSION

The results are presented such that they are consistent with the objectives and methodologies outlined in Chapter 3.

4.1 The effect of background Cu and Ni in the dissolution of Au from waste PCBs within an ammonium thiosulphate leaching system

4.1.1 Head grade analysis

The objective of this stage was to analyse the concentration of the following targeted metals Au, Cu, and Ni (even though Sn was also analysed) in the customised PCBs using aqua regia digestion and microwave assisted digestion analysis. The tests done on four different samples were reproducible within an average of ± 6.9% margin of error (value generated on excel). The average the head grade of the PCB, is given in Table 4-1 (see section 8.1 in the Appendices).

Table 4-1: Average head grade of PCBs

Condition of the samples tested	**Au** (mg/PCB)	**Cu** (mg/PCB)	**Ni** (mg/PCB)	**Sn** (mg/PCB)
Not Charred	3.44	8870	128	0
Charred	**4.01**	**10400**	**146**	**3.88**
Wt./wt. %	**0.0080**	**20.8**	**0.292**	**0.00776**

According to Table 4-1, the Au content for the charred and uncharred PCB samples is appreciable and stands at 4.01 mg and 3.44 mg, respectively, for each board weighing about 52 g. This amounts to at most 80.2 g Au/ton PCB (charred samples), which is more than an average of 5-15 g/ton that can be recovered from average natural ores, as reported in literature (Forti et al., 2020; Gámez et al., 2019; Kasper et al., 2018; Kaya, 2019).

The results for all samples also indicate that Cu is the most abundant metal at 20.75%. These findings somewhat concur with Behnamfard et al., (2013), Cui et al., (2020), Wu et al., (2017) and Li et al., (2012) in Table 2-1 from Chapter 2, particularly for Au, Ni and Cu content. Therefore, the results for the charred PCB samples were chosen and employed in all extraction efficiency calculations. It is important to note that, in these experiments, Sn was solely utilized in the measure of the efficiency of the digestion processes. In 2.5.1 it was established that the extraction of Sn is

not feasible in alkali solutions (thiosulphate systems) at room temperature. Therefore, its co-extraction along Au, Cu and Ni was not investigated in this study.

4.1.2 Simulation of Au dissolution in ammonium thiosulphate and cyanide leach using Au leaf

The aim of the simulation tests was to obtain baselines for the extraction of Au from PCBs without any interference of the other metals that are found in PCBs. Different runs were done in distinct solutions of $0.5\text{M}\ S_2O_3^{2-}$ and $0.5\text{M}\ CN^-$, with all other conditions as outlined in 3.1.2. Au dissolution from PCBs was simulated using Au leaf as a proxy while background Cu and Ni concentrations were introduced in a controlled manner. The quantities of Cu and Ni introduced were determined by using the head grade values (see Table 8-4 in the appendices). As mentioned earlier, this was done to keep the concentrations used in the simulated leaching of Au from waste PCBs as close as possible to that of the PCB samples used in the rest of the tests.

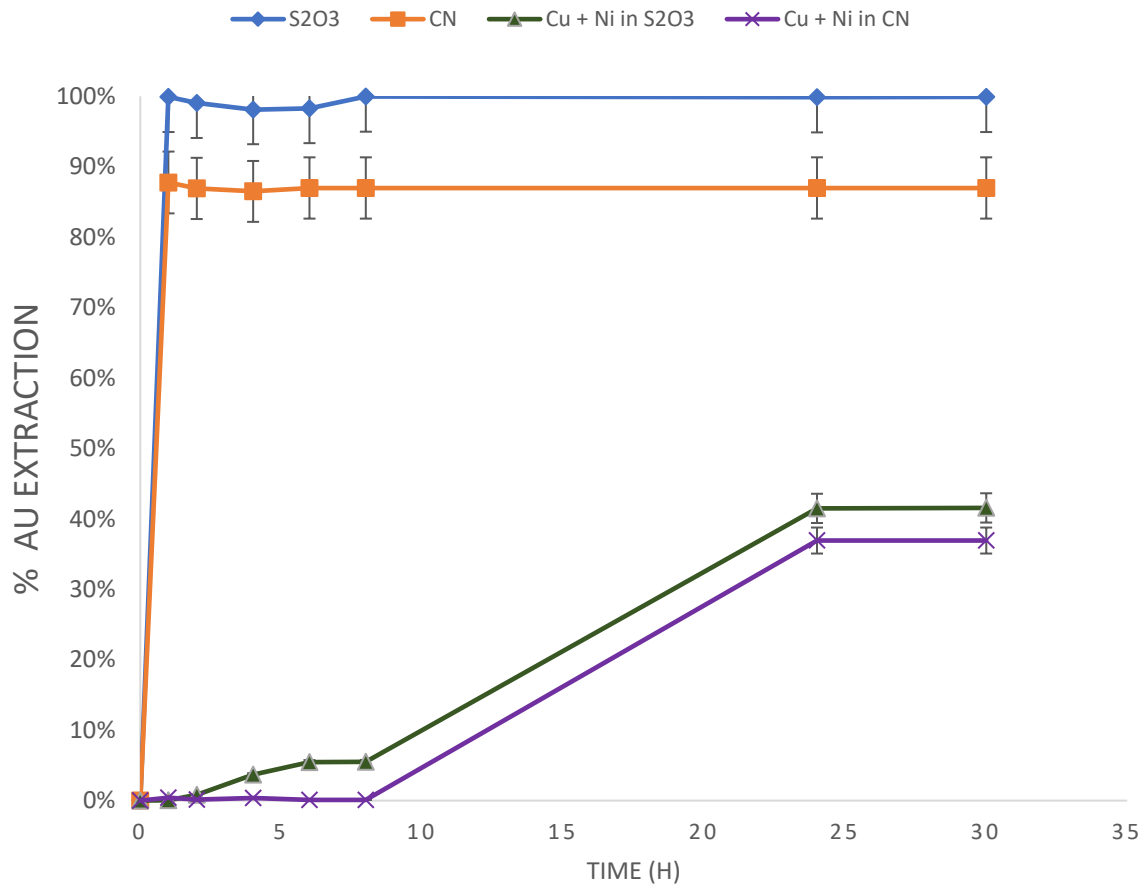

Figure 4-1: The percentage of Au extracted from simulated Au in concentrations of $0.5M\ S_2O_3^{2-}$ and $0.5M\ CN^-$ leaching solutions.

Figure 4-1 shows a summary of results obtained in both 0.5M $S_2O_3^{2-}$ and 0.5 M CN^- leaching systems. Additionally, it displays the percentage of Au extracted with and without the addition of Cu and Ni. The graphs show that the rate of Au extraction was extremely high for both solutions in the absence of background Cu and Ni. An extraction of 99% and 88% was achieved in 0.5M $S_2O_3^{2-}$ and 0.5M CN^-, respectively, within the first hour of leaching. When leaching proceeded further the dissolution of Au did not change significantly until 30 hours residence time was reached.

However, for the leaching done in the presence of Cu and Ni; the kinetics of Au extraction were very sluggish. The total Au extraction drastically reduced to at most 42% and 37% in 0.5M $S_2O_3^{2-}$ and 0.5 M CN^-, respectively. As observed for the results without the presence of background metals, the Au extraction in a 0.5M $S_2O_3^{2-}$ solution is marginally higher than that in a 0.5M CN^- solution in the presence of Cu and Ni.

The observations made during the leaching trials (in both 0.5M $S_2O_3^{2-}$ and 0.5M CN^- leaching systems) and what is depicted on the graph, in Figure 4-1, align. All the Au leaf had been dissolved into solution at the measured concentrations without background Cu and Ni after 30 minutes. However, in the presence of Ni and Cu, most of the Au leaf particles remained in suspension for a total of 30 hours. As the leaching progressed, black particles developed in the 0.5M $S_2O_3^{2-}$ solutions as depicted in Figure 4-2(a), in the presence of both Cu and Ni into solution.

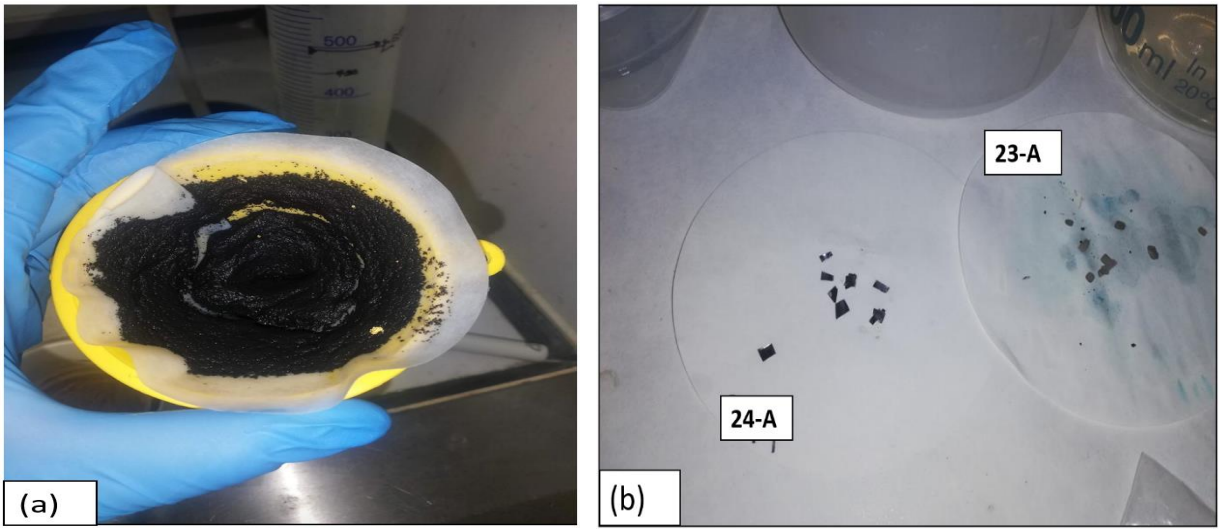

Figure 4-2: (a)LEFT- Black particles that formed in 0.5 M $S_2O_3^{2-}$ leaching system as the reaction progressed. RIGHT- (b) 23-A and 24-A showing the particles of unleached particles of Ni obtained after 30 hours of leaching from 0.5M $S_2O_3^{2-}$ and 0.5M CN^-, respectively.

Figure 4-2 (b) shows unleached Ni foil particles after 30 hours leaching in 0.5M $S_2O_3^{2-}$ (filter paper 23-A) and 0.5M CN^-(filter paper 24-A). On filter paper 24A, Ni can be seen to still be intact, showing no evidence of leaching in CN^-. Filter paper 23A shows a sample of similar Ni particles after leaching in $S_2O_3^{2-}$. These Ni particles were obtained from the black particles shown in Figure 4-2 (a). The sample showed evidence of leaching with the sample having visibly reduced in size. The individual graphs for the 0.5M $S_2O_3^{2-}$ and 0.5M CN^-leaching systems, in the presence of Cu and Ni, are presented in Figure 4-3 and Figure 4-4, respectively.

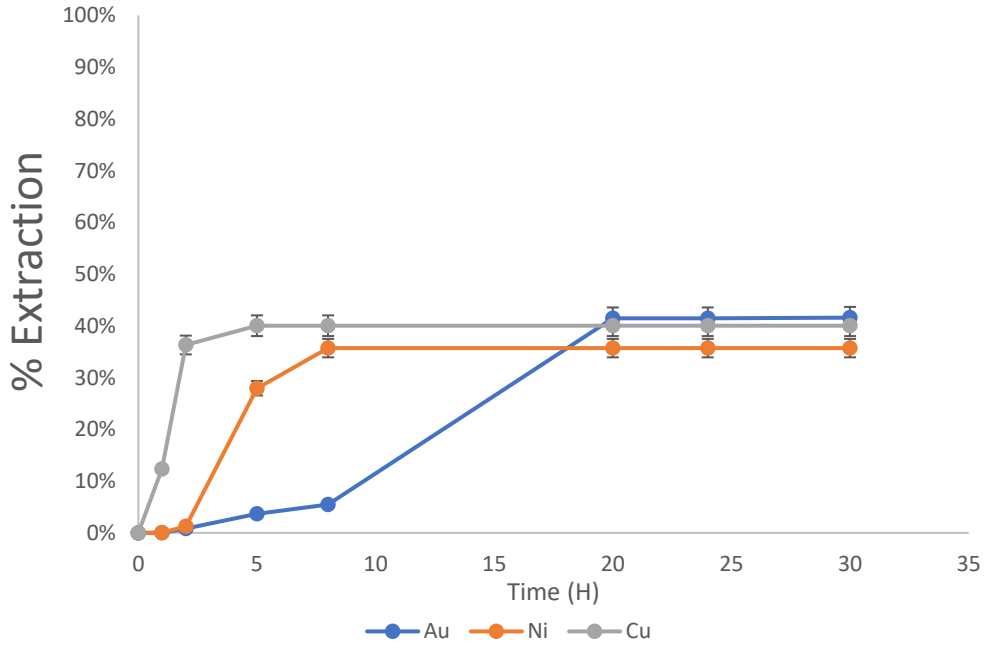

Figure 4-3: Simulated Au extraction kinetics in the presence of Cu and Ni in 0.5 M $S_2O_3^{2-}$ leaching solution.

The two plots in Figure 4-3 and Figure 4-4 demonstrate that Au leaching was hampered because the peak extraction for both graphs is between 37% and 42%, as previously stated. In Figure 4-3, within the first 5 hours, both Cu and Ni were extracted at least 6 times faster than Au, with Cu having the fastest leaching rates. Au, Cu and Ni were coextracted to a maximum of approximately 40% in the thiosulphate leaching system. An increase in residence time from 24 hours to 30 hours did not result in a significant change.

In section 2.7.1, equation 8 shows that 5 moles of $S_2O_3^{2-}$ are required to dissolve 1 mole of Au. The 500 ml lixiviant that was used, contained 0.25M $S_2O_3^{2-}$, which can theoretically extract 0.05

moles of Au. In the case of leaching Au leaf (14.35 mg of Au or 0.0729 mmol Au) without the presence of Cu and Ni, there was more than enough $S_2O_3^{2-}$to react with the total Au available.
In contrast, the presence of Cu and Ni were added in the following amounts: 11501.5 mg Cu and 518.5 mg Ni, (see section 8.2.1 of the Appendices). This corresponds to 181 mmoles of Cu, 0.0729 mmol Au and 8.84 mmol of Ni in the 500 ml $S_2O_3^{2-}$ lixiviant. When combined it results in a total of 190 mmol, all competing for $S_2O_3^{2-}$ with a capacity of 50 mmol Au. This means 0.25 moles of $S_2O_3^{2-}$ were insufficient.
Moreover, as was already mentioned in Sections 2.7 to 2.7.5, elemental Cu is dissolved by $Cu(NH_3)_4^{2+}$ to $Cu(NH_3)_2^{+}$ through the reaction given by equation 12.

$$Cu + Cu(NH_3)_4^{2+} \rightarrow 2Cu(NH_3)_2^{+} \quad (12)$$

This results in a decrease of the oxidizing agent (catalyst) available for Au leaching. The produced $Cu(NH_3)_2^{+}$ ions are converted to $Cu(S_2O_3)_3^{5-}$ species by reacting with 3 mol of $S_2O_3^{2-}$ ions which consumes the available lixiviant (see Figure 2-6 in section 2.7.1) (Aylmore et al., 2001; Oishi et al., 2007; Rudnik et al., 2016; Zhang et al., 2004).

The chemistry of Au leaching in the presence of other metals (Ni and Cu), is complicated by the presence of ammonia and thiosulphate complexing ligands, despite the fact that the stoichiometry of the leaching of Au in $S_2O_3^{2-}$ is well established (Aylmore et al., 2001; Jeon et al., 2018). The possible oxidative decomposition of thiosulphate to tetrathionate and other sulphur compounds further complicates the Au leaching chemistry (Aylmore et al., 2001; Oishi et al., 2007; Rudnik et al., 2016; Zhang et al., 2004).

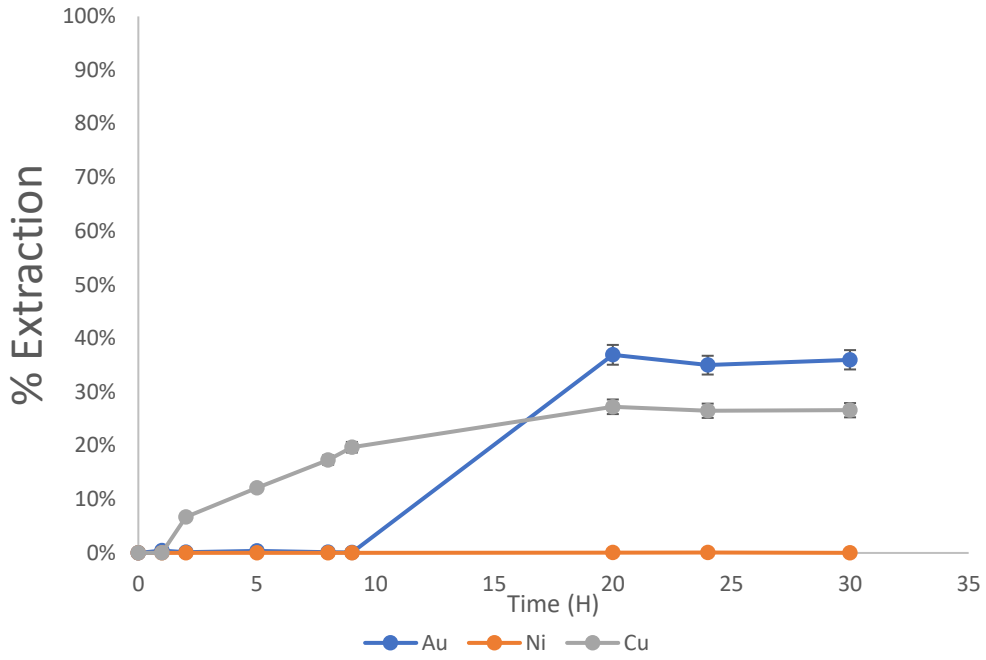

Figure 4-4: : Simulated Au extraction kinetics in the presence of Cu and Ni in 0.5M CN^- leaching solution.

Figure 4-4 shows that in the 0.5M CN^- leaching system, there was no evidence of Ni leaching, supporting the observations made in Figure 4-2(a). The residues in Figure 4-2(a) showed Ni foil to be intact and shiny compared to thin Ni foil particles left over after 0.5M $S_2O_3^{2-}$ leaching.

Compared to Au and Ni, Cu demonstrated relatively faster extraction rates over the first 10 hours. Within that period, no Au was extracted. Thereafter, Au extraction barely reached its peak and the maximum amount extracted was about 37% Au. Cu was only co-extracted to a maximum of 30%. This is because unlike pure Ni, pure Cu dissolution is feasible in the presence of a suitable oxidant, as Cu^+ is stabilised in CN^- system (Leaver et al., 1931; Marsden et al., 2006.; Sayiner et al., 2014). This ultimately leads to CN^- consumption previously mentioned in 2.6.1.

The curves in Figure 4-3 and Figure 4-4 plateau after roughly 20 hours which suggests that equilibrium had been reached in both experiments. As shown earlier in $S_2O_3^{2-}$ leaching, there was no longer lixiviant available for the extraction of any metals.

The pH remained within the desired range in both leaching systems (see Table 8-15 in the APPENDICES). The black precipitation observed was likely caused by a breakdown of

0.5M $S_2O_3^{2-}$ into black copper sulphides as aforementioned 2.7.3. This is a result of low potentials where oxidants are deemed insufficient especially in high Cu concentrations. As a result, the amount of oxygen in the system affects the precipitation rates and extent of formation copper sulphides (Byerley et al., 1975).

4.1.3 Limitations

While being able to provide baseline data and demonstrate the impact of BMs namely Cu and Ni, the following limitations need to be borne in mind when reviewing results from the simulations in relation to waste PCB leaching.

i. In contrast to simulations, metals in the simulated tests were in the form of granules for the Cu, thin metal foil for the Ni and Ni leaf for the Au. This means they were completely in contact with the lixiviant, each presenting a large surface area for leaching. In contrast, when metal is leaching from PCB, Au and Ni are alloyed and exist on the surface of the PCB, while Cu is found beneath the Au-Ni alloy and in the inner layers of the board. This means, not all metals in the PCb get to be fully in-contact with the lixiviants thereby reducing their chances of leaching.
ii. Other coexisting metals, such as Zn, Al, Fe, and Pb, are present in PCBs and may be co-extracted with Au during leaching. This study exclusively focused on Cu and Ni, due to the abundance of Cu and the fact that Au is typically found as an alloy of Au and Ni, which increases the possibility of those two metals being coextracted.

4.2 Investigation and selection of the reactor sequencing in an ammonium thiosulphate leaching system to maximize the amount of Au extracted from PCBs

4.2.1 Pre-treatment (particle size reduction)

Table 4-2 shows each pre-treatment method and the material losses experienced, which were slightly different from what Chirume, (2019) and (Prestele, 2020) reported.

Table 4-2: Material Losses Incurred

	Cut PCBs (3cm x 2cm pieces)	**PCB shreds** pieces after 6 cycles
Mass loss (g)	3.74	7.1
Mass retained (wt.%)	92.8	86

The material losses were all below 10%; however, there were considerable losses for the boards that were shredded as shown in Table 4-2. It is undesirable to lose some of the board material during pre-treatment. The installation of necessary equipment to collect the dust is expensive both financially and operationally. This can be avoided if the PCBs are treated as whole as previously stated in 3.2.1. This would have been ideal for the study, particularly for the sequences (A) and (D), however as was already mentioned, the PCBs could have not fit inside the reactors.

4.2.2 Reactor sequencing tests in an ammonium thiosulphate leaching system

Base metal extraction test results

During the ammonium sulphate-based Cu leaching stage, there were visible minute Au flakes suspended in the reactor 24 hours into the experiments. After 72 hours residence time , all the visible Au on the PCBs had completely peeled off and was visible at the bottom of each reactor. This is demonstrated in Figure 4-5. Part (a) depicts the bottom of the reactor just before leaching experiment and part (b) shows the bottom of the same reactor 72 hours later. These Au flakes were filtered off using a vacuum filter and 0.2 µm filter paper as demonstrated by (c). Thereafter, they were dried out in open air before being subjected Au leaching along with the PCBs they had peeled from, in the subsequent stage of Au leaching using $S_2O_3^{2-}$.

Figure 4-5: (a)Reactor at time t=0 hours (b) Au flakes t=72hours (c) filtration of the flakes (d) filtered flakes

Figure 4-6 and Figure 4-7, shows the metal extraction results for the sequences C and D (Cut and Shredded), respectively, during Cu leaching using ammonium sulphate. For both cut and shredded PCBs, Ni had the fastest leaching rates, with over 67% Ni being extracted within the first 24 hours. Cu rates of extraction were less than half of Ni rates, with 34% and 17% Cu extracted within the same period for shredded and cut PCBs, respectively. The leaching studies demonstrate after a 72-hour residence time that no Au was extracted during the Cu leaching stage, while a maximum of (71% and 80%) Ni and, (44% and 23%) Cu was extracted for shredded and cut PCBs respectively.

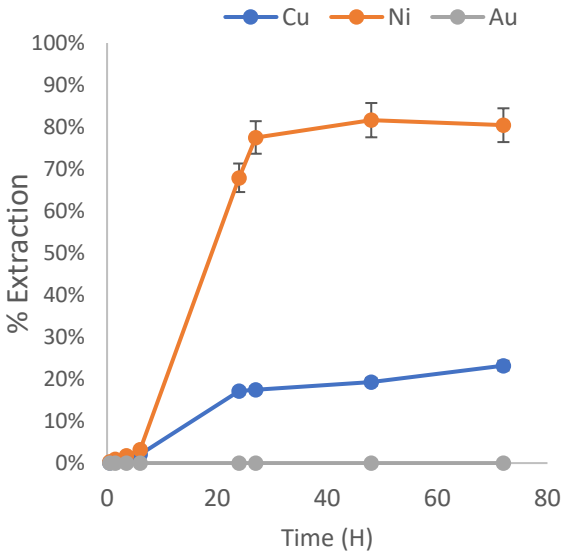

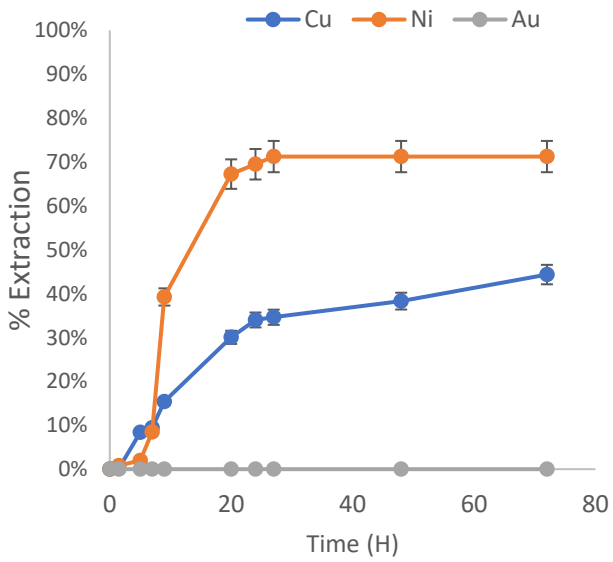

Figure 4-6: BM extraction for sequence C-Cut PCBs in $(NH_4)_2SO_4$ *Figure 4-7:BM extraction for sequence D-Shredded PCBs in $(NH_4)_2SO_4$*

The extent of Ni extraction was 9% higher for Cut PCBs than Shredded PCBs most probably due to the losses that were encountered during the shredding process. Most of the Au is presumably lost during size reduction (Ha et al., 2010; Kasper et al., 2018) . Since Ni is present in PCBs, as an Au-Ni alloy, it is lost in this manner, according to literature. This is demonstrated in section 4.2.1.

Ni had overall faster leaching rates than Cu because of its location of the PCBs as previously mentioned in 3.2.1. The Au-Ni alloy exists on the vias and upper and lower part of waste PCBs. However, in the case of Cu, if the top and bottom masks are removed, approximately 31% of the Cu layers are accessible to the lixiviant. The maximum Cu extraction from PCBs that were shredded was greater than that from PCBs that were cut, and an additional 13% of the Cu deemed to be inaccessible was also extracted. This implies that shredding exposes Cu layers to the lixiviant more so than cutting.

Au extraction test results

The section covers the total Au extracted from PCBs in the sequences A-D investigated. The total Au extraction was standardized against the initial head grade given in section 4.1.1. While the coextraction of Ni and Cu was standardized against the recalculated head grade, after the total mass of Ni and Cu extracted during the prior BM leaching stage was subtracted (see section 8.7 in Table 8-25).

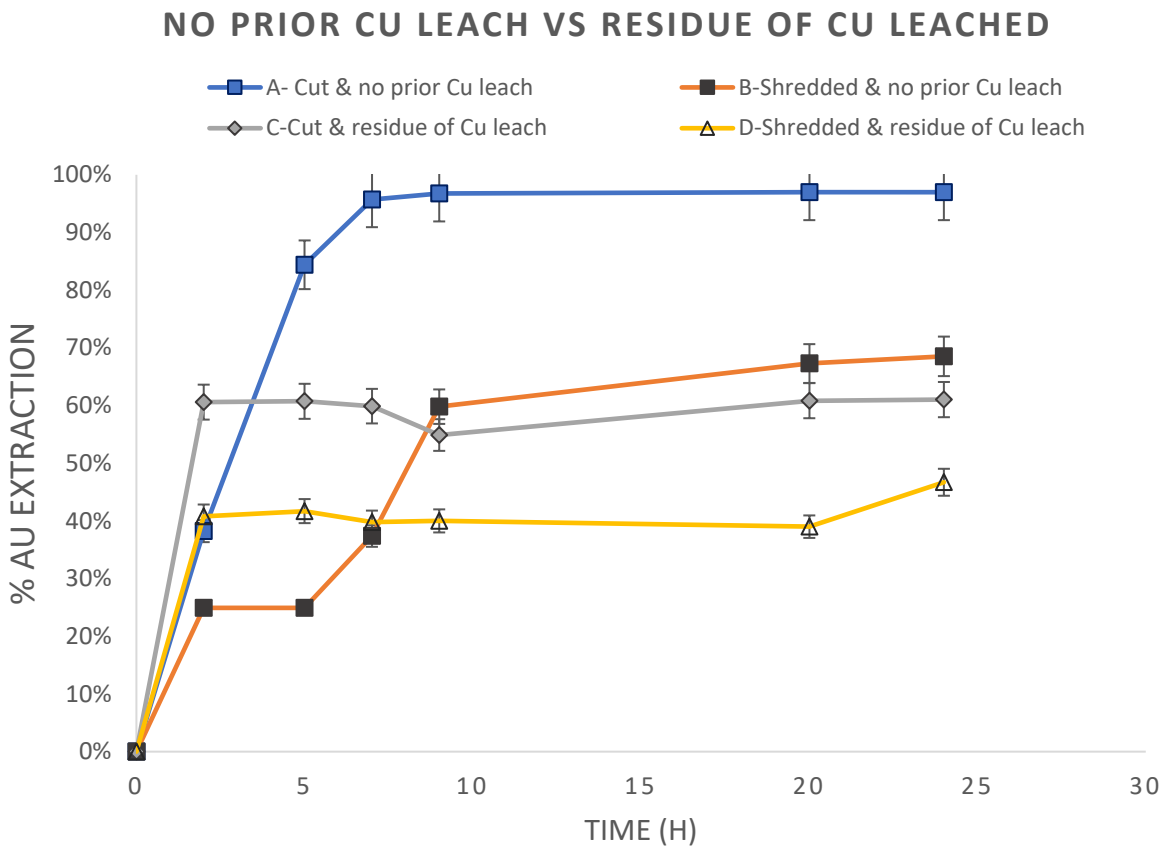

Figure 4-8: The four reactor sequences investigated in $(NH_4)_2S_2O_3$.

The summarized percentage Au extractions for sequences A through D is shown in Figure 4-8. Sequences C and D demonstrated faster Au leaching rates over the first two hours, with 30% Au extraction/hour and 20% Au extraction/hour, respectively. Based on this rate, A and B were outpaced by C by a factor of 1.6 and 2.5 respectively. Thereafter, the plateau in C and D rate indicates that equilibrium had been reached. After 7 and 9 hours, respectively, A and B also reached a plateau. Sequence A had the maximum Au extraction of nearly 97% after a total of 24 hours residence time, followed by B with 69%, and C and D with 61% and 47%, respectively.

Due to a previous Cu leaching step, Sequences C and D showed faster Au extraction rates and were able to reach equilibrium more rapidly than A and B. As was previously described during the Base metal extraction test results section, all the visible Au peeled off from the PCBs, generating very minute flakes of Au that were leached along the PCB residue they had peeled off from. The

minuscule Au particles were consequently freely suspended, highly exposed to the lixiviant, and so easily dissolved in solution. Additionally, studies have shown that smaller particle sizes favor fast leaching reaction kinetics (Tuncuk et al., 2012). Contrarily, in sequences A and B, where there was no stage of prior Cu leaching, the Au was still intact on the fresh PCBs at the onset of the experiments.

The low maximum Au leaching extractions demonstrated by C and D indicate an excessive amount of Au was lost. This was most likely caused by the shredding and filtration steps, given that no Au was dissolved during the Cu leaching, as indicated by Figure 4-6 and Figure 4-7.

Reactor Sequencing A vs Reactor Sequencing C

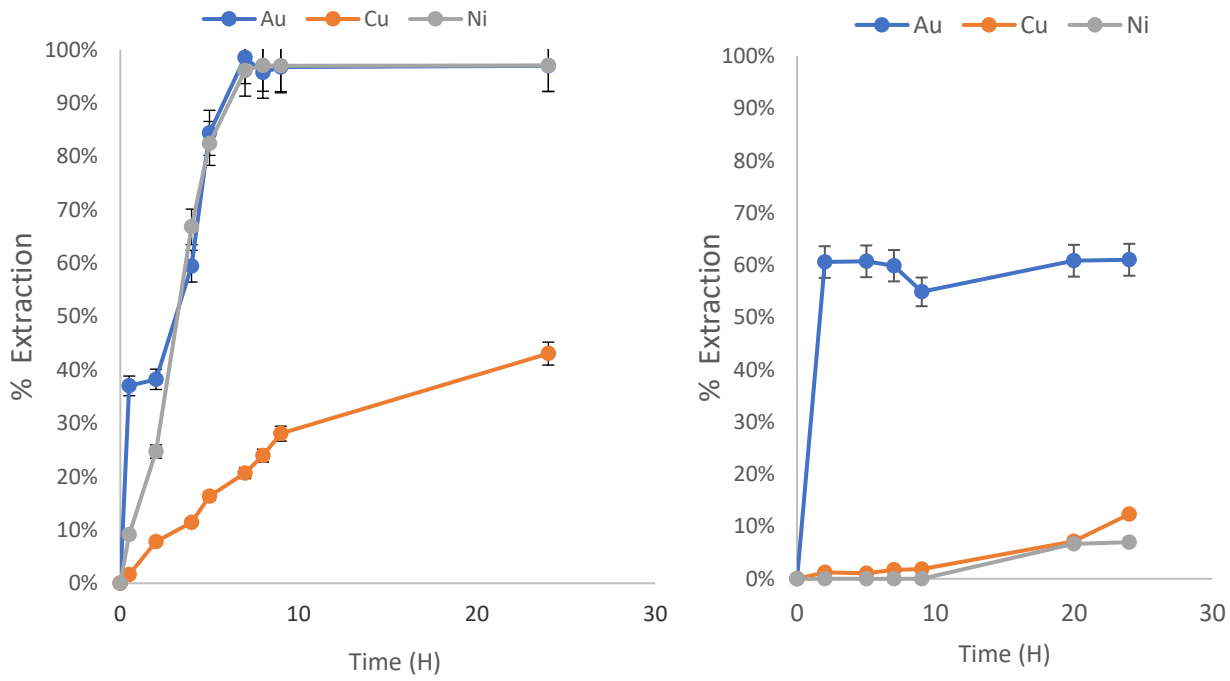

Figure 4-9: (a)Reactor Sequence A, Cut and no prior Cu leach PCBs & (b) Reactor Sequence C, Cut and PCB residue of Cu leach ,respectively.

Figure 4-9 (a) and (b) shows the focused, individual graphs for coextraction of Au, Cu and Ni of Sequence A and C, respectively. The Au extractions have already been discussed in the Au extraction test results section.

When focussing on the individual curves in Figure 4-9, overall, the boards that were processed through sequence C were found to have the least amount of co-extracted Cu and Ni. Ni was barely leached after attaining a maximum of 7% extraction, whereas in Sequence A, a total of 97% Ni was coextracted. With regards to Cu, the total Cu extracted in sequence A was almost 4 times higher than the total extracted during Sequence C.

In sequence A, in the first 2 hours, Au leached 1.6 times quicker than Ni, but both metals reached equilibrium after 8 hours and a combined maximum of 97% of each metal was extracted. The least amount of Cu was extracted, with a maximum extraction of 43% was attained. Whereas in C, of the remaining 20% Ni from the Cu pre-leach, only 0.35% of Ni was extracted. For Cu, an additional 12% of Cu was extracted from the Cu pre-leach.

As previously stated, the differences in particle size between sequences A and C led to variations in the rate of Au extraction. The differences in the extent of Au extraction was due to the losses incurred during the flaking and filtration processes as previously stated. As for Ni, other than the presumption that it was lost during shredding (as a Ni-Au alloy), most of it was had already been extracted during the prior Cu leaching stage, for Sequence C. Same goes for Cu, most of the leachable Cu had also been extracted during the Cu leaching stage.

Reactor Sequencing B vs Reactor Sequencing D

Figure 4-10 (a) and (b) focuses on the different graphs for the coextraction of Au, Cu, and Ni from Sequences B and D, respectively. The outcomes of the Au extraction tests were already covered in the Au extraction test results section.

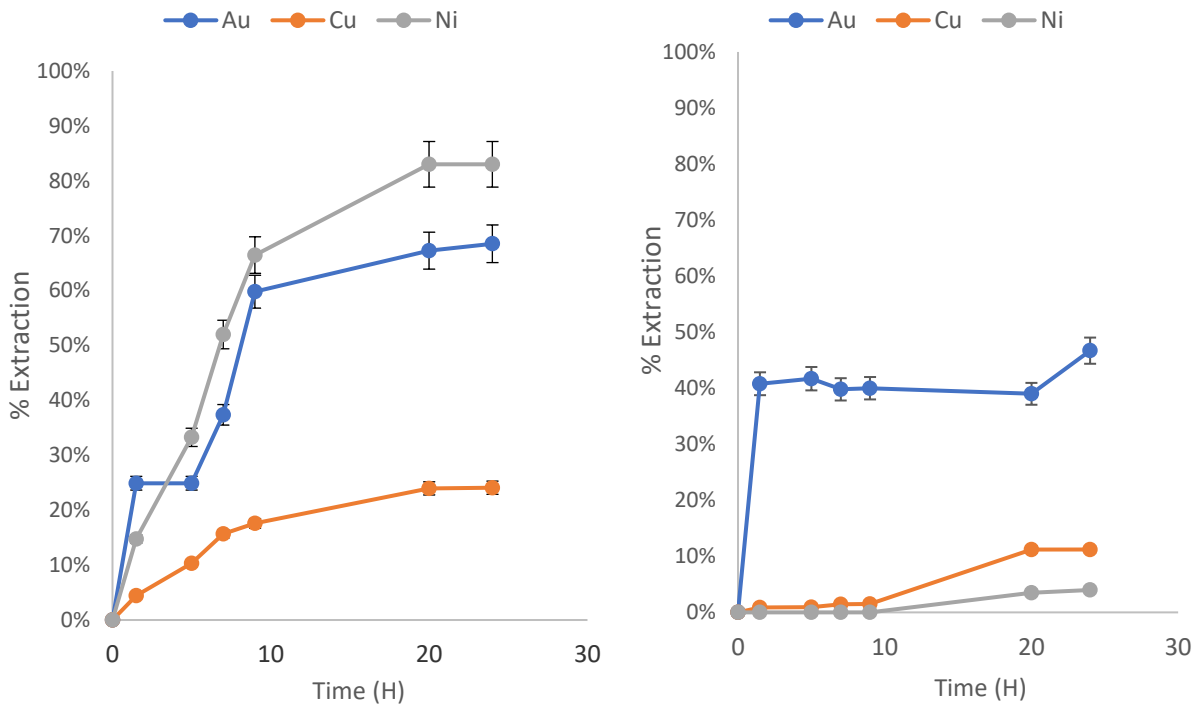

Figure 4-10: (a)Reactor Sequence B, Shredded and no prior Cu leach PCBs & (b) Reactor Sequence D, Shredded and PCB residue of Cu leach, respectively.

Figure 4 10 displays a pattern similar to Figure 4-9, except sequence B and D extracted less Au overall.

The PCBs that were processed through sequence D had the least amount of co-extraction of Cu and Ni overall, as demonstrated by a closer examination of the individual curves in Figure 4-10. In contrast to Sequence B, where a total of 83% Ni was coextracted, Ni was barely leached after reaching a maximum extraction of 4%. With regards to Cu, the overall percentage extracted during Sequence B was two times greater than the total amount extracted during Sequence D .

Au was extracted 1.6 times faster than Ni in the first 1.5 hours of Sequence B. Ni and Au were extracted to a maximum of 83% and 69%, respectively. The least amount of Cu was extracted, with a maximum of 24% Cu extraction achieved. Whereas in D, only 0.14% of the remaining 29% Ni from the Cu pre-leach was extracted (See Table 8-23 in the Appendices). An additional 11% of Cu was also extracted from the Cu pre-leach. Only 47% of the Au was extracted in total in D.

Overall Cu extraction variations in sequence B and D, were discussed in the Reactor Sequencing A vs Reactor Sequencing C portion of the previous section.

4.2.3 Selection of the optimal reactor sequencing in an ammonium thiosulphate leaching system that maximizes the amount of Au extracted from PCBs

Sequence A was selected as the best route since it had the highest overall Au extraction. These findings differ from those of Ficeriová et al., (2011). Without BM extraction, they were only able to extract a maximum of 16% Au under the same leaching conditions. However, these results, are an improvement over those of Tripathi et al., (2012) and Kasper et al., (2018) , who under the same conditions only extracted a maximum of 57% and 79%, respectively, of PCBs that did not undergo size reduction and BM extraction. The use of depopulated PCBs and the utilization of a higher concentration of thiosulphate in this study, (comparable to Ficeriová et al., (2011)) sets it apart from their studies.

Sequence A, however, had a higher rate of Cu and Ni co-extracted. 2143.2 mg of Cu and 140,10 mg of Ni were coextracted along with the highest Au extraction of 3,89 mg, after approximately 7 hours, which may not be favorable for downstream processes (See Table 8-7 in the Appendices)

On the other hand, according to Tripathi et al., (2012), Aylmore et al., (2001) and the results obtained in this study, sequence B has drawbacks such as significant losses during size reduction. Additionally, an increased coextraction of Cu, during Au leaching, results in larger losses of thiosulphate ions by its conversion to tetrathionate and other polythionates. As a result, there is a lower extraction of Au from shred PCBs because such ions are not useful in the extraction of Au.

BMs are removed in large quantities during the prior leaching stage of sequences C and D, which is advantageous for subsequent procedures. But it comes at a cost of Au loss during mechanical size reduction, especially for sequence D (Table 4-2), and a further loss in the form of tiny flakes during filtration demonstrated by Figure 4-5. As a result, a total of 53% Au was lost during the methods used in sequence D (See Table 8-23 of the Appendices). For the PCBs processed through sequence C, there was a 35% total in Au loss. No Au was extracted during the leaching of BMs,

indicating that the loss of Au was a direct result of the stages that came before the Cu leaching stage (see Table 8-23 in the Appendices).

4.3 The optimization of Au extraction from PCBs over a selected range of parameters using the best reactor sequencing obtained in 4.2

4.3.1 Optimisation step

The trial combinations from 1 to 8, each of which corresponds to the leaching parameters investigated, are listed in Table 4-3. The 3 factors optimized were, NH_3, $S_2O_3^{2-}$ and S/L ratio, in the levels of (0.5 and 1)M, (0.25 and 0.5)M, and (50 and 100) g/L.

Table 4-3:Trial combinations generated by the full factorial analysis.

Trial Combination	**NH_3 (M)**	**$S_2O_3^{2-}$ (M)**	**S/L ratio (g/L)**
1	0.5	0.25	100
2	0.5	0.25	50
3	0.5	0.5	100
4	0.5	0.5	50
5	1	0.25	100
6	1	0.25	50
7	1	0.5	100
8	1	0.5	50

These levels are within the range of optimum leaching parameters identified in the literature and listed in Table 2-6 in section 2.7.6. Using the optimal reactor sequence identified in 4.2.3, Au extraction from PCBs by thiosulphate leaching was optimized using a full factorial design method.

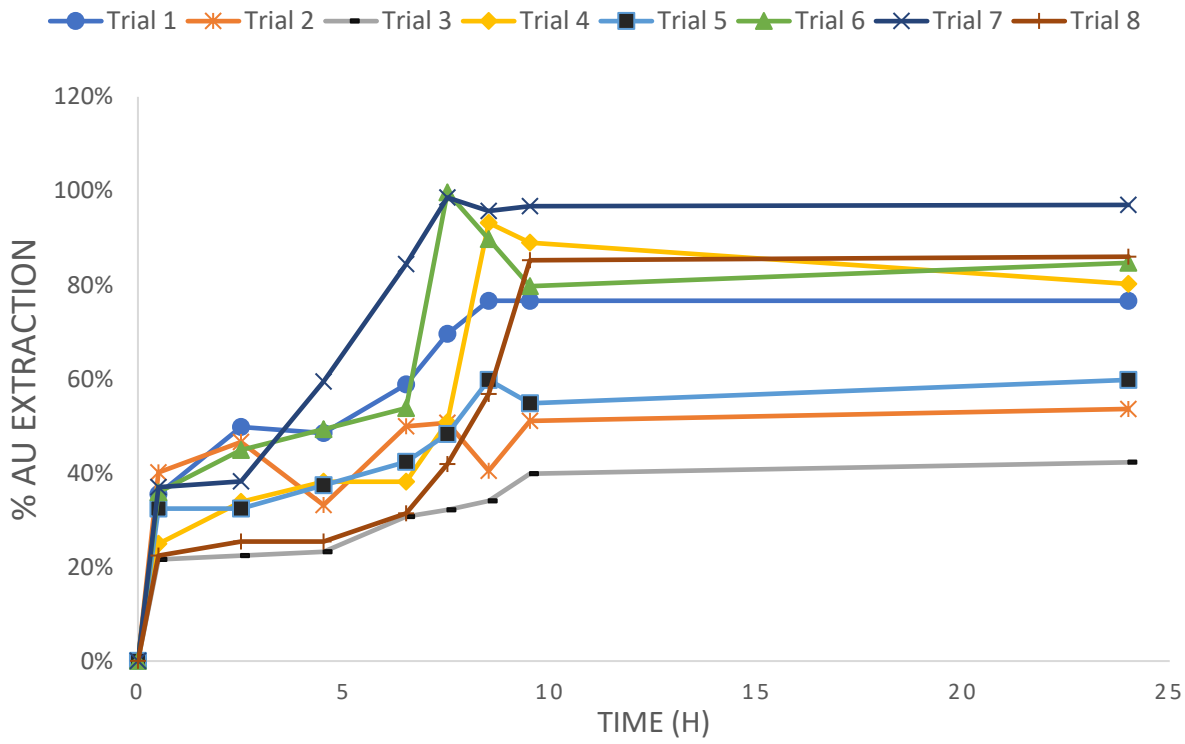

Figure 4-11: Au extraction per leaching trial, over a period of 24 hours residence time.

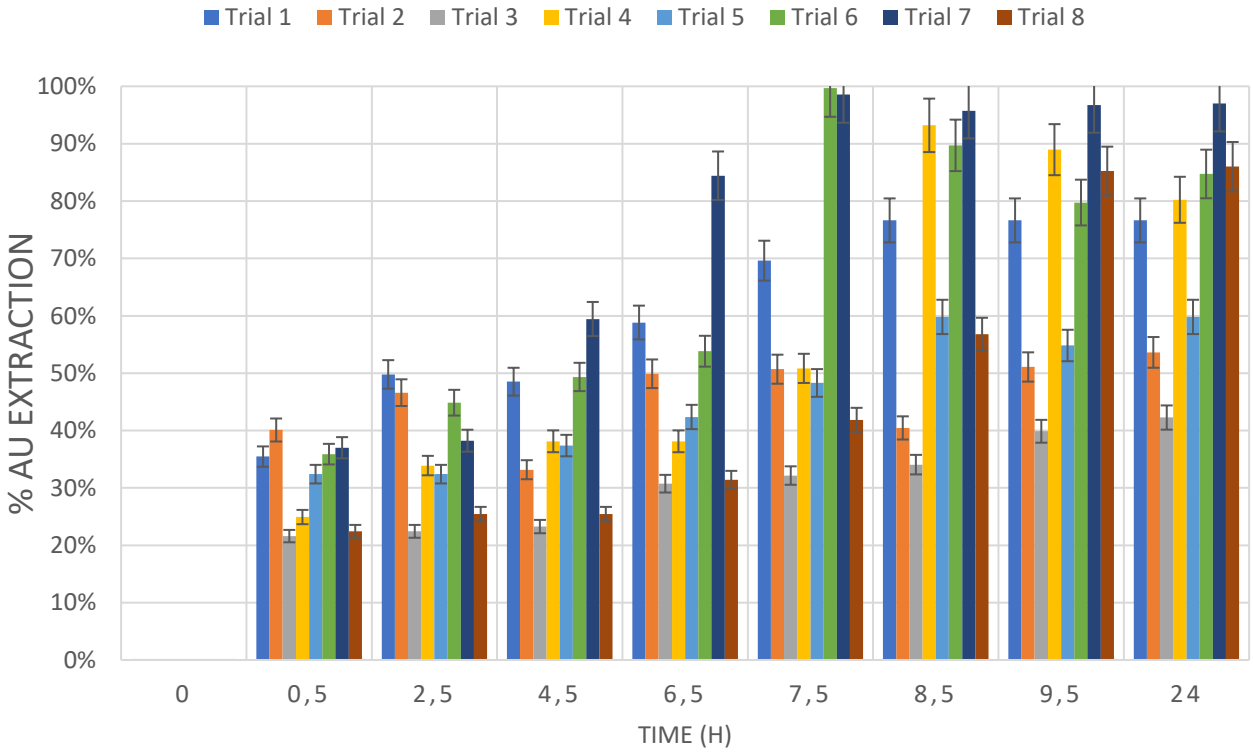

Figure 4-12: Au extraction per leaching trial, over a period of 24 hours residence time.

The results of the leaching trials 1–8 are shown in Figure 4-11 and Figure 4-12. Both figures indicate that most trials had attained their highest extraction after 7.5 hours. Trial 1 experienced the fastest leaching rate within the first 2.5 hours, at 20% Au/hour.

This was twice as fast as Trial 3, whose rate was the slowest throughout the entire leaching process. Trial 2 maintained its initial rate but was overtaken by Trial 7 two hours later. For the following 3.5 hours, Trial 7 kept the lead with a 33% Au/hour rate. In a total of 7.5 hours, the highest extraction of almost 99% Au was achieved. Trial 6 was next, managing to achieve greater than 99% Au extraction. However, after an hour, the extraction fell to roughly 90%, and after the entire leaching period, it fell by another 10%.

The lowest total extractions were achieved by in Trials 3, 2, and 5, each reaching at 42%, 54%, and 60%, respectively. The pH was stable in all trials in the range between 10 and 10.4. This with the exception of trial 3 and 4, the pH fluctuated between a pH of 9.8 and 9.9 (see Table 8-17 and Figure 8-1 in the Appendices)

The findings demonstrate how crucial it is to carry out the leaching using the correct ratio of $S_2O_3^{2-}$ to NH_3. Literature shows that this ensures that Au dissolves faster, the maximum extraction is soon reached, and the produced Au complexes manage to remain in solution rather than precipitate out. Overall, Trials 1, 2, 7, and 8 had a $S_2O_3^{2-}/NH_3$ ratio of 0.5 as shown in Table 4-3. Throughout the leaching experiment, total Au extraction values did not drop, unlike other trials. This suggests that stability of the Au complexes was higher, than other trials. However, Trial 1 and Trial 2 achieved lower total Au extractions compared to the other two trials, likely due to the differences in concentration. Still maintaining 24 hours as a basis and comparing either Trial 1 to 7 or Trial 2 and 8 (all of which had a $S_2O_3^{2-}/NH_3$ ratio of 0.5 but different S/L ratio), Trials with a higher S/L ratio showed a higher Au extraction.

The decrease in Au extraction for trial 6 after 7.5 hours was likely caused by the thiosulphate Au complex precipitating as a result of potential reactions between the thiosulphate and oxygen. This could have resulted in a precipitation of sulfur, a substance that encourages the passivation of the metallic surface of the Au and prevents its further dissolution (Grosse et al., 2003).

The slowest kinetics and overall low extraction observed in Trial 3 can be attributed low concentration of NH_3 in the system. The ratio of $S_2O_3^{2-}$ to NH_3 was 1:1 and the S/L ratio was 100

g/L. This system had lower pH unlike other trials save for Trial 4. This demonstrates the importance of a proper balance between $S_2O_3^{2-}$, NH_3 and S/L ratio. As seen in section 2.7.3, if there is too much thiosulphate present, it may react with present Cu from PCBs to create $Cu(S_2O_3)_3^{5-}$. This specie, is ineffective for extracting Au because copper tetramine complexes are required to dissolve Au (Senanayake, 2007). This also may explain why Trial 4 had a higher Au extraction compared to Trial 3.

From literature, the extraction of Au from the PCBs is enhanced at a lower S/L ratio. According to Gámez et al., (2019), this is because there is a greater supply of the reagent available per unit weight of PCBs. This was the general pattern seen throughout Trial 3, 4, 5 and 6. However, the rest of the trials conflicted with this assertion, as illustrated in Figure 4-11 and Figure 4-12. The difference between these trials was the $S_2O_3^{2-}/NH_3$ ratio, which was equal to 0.5 in Trials 1, 2, 7 and 8. This observation suggests that within a total leaching period of 24 hours, a S/L ratio of 100g/L is conducive as long as the $S_2O_3^{2-}/NH_3$ is 0.5.

The observation that at 7.5 hours, most trials had reached their maximum extraction, suggests that approximately 8 hours is the optimal leaching time, since the extent of extraction does not change significantly, thereafter.

Overall, the findings demonstrate that trials 6, 7, and 8 were successful in achieving significantly high Au extraction above 80% during a 24-hour period. At the optimal leaching of 7.5 hours, Trial 6 had the highest Au extraction above 99%, while Trial 7 had at most 99%. Trial 7 demonstrated a better stability of the Au complex than Trial 6, nonetheless. Additionally, it was able to attain equilibrium more quickly than any other trial. As a result, Trial 7, of a 1M NH_3 and 0.5M $S_2O_3^{2-}$ concentration, a S/L ratio of 100g/L and 8 hours, was chosen as the optimum, since it has faster leaching kinetics and displays a high level of stability for the dissolved Au in solution.

4.3.2 Rate limiting step

For flat surfaces similar to Au in PCBs, Levenspiel, (1973) offered an extension of the Shrinking core model discussed in 2.7.4. It was determined that the Au dissolution from PCBs is only limited by film diffusion and chemical reaction described by equation 11-A in section 2.7.4,. In order to verify whether the leaching experiments during the optimization stage were limited by chemical reaction and film diffusion, equation 11-A was applied.

Table 4-4: Contrasting the various rate-limiting models.

Trial	**Film diffusion and reaction controlled (R^2)**	**Rate constant $\frac{1}{\tau}$ (hrs^{-1})**
1	0.92	0.0970
2	0.78	0.0676
3	0.89	0.0457
4	0.91	0.0856
5	0.90	0.0715
6	0.93	0.112
7	0.96	0.126
8	0.92	0.0603

The output values obtained from the equation 11-A (in section 2.7.4), for each trial (at the established optimum time of 8 hours), were plotted against time and linear trendlines were fitted (see Figure 8-11 in the Appendices) in section 2.7.4,. In order to verify whether the leaching experiments during the optimization stage were limited by chemical reaction and film diffusion, equation 11-A was applied.

Table 4-4 shows the R^2 values and the rate constant obtained after plotting the output values for each trial. The R^2 values are all high enough which suggests that the rate limiting step was indeed chemical reaction and film diffusion. In section 2.7.4, it was highlighted that for the Shrinking Core model extension for flat plates, the equations for a chemical reaction and film diffusion-controlled reaction, are identical. Since the equations are the same ,they produce the same plots. However, this does not mean both mechanisms apply. It cannot be concluded with certainty which one applies from the model analysis alone.

4.3.3 Optimization of Au extraction based on surface response method

The 2-level full factorial design generated 8 combinations which are given in Table 4-3. The 3 factors, NH_3, S_2O_3 and S/L ratio in the levels of (0.5 and 1)M, (0.25 and 0.5)M, and (50 and 100) g/L , respectively, were analyzed using the composite design functionality within response surface methodology in Minitab. The Au extraction values were taken at the optimal leaching time of 7.5

hours as aforementioned in 4.3.1. The central composite design generated 20 runs which were not replicated. An R^2 of 0.75 suggested that the model could only explain 75% of the variation in the Au extraction. The fitted surface plots are given in the appendices in section 8.8

Table 4-5: Analysis of variance (ANOVA) of a full factorial design phase

Source	**DF**	**Adj SS**	**Adj MS**	**F-Value**	**P-Value**
Model	9	0,84607	0,094008	3,02	0,050
Linear	3	0,40465	0,134883	4,33	0,034
S_2O_3	1	0,02750	0,027498	0,88	0,70
NH_3	1	0,29220	0,292198	9,37	0,009
S/L Ratio	1	0,08495	0,084953	2,73	0,130
Square	3	0,36728	0,122426	3,93	0,043
$S_2O_3 * S_2O_3$	1	0,26278	0,262776	8,43	0,013
NH_3*NH_3	1	0,12454	0,124538	4,00	0,074
S/L ratio*S/L ratio	1	0,03553	0,035526	1,14	0,311
2-Way Interaction	3	0,07414	0,024715	0,79	0,525
S_2O_3*NH_3	1	0,04560	0,045602	1,46	0,254
S_2O_3*S/L ratio	1	0,02060	0,020605	0,66	0,435
NH_3*S/L ratio	1	0,00794	0,007938	0,25	0,625
Error	10	0,31173	0,031173		
Lack-of-Fit	5	0,31173	0,062345	*	*
Pure Error	5	0,00000	0,000000		
Total	19	1,15780			

Table 4-5 shows the analysis of variance (ANOVA) between the investigated factors and the values fitted by the model. The p-value of NH_3 and the $S_2O_3 \times S_2O_3$ shows that those two parameters were statistically significant amongst other parameters. This essentially means that other parameters and their interactions did not have a statistically significant effect on Au extraction. This suggests these parameters had significant influence on the Cu-NH_3-S_2O_3 leaching system, which is supported by the literature and the findings obtained during the examination of the optimization results in section 4.3.1.

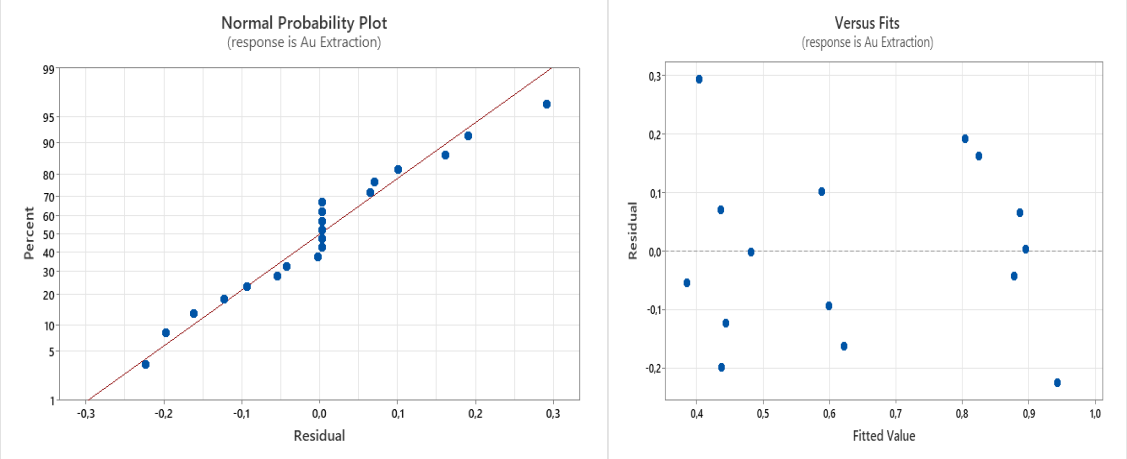

Figure 4-13: (a)Normal probability plot of residuals (b) Raw residuals vs fitted values

Figure 4-13 (a) illustrates the normal probability plot of residuals while (b) shows the plot of the residual values against the fits. The residual errors are normally distributed except for 5 points which are outliers, this is also indicated in Table 4-5. The residuals vs fits dots are in a reasonable parallel band, this means that the variation throughout is quite even. Therefore, this is reasonably satisfactory.

Non-statistically significant factors were eliminated to create a better model that would fit the data more accurately. A model with an R^2 of 0.34 value was generated. As a result of this being too low, the model initially generated and provided by equation 13 was employed.

$$Au\ extraction = -1{,}09 + 3{,}81\,S_2O_3 + 2{,}29\,NH_3 + 0{,}0065\,S/L\ Ratio - 8{,}64\,S_2O_3 * S_2O_3 - 1{,}487\,NH_3 * NH_3 - 0{,}000079\,S/L\ Ratio * S/L\ Ratio + 2{,}42\,S_2O_3 * NH_3 + 0{,}0162\,S_2O_3 * S/L\ Ratio - 0{,}00504\,NH_3 * S/L\ Ratio \quad (13)$$

This model predicts that at 8 hours leaching time, the Au extraction at 1M NH_3 and 0.5M $S_2O_3^{2-}$ concentration, a S/L ratio of 100g/L will be equal to 82%. This is not comparable to 99% Au extraction that was achieved during the leaching experiments. The model also predicts that the optimal Au leaching are conditions are a concentration of 0.42M $S_2O_3^{2-}$ and 1M NH_3 and, a S/L ratio of 60 g/L at an optimal leaching time of 7.5 hours.

Therefore, the model does not accurately fit the data. Future experiments would need to include more replicates and testing at wider parameter ranges in order to create a model that is more accurate. Additionally, other parameters may need to be included in the experimental design.

4.4 Comparing the best PCB leaching method with the cyanide-based leaching of Au from PCBs using ammonium thiosulphate, which was achieved in step (4.3)

The optimal reagent mix established from section 4.3 was then compared against Au leaching using cyanide. The cyanide concentrations that were investigated were 0.025M, 0.05M, 0.25M, and 0.5M, as previously indicated in the methodology in section 3.4.1.

Table 3-7 lists all other parameters that were kept identical to those for leaching Au using thiosulphate. The findings of Au leaching at various cyanide concentrations are presented in Figure 4-14.

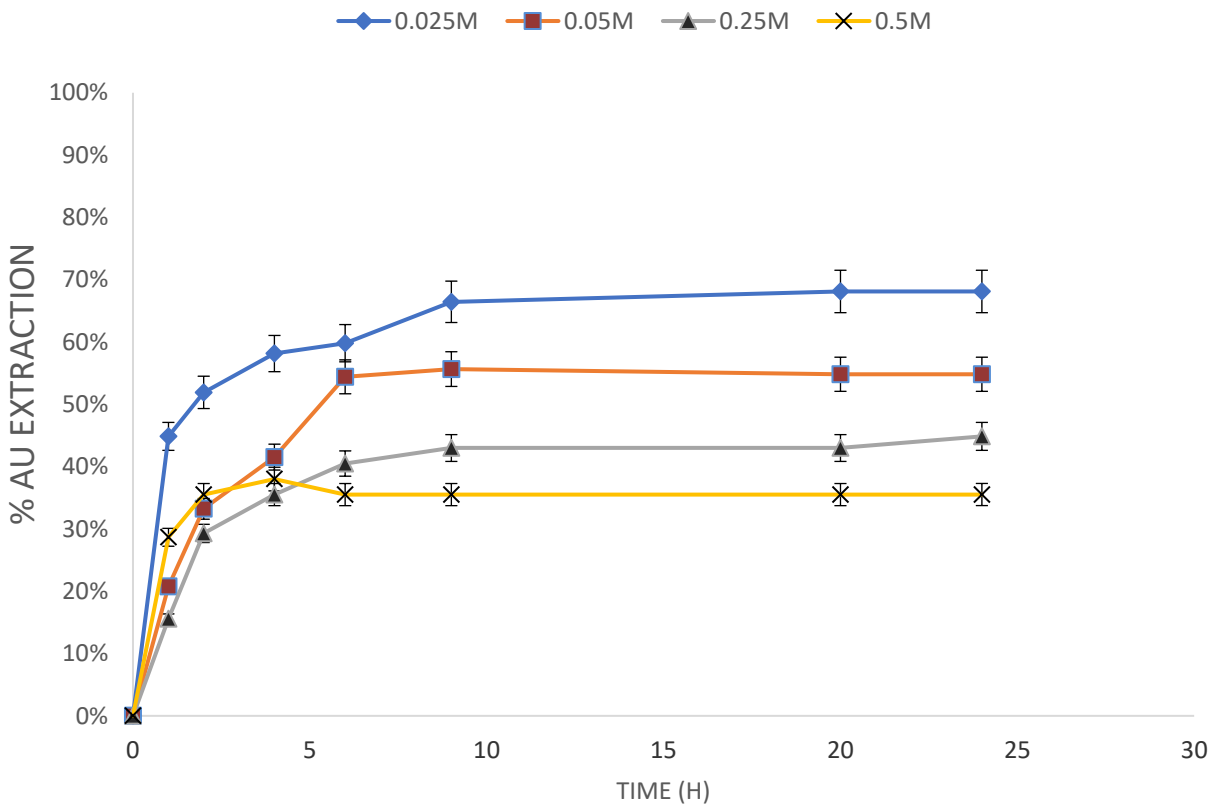

Figure 4-14:Au extraction from Cut PCBs at different NaCN leaching concentration of 0.025M. 0.05M, 0.25M and 0.5M.

Figure 4-14 shows the Au extracted against CN^-concentration over a total leaching period of 24 hours. The quickest leaching kinetics and highest extraction occurred at a concentration of 0.025M CN. During the first hour, the rate of Au extraction for 0.025M CN^-, was about 45% Au/hr. This was more than double the rate the rate of 0.05M CN^- and almost triple than that of 0.25M CN^-. 0.5M CN^-concentration had the second fastest rate of about 29% Au/hr. However, its rate declined

thereafter as it plateaued after 2 hours, yielding the lowest total extraction of 36% Au after a total of 24 hours residence time. The lowest concentration, 0.025M CN^-, had the highest Au extraction of 68%. This was followed by (0.05M, 0.25M, and lastly, 0.5M) CN^-, each yielding a maximum Au extraction of 56%, 45% and 55%, respectively.

A trend was observed that the percentage of Au extraction tends to decline as CN^-concentration rises, and this is elaborated in Figure 4-15. The lowest concentration of 0.025M achieved the highest extraction of almost 70%, followed by 0.05M with almost 55%. However, the highest concentrations of 0,5M achieved a Au extraction almost half that of 0.025M, while that for 0.25M was below 50%.

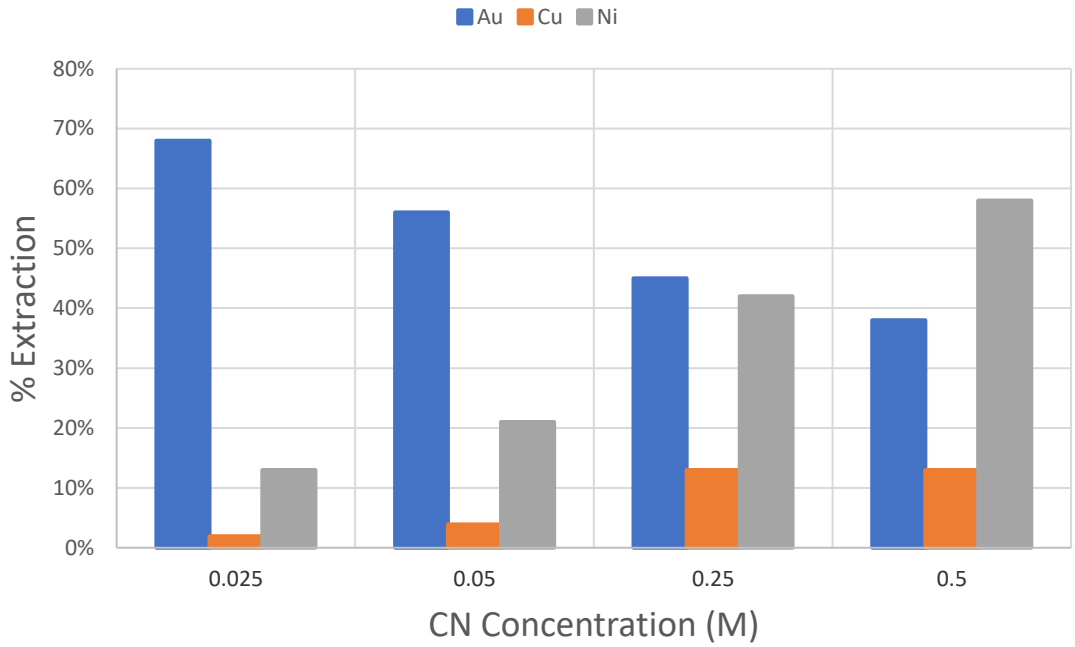

Figure 4-15: Metal co-extraction against CN concentration 0.025M. 0.05M, 0.25M and 0.5M.

Upon comparing the BM extraction for each concentration displayed in Figure 4-15, a reverse trend was observed. The highest concentration, 0.5M, exhibited the highest co-extraction of BMs, Ni and Cu of 59% and 13%, respectively. While that of 0.025M extracted Ni and Cu almost 5 and 7 times lower that a concentration of 0.5M.

This suggests that the Au extraction was most likely hampered by Ni and Cu competing for the lixiviant . These results, however, do not match up with what was demonstrated in the Au leaching simulation experiments (using Au leaf in the presence of elemental Cu and Ni), discussed in section 4.1.2., particularly in the case of Ni extraction.

This is most likely because the Ni in the PCBs is in a form of a Au-Ni alloy, which, as was already discussed in 3.1.1, is more easily leached in CN^- than pure Ni (Leaver et al., 1931; Sayiner et al., 2014). However, unlike Ni, native Cu readily dissolves even at low concentrations of CN^- which leads to its high consumption and concomitant decrease of Au extraction (Marsden et al., 2006.) In this study, the Cu extractions were quite low compared to Ni, due to the reason that was discussed in 4.2.2, that approximately for cut PCBs approximately 31% of the Cu is accessible to the lixiviant.
The results also concur with the study by Montero et al., (2012). At a high CN^- concentration of approximately 0.2 M, they achieved Au extraction of 48%, while the level of Cu coextraction was quite high (77%), as previously stated in section 2.6.1

Unlike the optimal leaching of waste PCBs obtained in section 4.2.2 and 4.2.3 via thiosulphate leaching, it is difficult to implement the sequence A and B in the leaching of waste PCBs using a concentration of 0.5M CN^-. Other than its level of toxicity, it requires implementation of the prior removal of BMs before leaching of Au. Even though the lowest CN^- concentration resulted in high Au extraction of 68%, this value was still lower than the 99% achieved by 0.05M $S_2O_3^{2-}$. Additionally, equilibrium during $S_2O_3^{2-}$ leaching could be attained as early as 7.5 hours, this compared to approximately 10 hours leaching time required by CN^-, under the same conditions. Additionally, this study showed that the advantage CN^- has over $S_2O_3^{2-}$ leaching is the low co-extraction of Ni and Cu.

5. CONCLUSION

The findings of the characterization tests demonstrated that waste PCBs contain a considerable amount of 80.2 g Au/ton PCB in their composition. Since the average levels found in ores are only 5-15 g Au/t, it makes recycling commercially interesting as a result. Even though waste PCBs contain a significant amount of Au, other metals like Cu and Ni may prevent it from being effectively extracted using the conventional leaching route for the thiosulphate leaching of waste PCBs.

In this regard, simulations of Au leaching using Au leaf (14.3 mg Au per leaf) and elemental Cu and Ni were a good way of getting baseline studies on the extent to which Cu and Ni affect the $(NH_4)_2S_2O_3$ and NaCN leaching of waste PCBs despite a few limitations. Within the first hour of leaching, 99% and 88% of the Au was extracted from the Au leaf in $0.5M\ S_2O_3^{2-}$ and $0.5M\ CN^-$, respectively, in the absence of Cu and Ni. In the presence of 11500 mg Cu and 519 mg Ni (proportional to accessible Cu and Ni in head grade) the total Au extraction reduced to at most 42% and 37% in $0.5M\ S_2O_3^{2-}$ and $0.5M\ CN^-$, respectively. The actual leaching of PCB in the same concentrations of $(NH_4)_2S_2O_3$ and NaCN gave 97% and 38% Au extraction, respectively.

Under the same leaching conditions, ammonium thiosulphate was proven to have a number of advantages over cyanide. These include faster rates and higher extent of Au extraction, and less interference from foreign ions. The primary drawback to using thiosulphate is that it requires strict control of process variables due to the complicated nature of the reactions involved, some of which are difficult to interpret because they are not fully understood. It also requires a higher dosage compared to CN.

Sequence A, of cut PCBs without any prior Cu leach step, was selected as the best route, as it stood out as having the maximum Au extraction. However, compared to Sequence C-D, it had a higher percentage of Cu and Ni co-extraction. The results showed that through this sequence, 2143 mg of Cu and 140 mg of Ni were coextracted along 3.89 mg Au after 7 hours of leaching. This translates to 21% Cu, 96% Ni and 97% Au extracted using 0.5M $S_2O_3^{2-}$, 1M NH_3 and 0.04M $CuSO_4$ solution mixture and a S/L ratio of 100 g/L. This co-extraction extent may not be favorable especially for downstream processes.

On the other hand, other sequences have the key drawback of significant Au losses during size reduction. Sequence D suffered severe loss as high as 53% while Sequence C and B suffered a total of 20% and 26% Au. Furthermore, a higher coextraction of Cu, especially for Sequence B, led to depletion of thiosulphate ions, which was suggested to be the result of its conversion to tetrathionate and other polythionates. As a result, there was a decrease in the extraction of Au from shredded PCBs. The leaching results also demonstrated that no Au was leached during Cu leaching suggesting that it is inert and simply peels off during the Cu leaching step.

Three factors, NH_3, S_2O_3 and S/L ratio, were optimized using the 2-level full factorial at specific levels of (0.5 and 1)M, (0.25 and 0.5)M, and (50 and 100) g/L. At 7.5 hours residence time, Trial 7 which was conducted at a concentration of 0.5M $S_2O_3^{2-}$ and 1M NH_3, and a S/L ratio of 100 g/L was found to be optimal. The optimization step also showed that it is essential to maintain a suitable thiosulphate/ammonia ratio to achieve a higher Au extraction. Trial 7, having a $S_2O_3^{2-}/NH_3$ ratio of 0.5 was able to attain equilibrium more quickly than any other trial. This Trial also exhibited faster leaching kinetics after managing to extract about 99% Au within 7.5 hours. In contrast to other trials, which saw fluctuating extractions after achieving the maximum extractions, Trial 7 was able to sustain the Au extracted in solution, thereby demonstrating stability for the dissolved Au in solution.

The results were also analyzed using the composite design functionality within the response surface methodology. The model showed that NH_3 and the $S_2O_3^{2-}$ interactions were the most statistically significant amongst other parameters which agreed which the optimization results. The generated model predicted that at 7.5 hours leaching time, the Au extraction at 1M NH_3 and 0.5M $S_2O_3^{2-}$ concentration and a S/L ratio of 100g/L would be 82%. This was not comparable to 99% Au extraction that was achieved during the leaching experiments. It was concluded that the model did not accurately fit the data.

6. RECOMMENDATIONS

A few things could be implemented to improve the extraction of Au from waste PCBs.

- The first step should be to perform leaching tests on completely whole waste PCBs that are not reduced in size. This would ensure that less Cu and other BM are not exposed to the leaching system during Au extraction using ammonium thiosulphate.
- It would be ideal to then apply the optimized Au leaching process further on actual e-waste to see or test the practicality of the method on actual waste PCBs.
- BMs that were not examined in this study should also be looked at, since they may affect the thiosulphate leaching of waste PCBs.
- In order to determine how much thiosulphate was degraded and the residual amount after leaching, it would also be helpful to do an iodometry-based analysis for residual thiosulphate.
- It would also be better to use fire assaying as it is more accurate to characterize waste PCBs and therefore accurately calculate the head grade of the waste PCBs.
- Lower concentrations less than 0.025M of CN should also be investigated and optimized, since the lowest concentration of cyanide gave higher extraction of Au and less co-extraction of BMs.
- To improve the Au extraction model generated by response surface methodology, further testing at wider parameter ranges and more replicates should be conducted in future tests to produce a more accurate model. Other parameters can also be added in the experimental design.

7. REFERENCES

1. Abbruzzese, C., Fornari, P., Massidda, R., Vegliò, F. & Ubaldini, S. 1995. Thiosulphate leaching for gold hydrometallurgy. *Hydrometallurgy.* 39(1):265-276. DOI:https://doi.org/10.1016/0304-386X(95)00035-F.
2. Akcil, A., Erust, C., Gahan, C.S., Ozgun, M., Sahin, M. & Tuncuk, A. 2015. Precious metal recovery from waste printed circuit boards using cyanide and non-cyanide lixiviants – A review. *Waste Management.* 45:258-271. DOI:https://doi.org/10.1016/j.wasman.2015.01.017.
3. Albertyn, P.W. 2017. Ammonium Thiosulphate Leaching of Gold from Printed Circuit Board Waste. Stellenbosch University. [13 September 2022].
4. Aylmore, M.G. & Muir, D.M. 2001. Thiosulfate leaching of gold—A review. *Minerals Engineering.* 14(2):135-174. DOI:https://doi.org/10.1016/S0892-6875(00)00172-2.
5. Baldé, C., Forti, V., Gray, V., Kuehr, R. & Stegmann, P. 2017. *The Global E-waste Monitor 2017: Quantities, Flows, and Resources.*
6. Bari, M., Begum, N., Hamaludin, S.B. & Kamarudin, H. 2009. Selective leaching for the recovery of copper from PCB, proceedings of the Malaysian Metallurgical Conference '09, 1-1.12 2009. *Kuala Perlis.*1-4.
7. Behnamfard, A., Salarirad, M.M. & Veglio, F. 2013. Process development for recovery of copper and precious metals from waste printed circuit boards with emphasize on palladium and gold leaching and precipitation. *Waste Management.* 33(11):2354-2363. DOI:https://doi.org/10.1016/j.wasman.2013.07.017.
8. Birich, A. 2020. Early Stage Gold Recovery from Printed Circuit Boards via Thiosulfate Leaching. RWTH Aachen University.
9. Birloaga, I., Michelis, I., Ferella, F., Buzatu, M. & Veglio, F. 2013. Study on the influence of various factors in the hydrometallurgical processing of waste printed circuit boards for copper and gold recovery. *Waste management (New York, N.Y.).* 33. DOI:10.1016/j.wasman.2013.01.003.
10. Breuer, P. & Jeffrey, M.I. 2002. An electrochemical study of gold leaching in thiosulfate solutions containing copper and ammonia. *Hydrometallurgy.* 65:145-157. DOI:10.1016/S0304-386X(02)00086-5.

11. Breuer, P.L. & Jeffrey, M.I. 2000. Thiosulfate leaching kinetics of gold in the presence of copper and ammonia. *Minerals Engineering.* 13(10):1071-1081. DOI:https://doi.org/10.1016/S0892-6875(00)00091-1.
12. Byerley, J.J., Fouda, S.A. & Rempel, G.L. 1973. Kinetics and mechanism of the oxidation of thiosulphate ions by copper(II) ions in aqueous ammonia solution. *Journal of the Chemical Society, Dalton Transactions.* 10.1039/DT9730000889(8):889-893. DOI:10.1039/DT9730000889.
13. Byerley, J.J., Fouda, S.A. & Rempel, G.L. 1975. Activation of copper(II) ammine complexes by molecular oxygen for the oxidation of thiosulphate ions. *Journal of the Chemical Society, Dalton Transactions.* 10.1039/DT9750001329(13):1329-1338. DOI:10.1039/DT9750001329.
14. Cadence®, C.P.S. 2023. *An Introduction to Printed Circuit Boards*. Cadence Design Systems. Available: https://www.cadence.com/en_US/home/tools/pcb-design-and-analysis.html [2023].
15. Cao, C., Hu, J. & Gong, Q. 1992. Leaching gold by low concentration thiosulfate solution. *Transactions of the Nonferrous Metals Society of China(China).* 2(4):21-25.
16. Cerchier, P., Dabalà, M. & Brunelli, K. 2017. Gold Recovery from PCBs with Thiosulfate as Complexing Agent. *Materials Science Forum.* 879:289-294. DOI:10.4028/www.scientific.net/MSF.879.289.
17. Chirume, B.H. 2019. *Investigation of a hydrometallurgical process route to recover metals from waste printed circuit boards.* Faculty of Engineering and the Built Environment.
18. Chu, C.K., Breuer, P.L. & Jeffrey, M.I. 2003. The impact of thiosulfate oxidation products on the oxidation of gold in ammonia thiosulfate solutions. *Minerals Engineering.* 16(3):265-271. DOI:https://doi.org/10.1016/S0892-6875(02)00369-2.
19. Cui, H. & Anderson, C. 2016. Literature Review of the Hydrometallurgical Recycling of Printed Circuit Boards (PCBs). *Journal of Advanced Chemical Engineering.* 6:11. DOI:10.4172/2090-4568.1000142.
20. Cui, H. & Anderson, C. 2020. Hydrometallurgical Treatment of Waste Printed Circuit Boards: Bromine Leaching. 10.3390/met10040462:18. DOI:10.3390/met10040462.

21. Cui, J. & Zhang, L. 2008a. Metallurgical recovery of metals from electronic waste: a review. *J Hazard Mater.* 158(2-3):228-256. DOI:10.1016/j.jhazmat.2008.02.001.
22. Cui, J. & Zhang, L. 2008b. Metallurgical recovery of metals from electronic waste: A review. Journal of Hazardous Materials, 158, 228-256. *Journal of hazardous materials.* 158:228-256. DOI:10.1016/j.jhazmat.2008.02.001.
23. EPA, U.S. 2015. *Report on the 2015 U.S. Environmental Protection Agency (EPA) International Decontamination Research and Development Conference*. (310425). Washington, DC. Available: https://cfpub.epa.gov/si/si_public_record_report.cfm?dirEntryId=310425&Lab=NHSRC&fed_org_id=1253&subject=Homeland%20Security%20Research&view=desc&sortby=pubDateYear&showcriteria=1&count=25.
24. Ficeriová, J., Baláž, P. & Gock, E. 2011. Leaching of gold, silver and accompanying metals from circuit boards (PCBs) waste. *Acta Montanistica Slovaca.* 16.
25. Flynn, C.M. & Haslem, S.M. 1995. *Cyanide Chemistry : Precious Metals Processing and Waste Treatment.* Washington D.C.
26. Forti, V., Baldé, C., Kuehr, R. & Bel, G. 2020. *The Global E-waste Monitor 2020. Quantities, flows, and the circular economy potential.*
27. Gámez, S., Garcés, K., De La Torre, E. & Guevara, A. 2019. Precious metals recovery from waste printed circuit boards using thiosulfate leaching and ion exchange resin. *Hydrometallurgy.* 186. DOI:10.1016/j.hydromet.2019.03.004.
28. Gertjegerdes, T. & Latacz, D. Eds. 2022. WEEE Recycling Routes and Alternatives. University of Cape Town, New Engineering Building, 7 November 2022. RWTH Aachen University.
29. Grosse, A.C., Dicinoski, G.W., Shaw, M.J. & Haddad, P.R. 2003. Leaching and recovery of gold using ammoniacal thiosulfate leach liquors (a review). *Hydrometallurgy.* 69(1):1-21. DOI:https://doi.org/10.1016/S0304-386X(02)00169-X.
30. Guo, X., Liu, J., Qin, H., Liu, Y., Tian, Q. & Li, D. 2015. Recovery of Metal Values from Waste Printed Circuit Boards using an Alkali Fusion-Leaching-Separation Process. *Hydrometallurgy.* 156. DOI:10.1016/j.hydromet.2015.06.011.

31. Ha, Lee, J.C., Jeong, J., Hai, H.T. & Jha, M.K. 2010. Thiosulfate leaching of gold from waste mobile phones. *J Hazard Mater.* 178(1-3):1115-1119. DOI:10.1016/j.jhazmat.2010.01.099.
32. Ha, Hung, V., Lee, J.-c., Huynh, T.H., Jeong, J. & Pandey, B.D. 2014. Optimizing the thiosulfate leaching of gold from printed circuit boards of discarded mobile phone. *Hydrometallurgy.* 149:118-126.
33. Hageluken, C. Ed. 2006. Improving metal returns and eco-efficiency in electronics recycling - a holistic approach for interface optimisation between pre-processing and integrated metals smelting and refining. 8-11 May 2006. 218-223.
34. He, Y. & Xu, Z. 2015. Recycling gold and copper from waste printed circuit boards using chlorination process. *RSC Advances.* 5(12):8957-8964. DOI:10.1039/C4RA16231E.
35. Hemmati, M. 1987. A study of thiosulfate leaching of gold from carbonaceous ore and the quantitative determination of thiosulfate in the leached solution. University of Nevada, Reno. Available: http://hdl.handle.net/11714/1361 [2017-06-30T19:38:34Z].
36. Hossain, M.S., Al-Hamadani, S. & Rahman, M.T. 2015. E-waste: A Challenge for Sustainable Development. *J Health Pollut.* 5(9):3-11. DOI:10.5696/2156-9614-5-9.3.
37. Işıldar, A., Rene, E., van Hullebusch, E. & Lens, P.N.L. 2017. Two-Step Leaching of Valuable Metals from Discarded Printed Circuit Boards, and Process Optimization Using Response Surface Methodology. *Advances in Recycling & Waste Management.* 02. DOI:10.4172/2475-7675.1000132.
38. Jeon, S., Tabelin, C.B., Takahashi, H., Park, I., Ito, M. & Hiroyoshi, N. 2018. Interference of coexisting copper and aluminum on the ammonium thiosulfate leaching of gold from printed circuit boards of waste mobile phones. *Waste Manag.* 81:148-156. DOI:10.1016/j.wasman.2018.09.041.
39. Jeon, S., Tabelin, C.B., Park, I., Nagata, Y., Ito, M. & Hiroyoshi, N. 2020a. Ammonium thiosulfate extraction of gold from printed circuit boards (PCBs) of end-of-life mobile phones and its recovery from pregnant leach solution by cementation. *Hydrometallurgy.* 191. DOI:10.1016/j.hydromet.2019.105214.
40. Jeon, S., Tabelin, C.B., Park, I., Nagata, Y., Ito, M. & Hiroyoshi, N. 2020b. Ammonium thiosulfate extraction of gold from printed circuit boards (PCBs) of end-of-life mobile

phones and its recovery from pregnant leach solution by cementation. *Hydrometallurgy*. 191:105214. DOI:https://doi.org/10.1016/j.hydromet.2019.105214.

41. Jergensen, G.V. 1999. *Copper leaching, solvent extraction, and electrowinning technology*. SME.
42. Kasper, A. & Veit, H. 2018. Gold recovery from printed circuit boards of mobile phones scraps using a leaching solution alternative to cyanide. *Brazilian Journal of Chemical Engineering*. 35:931-942. DOI:10.1590/0104-6632.20180353s20170291.
43. Kaya, M. 2019. *Electronic Waste and Printed Circuit Board Recycling Technologies*. 1. Springer ChamDOI:https://doi.org/10.1007/978-3-030-26593-9.
44. Kerley Jr, B. 1983. Recovery of precious metals from difficult ores. *Off. Gaz.*
45. Kholmogorov, A.G., Kononova, O.N., Pashkov, G.L. & Kononov, Y.S. 2002. Thiocyanate solutions in gold technology. *Hydrometallurgy*. 64(1):43-48.
46. Koyama, K., Tanaka, M. & Lee, J.-c. 2006. Copper Leaching Behavior from Waste Printed Circuit Board in Ammoniacal Alkaline Solution. *MATERIALS TRANSACTIONS*. 47(7):1788-1792. DOI:10.2320/matertrans.47.1788.
47. Leaver, E.S. & Woolf, J.A. 1931. *Copper and zinc in cyanidation sulphide-acid precipitation*. US Bureau of Mines.
48. Levenspiel, O. 1973. Chemical reaction engineering, Octave , Wiley, New York (1972). 578 pages. $16.95. *AIChE Journal*. 19(1):206-207. DOI:https://doi.org/10.1002/aic.690190143.
49. Li, J.Y., Xu, X.L. & Liu, W.Q. 2012. Thiourea leaching gold and silver from the printed circuit boards of waste mobile phones. *Waste management (New York, N.Y.)*. 32:1209-1212. DOI:10.1016/j.wasman.2012.01.026.
50. Liddell, K. 2005. Shrinking core models in hydrometallurgy: What students aren't being told about the pseudo-steady approximation. *Hydrometallurgy*. 79:62-68. DOI:10.1016/j.hydromet.2003.07.011.
51. Long, H., Jeong, J., Lee, J.-C., Pandey, B.D., Yoo, J.-M. & Huyunh, T.H. 2011. Hydrometallurgical Process for Copper Recovery from Waste Printed Circuit Boards (PCBs). *Mineral Processing and Extractive Metallurgy Review*. 32(2):90-104. DOI:10.1080/08827508.2010.530720.

52. Lucheva, B., Iliev, P. & Kolev, D. 2017. Recovery Of gold from electronic waste by iodine-iodide leaching. *Journal of Chemical Technology and Metallurgy*. 52:326-332.
53. Lydall, M., Nyanjowa, W. & James, Y. 2017. *Mapping South Africa's Waste Electrical and Electronic Equipment (WEEE) Dismantling, Pre-Processing and Processing Technology Landscape*. Johannesburg.
54. Macrotrends©, L.-. 2023. *Gold Prices - 100 Year Historical Chart*. Available: https://www.macrotrends.net/1333/historical-gold-prices-100-year-chart [2023, 06/02/2023].
55. Marsden, J. & House., C.I. 2006. *Chemistry of Gold Extraction* second. Littleton: SME. Available: https://search.ebscohost.com/login.aspx?direct=true&scope=site&db=nlebk&db=nlabk&AN=435087.
56. Mecucci, A. & Scott, K. 2002. Leaching and electrochemical recovery of copper, lead and tin from scrap printed circuit boards. *Journal of Chemical Technology & Biotechnology*. 77(4):449-457. DOI:https://doi.org/10.1002/jctb.575.
57. Mishra, G., Jha, R., Rao, M., Meshram, A. & Singh, K. 2021. Recovery of Silver from Waste Printed Circuit Boards (WPCBs) through Hydrometallurgical Route: A Review. *Environmental Challenges*. 4:100073. DOI:10.1016/j.envc.2021.100073.
58. Montero, R., Guevara, A. & De La Torre, E. 2012. Recovery of gold, silver, copper and niobium from printed circuit boards using leaching column. 2:590-595.
59. Moyo, T., Chirume, B.H. & Petersen, J. 2020. Assessing alternative pre-treatment methods to promote metal recovery in the leaching of printed circuit boards. *Resources, conservation and recycling*. 152:104545. DOI:https://doi.org/10.1016/j.resconrec.2019.104545.
60. Nesakumar, R. & K, C. 2014. Copper extraction from the discarded printed circuit board by leaching. *International Journal of Chemical & Petrochemical Technology (IJCPT)*. 4:11-16.
61. Ogunniyi, I.O. & Vermaak, M.K.G. 2009. FROTH FLOTATION FOR BENEFICIATION OF PRINTED CIRCUIT BOARDS COMMINUTION FINES: AN OVERVIEW. *Mineral*

Processing and Extractive Metallurgy Review. 30(2):101-121. DOI:10.1080/08827500802333123.

62. Oishi, T., Koyama, K., Alam, S., Tanaka, M. & Lee, J.C. 2007. Recovery of high purity copper cathode from printed circuit boards using ammoniacal sulfate or chloride solutions. *Hydrometallurgy.* 89(1):82-88. DOI:https://doi.org/10.1016/j.hydromet.2007.05.010.
63. Panda, R., Dinkar, O., Kumari, A. & Jha, M. 2020. Hydrometallurgical processing of waste integrated circuits (ICs) to recover Ag and generate mix concentrate of Au, Pd and Pt. *Journal of Industrial and Engineering Chemistry.* 10.1016/j.jiec.2020.10.007. DOI:10.1016/j.jiec.2020.10.007.
64. Peng, P. & Park, A.-H. 2020a. Supercritical CO 2 -induced alteration of polymer-metal matrix and selective extraction of valuable metals from waste printed circuit boards. *Green Chemistry.* 22. DOI:10.1039/D0GC02521F.
65. Peng, P. & Park, A.-H.A. 2020b. Supercritical CO2-induced alteration of a polymer–metal matrix and selective extraction of valuable metals from waste printed circuit boards. *Green Chemistry.* 22(20):7080-7092. DOI:10.1039/D0GC02521F.
66. Petter, P., Veit, H. & Bernardes, A. 2013. Evaluation of gold and silver leaching from printed circuit board of cellphones. *Waste management (New York, N.Y.).* 34. DOI:10.1016/j.wasman.2013.10.032.
67. Prestele, M.P. 2020. Assessment of a Shredding Technology of Waste Printed Circuit Boards in preparation for Ammonia-based Copper leaching. Available: http://hdl.handle.net/11427/32969.
68. Radmehr, V., Koleini, S.M.J., Khalesi, M.R. & Tavakoli Mohammadi, M.R. 2013. Ammonia Leaching: A New Approach of Copper Industry in Hydrometallurgical Processes. *Journal of The Institution of Engineers (India): Series D.* 94:95-104. DOI:10.1007/s40033-013-0029-x.
69. Rudnik, E., Pierzynka, M. & Handzlik, P. 2016. Ammoniacal leaching and recovery of copper from alloyed low-grade e-waste. *Journal of Material Cycles and Waste Management.* 18(2):318-328. DOI:10.1007/s10163-014-0335-x.
70. Sayiner, B. & Acarkan, N. 2014. Effect of silver, nickel and copper cyanides on gold adsorption on activated carbon in cyanide leach solutions. *Fizykochemiczne Problemy*

Mineralurgii - Physicochemical Problems of Mineral Processing. 50:277-287. DOI:10.5277/ppmp140123.

71. Senanayake, G. 2005. Gold leaching by thiosulphate solutions: a critical review on copper(II)–thiosulphate–oxygen interactions. *Minerals Engineering.* 18(10):995-1009. DOI:https://doi.org/10.1016/j.mineng.2005.01.006.
72. Senanayake, G. 2007. Review of rate constants for thiosulphate leaching of gold from ores, concentrates and flat surfaces: Effect of host minerals and pH. *Minerals Engineering.* 20(1):1-15. DOI:https://doi.org/10.1016/j.mineng.2006.04.011.
73. Senanayake, G., Perera, W. & Nicol, M. 2003. Thermodynamic studies of the gold (III)/(I)/(0) redox system in ammonia-thiosulphate solutions at 25 C.
74. Shuey, S.A., Vildal, E.E. & Taylor, P.R. 2006. Pyrometallurgical processing of electronic waste. *SME Annual Meeting.* Available: https://www.scopus.com/inward/record.uri?eid=2-s2.0-60249095285&partnerID=40&md5=af9e900765b376cc9fb56e6671bf2eda:1-8.
75. Sitando, O., Senanayake, G., Dai, X., Nikoloski, A. & Breuer, P. 2018. A review of factors affecting gold leaching in non-ammoniacal thiosulfate solutions including degradation and in-situ generation of thiosulfate. *Hydrometallurgy.* 178. DOI:10.1016/j.hydromet.2018.02.016.
76. Tanisali, E., Özer, M. & Burat, F. 2021. Precious Metals Recovery from Waste Printed Circuit Boards by Gravity Separation and Leaching. *Mineral Processing and Extractive Metallurgy Review.* 42(1):24-37. DOI:10.1080/08827508.2020.1795849.
77. Tripathi, A., Kumar, M., Sau, D., Agrawal, A., Chakravarty, S. & Mankhand, T. 2012. Leaching of Gold from the Waste Mobile Phone Printed Circuit Boards (PCBs) with Ammonium Thiosulphate. *International Journal of Metallurgical Engineering.* 1:17-21. DOI:10.5923/j.ijmee.20120102.02.
78. Tuncuk, A., Stazi, V., Akcil, A., Yazici, E.Y. & Deveci, H. 2012. Aqueous metal recovery techniques from e-scrap: Hydrometallurgy in recycling. *Minerals Engineering.* 25(1):28-37. DOI:https://doi.org/10.1016/j.mineng.2011.09.019.
79. Tykodi, R.J. 1990. In praise of thiosulfate. *Journal of Chemical Education.* 67(2):146. DOI:10.1021/ed067p146.

80. Veit, H.M. & Bernardes, A.M. 2015. Electronic waste. *Recycling Techniques.* 165.
81. Vijayaram, R., Nesakumar, D. & Chandramohan, K. 2013. Copper extraction from the discarded printed circuit board by leaching. *Research Journal of Engineering Sciences.* 2:11-14
82. Wan, R. & Brierly, J. 1997. Thiosulfate leaching following biooxidation pretreatment for gold recovery from refractory carbonaceous-sulfidic ore. *Mining Engineering(Colorado)(USA).*76-80.
83. Wang, R., Chenglong, Z., Zhao, Y., Zhou, Y., En, M., Bai, J. & Wang, J. 2020. Recycling Gold from Printed Circuit Boards Gold-plated Layer of Waste Mobile Phones in "Mild Aqua Regia" System. *Journal of Cleaner Production.* 278:123597. DOI:10.1016/j.jclepro.2020.123597.
84. Widmer, R., Oswald-Krapf, H., Sinha-Khetriwal, D., Schnellmann, M. & Böni, H. 2005. Global perspectives on e-waste. *Environmental Impact Assessment Review.* 25(5):436-458. DOI:https://doi.org/10.1016/j.eiar.2005.04.001.
85. Wu, Z., Yuan, W., Li, J., Wang, X., Liu, L. & Wang, J. 2017. A critical review on the recycling of copper and precious metals from waste printed circuit boards using hydrometallurgy. *Frontiers of Environmental Science & Engineering.* 11. DOI:10.1007/s11783-017-0995-6.
86. Xiu, f.-r., Qi, Y. & Zhang, F.-S. 2015. Leaching of Au, Ag, and Pd from waste printed circuit boards of mobile phone by iodide lixiviant after supercritical water pre-treatment. *Waste management (New York, N.Y.).* 41. DOI:10.1016/j.wasman.2015.02.020.
87. Xu, B., Kong, W., Li, Q., Yang, Y. & Liu, X. 2017. A Review of Thiosulfate Leaching of Gold: Focus on Thiosulfate Consumption and Gold Recovery from Pregnant Solution. *Metals.* 7:222. DOI:10.3390/met7060222.
88. Yang, H., Liu, J.a. & Yang, J. 2011. Leaching copper from shredded particles of waste printed circuit boards. *Journal of hazardous materials.* 187:393-400. DOI:10.1016/j.jhazmat.2011.01.051.
89. Yang, T., Xu, Z., Wen, J. & Yang, L. 2009. Factors influencing bioleaching copper from waste printed circuit boards by Acidithiobacillus ferrooxidans. *Hydrometallurgy.* 97(1):29-32. DOI:https://doi.org/10.1016/j.hydromet.2008.12.011.

90. Yang, T., Zhu, P., Liu, W., Chen, L. & Zhang, D. 2017. Recovery of tin from metal powders of waste printed circuit boards. *Waste Management.* 68:449-457. DOI:https://doi.org/10.1016/j.wasman.2017.06.019.
91. Yu, J., Williams, E. & Ju, M. Eds. 2009. Review and prospects of recycling methods for waste printed circuit boards. 18-20 May 2009. 1-5.
92. Zhang, X.M., Senanayake, G. & Nicol, M.J. 2004. A study of the gold colloid dissolution kinetics in oxygenated ammoniacal thiosulfate solutions. *Hydrometallurgy.* 74(3):243-257. DOI:https://doi.org/10.1016/j.hydromet.2004.05.007.
93. Zhukov, V., Sharikov, Y. & Turunen, I. 2013. Modeling of Gold Leaching with Thiosulphate Solutions in Different Types of Reactor. *Computer Aided Chemical Engineering.* 32:1045-1050. DOI:10.1016/B978-0-444-63234-0.50175-5.
94. Zipperian, D., Raghavan, S. & Wilson, J.P. 1988. Gold and silver extraction by ammoniacal thiosulfate leaching from a rhyolite ore. *Hydrometallurgy.* 19(3):361-375. DOI:https://doi.org/10.1016/0304-386X(88)90041-2.

8. APPENDICES

8.1 Determination of the head grade

8.1.1 Raw data for digestion tests using Aqua Regia Leach

Table 8-1 shows the mass lost after pulverization, in preparation for the digestion tests using both reverse aqua regia and aqua regia leach. The mass of the PCBs (before pulverisation) was taken as an average mass of population size (n) =21 PCBs. Average mass of the PCBs (after pulverisation) was taken as an average mass of sample size (n) = 5 PCBs

Table 8-1: Particle size reduction in preparation for digestion tests

	Average mass of PCB (g)	**Sample size**	**Standard Deviation**	**Standard Error**
Before pulverisation	**51.8**	21	0.416	0.09084
After Pulverisation	**45.7**	5	0.6707	0.146
Loss	6.0423			

The loss and standard error (SE) were calculated using the equation A1 and A2 below.

$$Loss = mass\ of\ the\ PCB\ before\ pulverization - mass\ of\ the\ PCB\ after\ pulverization \quad \text{(A1)}$$

$$Standard\ Error\ (SE) = \frac{Standard\ Deviation\ (SD)}{\sqrt{Sample\ Size\ (n)}} \quad \text{(A2)}$$

8.1.2 Head grade calculation

The masses of Au, Cu, and Ni extracted in each stage of PCB digestion are displayed in Table 8-2. Equation A3 is the formula used to calculate the head grade of each PCB. Each PCB weighs approximately 51.77g. After pulverization it reduced to 45.7g as shown in Table 8-1. The following notation in Table 8-2, represent the following:

(1)-Reverse aqua regia of fresh sample

(2)-Aqua regia of residue from (1)

(3)-microwave assisted digestion analysis from (2)

Table 8-2: Head grade calculation from the digestion tests

Test	***mg of each metal extracted in each test***							
	Au	***Cu***	***Ni***	***Sn***	***Au***	***Cu***	***Ni***	***Sn***
	Charred PCB				***Uncharred PCB***			
(1)	3.44	8865.50	127.78	0.043	3.14	7897.18	114.29	0
(2)	0.046	295.52	0.42	0	0	63.37	1.64	0
(3)	0.057	3.31	0.56	0	0	0	0	0
Total mass Pulverized PCB	3.54	9164.32	128.75	3.59	3.14	7960.55	115.93	0
Total mass Fresh PCBs (Head grade) (3 sf)	**4.01**	**10400**	**146**	**3.88**	**3.55**	**9010**	**131**	**0**

$$Head\ grade\ (mg/PCB) = \\ = total\ mass\ of\ metal\ (pulverised\ PCB) \times \frac{mass\ of\ fresh\ PCBs}{mass\ of\ pulverized\ PCBs} \quad \text{(A3)}$$

8.2 Simulation of Au leaching from PCBs using Au leaf and Metallic Cu and Ni

8.2.1 Determination of the composition of Au leaf

The total mass of Au, Cu, and Ni, respectively, extracted during the aqua regia tests from each Au leaf, after a 24-hour residence time, is shown in Table 8-3. The mass of each metal extracted was calculated using equations A4 and A5. Table 8-4 shows the calculated masses of each metal, introduced into the leaching system during the simulation tests. The total leachable percentages outlined in Table 8-4, were each obtained from a study done by Chirume, (2019) on similar PCBs, detailed in section 3.1.1.

Table 8-3: Mass of metal extracted from digestion of Au leaf

Test	***Mass of Au leaf (mg)***	***mg of each metal extracted from digestion***		
		Au	***Cu***	***Ni***
1	16.22	15.1	0.99	0.005
2	14.32	13.36	0.33	0.004
3	15.68	14.6	0.17	0.004
Average	**15.4**	**14.4**	**0.50**	**0.004**
%	**100%**	**93.2%**	**3.2%**	**0.026%**
SD	0.8	0.73	0.00036	0.36
SE	0.46	0.42	0.00021	0.21

Where;

$$Mass\ of\ metal\ extracted\ (mg) = \frac{Initial\ volume\ of\ the\ lixiviant}{mass\ of\ Au\ leaf\ sample} \times metal\ concentration\ detected\ in\ aliquot\ \times mass\ of\ original\ Au\ leaf\ sample \quad \text{(A4)}$$

OR

$$Mass\ of\ metal\ extracted\ (mg) = \frac{1}{S{:}L\ (Ratio)}\left(\frac{L}{g}\right) \times\ metal\ concentration\ detected\ in\ aliquot\ \left(\frac{mg}{L}\right) \times mass\ of\ original\ Au\ leaf\ sample\ (g) \quad \text{(A5)}$$

The same formula was used to calculate the Au, Cu and Ni extraction from all MP-AES results from each aliquot.

Table 8-4:Mass of each element to be added in the simulation test

Test	***Mass***	***Metal***		
		Au	***Cu***	***Ni***
Head grade	51.8 g/PCB	4.01mg/PCB	10 400 mg/PCB	146 mg/PCB
Total leachable % of each metal in 1 PCB		100%	31%	100%
Corresponding % To be added during simulation.	100% Au leaf (1 leaf per experiment)	93.1% Au (concentration of Au per Au leaf (Table 8-3))	31% of 10 400 mg Cu (estimated % of the leachable Cu in 1 PCB)	100% Ni of Ni foil (estimated % of the

				leachable Ni in1 PCB)
Mass to be added during simulation.	**15.4 g (total mass of 1 Au leaf)**	**14.4 mg (per Au leaf)**	**11500 mg**	**519 mg**

$$mass\ of\ Cu\ to\ be\ added\ during\ simulation = \frac{14.34\ mg}{4.01\ mg} \times 0.31(10375\ mg) = \mathbf{11500\ mg\ to\ 3sf} \quad \text{(A6)}$$

$$mass\ of\ Ni\ to\ be\ added\ during\ simulation = \frac{14.34\ mg}{4.01\ mg} \times 1\ (145\ mg) = \mathbf{519\ mg\ (3sf)} \quad \text{(A7)}$$

8.2.2 Simulation tests

The total mass of Au extracted from each aliquot is displayed in Table 8-6. Table 8-5 also lists the amounts of Cu and Ni that were simultaneously extracted from each aliquot at the specified time. Each metal mass is an average of the three leaching tests that were carried out for each test. The mass extracted and consequently the percentage of metal extraction per aliquot were then determined using Equation A8–10.

Table 8-5: mg of metals extracted in the leaching of Au leaf in the presence of Cu and Ni

Time (Hours)	***Au mg/leaf in 0.5 M $S_2O_3^{2-}$ + Cu + Ni***			***Au mg/leaf in 0.5 M CN^- + Cu + Ni***		
	Au	***Cu***	***Ni***	***Au***	***Cu***	***Ni***
0	0	0	0	0	0	0
1	0	1420	0.20	0	0	0
2	0.0001	4190	6.56	0	0	0
5	0.0005	4620	146	0	0	0
8	0.0008	4620	187	0	0	0
9	-	-	-	0	0	0
20	0.0058	4620	187	0	0	0
24	0.0056	4620	187	0.0049	5.78	139
30	0.0055	4620	187	0.0050	5.20	139

$$Mass\ of\ metal\ extracted\ (mg) = \frac{1}{S{:}L\ (Ratio)}\left(\frac{L}{g}\right) \times\ metal\ concentration\ detected\ in\ aliquot\ \left(\frac{mg}{L}\right) \times mass\ of\ original\ PCB\ sample\ (g\ ) \quad \text{(A8)}$$

$$\%Extraction = \frac{mass\ of\ metal\ extracted\ (mg)}{total\ metal\ mass\ from\ Head\ Grade\ calculation\ (mg)} \times 100\% \quad \text{(A9)}$$

For thiosulphate leaching:

$$\%\ Cu\ Extraction = \frac{mass\ of\ metal\ extracted\ (mg) - initial\ Cu^{2+}\ added\ initially\ into\ lixiviant\ (mg)}{total\ metal\ mass\ from\ Head\ Grade\ calculation\ (mg)} \times 100\% \quad \text{(A10)}$$

Table 8-6: mg Au extracted in the leaching of Au leaf without any interference

Time (Hours)	***Au mg/leaf without any interference***	
	0.5 M $S_2O_3^{2-}$	***0.5 M*** CN^-
0	0	0
1	0.0140	0.0123
2	0.0139	0.0122
4	0.0137	0.0121
6	0.0136	0.0122
8	0.0140	0.0122
24	0.0140	0.0122
30	10.2	11

8.3 Sequencing Tests

The masses calculated for each leaching sequence A–D are shown in Table 8-7 and Table 8-8, respectively. The computations for each value followed the steps outlined in equations A8–A10 for the prior calculations.

Table 8-7: Leaching results for sequence A and B (Au leaching)

Time	***Sequence A- mg/PCB***			***Sequence B- mg/PCB***		
(Hours)	***Au***	***Cu***	***Ni***	***Au***	***Cu***	***Ni***
0	0	0	0	0	0	0
0.5	1.48	170	13.7	-	-	-
2	1.53	809	36.0	1	1070	48.5
4	2.39	1180	97.4	1	1070	48.5
5	3.39	1690	120	1.5	1630	75.8
7	3.96	2140	140	2.4	1830	96.9
8	3.84	2480	142	2.5	2068	107.2
9	3.88	2910	141	2.7	2490	121
24	3.89	4360	142	2.75	2500	121
Cu leaching tests for sequence C and D						
Time	***Sequence C- mg/PCB***			***Sequence D- mg/PCB***		
(Hours)	***Au***	***Cu***	***Ni***	***Au***	***Cu***	***Ni***
0	0	0	0	0	0.00	0.00
1.5	0	9.25	0.45	0	14.5	1.21
3.5	0	52.8	1.4	0	871	2.90
6	0	111	2.53	0	978	0.34
9	0	212	4.65	0	1596	57.2
24	0	1780	99	0	3117	98.02
27	0	1810	113	0	3530	101
48	0	2004.5	119	0	3590	103.8
72	0	2390	117	0	4601	103.8

Table 8-8: Leaching results for sequence C and D Au leaching

Time (Hours)	***Sequence C- mg/PCB***			***Sequence D- mg/PCB***		
	Au	***Cu***	***Ni***	***Au***	***Cu***	***Ni***
0	0.00	0.00	0	0.00	0.00	0
0.5	119	32	0	42.6	19.8	0
2	2.41	63.9	0	80.23	42.6	0
4	2.43	129	0	1.64	91.7	0
5	2.44	109.5	0	1.67	96.3	0
7	2.40	178	0	1.60	149	0
8	2.20	190.4	0	1.61	158	0
9	2.44	435	0	1.57	643	0
24	2.45	972	0.02	1.87	646	0.01

8.4 Optimisation

Table 8-9 to Table 8-12 list the mass of each metal that was extracted from trials 1 through 8. The calculations for each value followed the steps outlined in equations A8–A10 for the prior calculations.

Table 8-9: Leaching results for trial 1 and 2

Time (Hours)	***Trial 1- mg/PCB***			***Trial 2- mg/PCB***		
	Au	***Cu***	***Ni***	***Au***	***Cu***	***Ni***
0	0	0	0.45	0	0	1.48
0.5	2	230	2.26	1.87	721	1.72
2.5	2.01	87.7	5.34	1.87	-	9.23
4.5	1.95	805	10.42	1.33	1060	7.10
6.5	2.36	1520	18.03	2.00	1150	24.5
7.5	2.79	1590	20.69	2.03	1390	32.2
8.5	3.08	1730	43.2	1.62	1930	38.8
9.5	3.08	1570	51.3	2.04	2640	45.3
24	3.08	1740	54.3	2.15	3630	56.6

Table 8-10:Leaching results for trial 3 and 4

Time (Hours)	***Trial 3- mg/PCB***			***Trial 4- mg/PCB***		
	Au	***Cu***	***Ni***	***Au***	***Cu***	***Ni***
0	0	0	0	0	0	0
0.5	0.87	181	5.77	1	340	11.2
2.5	0.9	268	19.5	1.36	490	26.5
4.5	0.93	589	36.2	1.53	1014	58.3
6.5	1.23	834	48.1	1.53	1330	66.3
7.5	1.29	1170	70.4	2.04	1900	103
8.5	1.37	1410	81.2	3.74	2800	168
9.5	1.6	1520	91.8	3.57	2630	170
24	2.9	2270	137	3.22	2750	141

Table 8-11: Leaching results for trial 5 and 6

Time (Hours)	***Trial 5- mg/PCB***			***Trial 6 mg/PCB***		
	Au	***Cu***	***Ni***	***Au***	***Cu***	***Ni***
0	0	0	0	0	0	0
0.5	1.3	457	16.1	1.44	369	11.3
2.5	1.3	635	28.3	1.8	763	22.7
4.5	1.5	134	59.1	1.98	1360	58.0
6.5	1.7	1470	68.6	2.16	1460	68.8
7.5	1.8	1080	56.4	4	2640	108
8.5	2.4	1890	123	3.6	2520	137
9.5	2.2	1940	129	3.2	2520	144
24	2.4	1840	130	3.4	2600	139

Table 8-12: Leaching results for trial 7 and 8

Time (Hours)	***Trial 7- mg/PCB***			***Trial 8- mg/PCB***		
	Au	***Cu***	***Ni***	***Au***	***Cu***	***Ni***
0	0	0	0	0	0	0
0.5	1.48	170	13.3	0.9	79.2	13.3
2.5	1.53	809	36.0	1.02	602	35.5
4.5	2.39	1180	97.4	1.02	909	50.3
6.5	3.39	1690	120	1.26	1690	89.8
7.5	3.96	2140	140	1.68	1790	102
8.5	3.84	2480	142	2.28	1940	114
9.5	3.88	2910	141	3.42	2860	144
24	3.89	4360	142	3.45	2960	146

8.5 Cyanide Leaching

The calculated mass for each cyanide leaching test is shown in Table 8-13 and Table 8-14, respectively. Each table's concentrations range from 0.025M to 0.5M, accordingly.

Table 8-13:Leaching results of cut PCBs in 0.025M and 0.05M CN, respectively.

Time (Hours)	***mg/PCB in 0.025 M CN***			***mg/PCB 0.05 M CN***		
	Au	***Cu***	***Ni***	***Au***	***Cu***	***Ni***
0	0.0	0.0	0.0	0.0	0.0	0.0
1	1.8	12.6	0.1	0.8	15.0	0.2
2	2.1	32.1	0.8	1.3	44.8	0.8
4	2.3	64.0	2.0	1.7	68.2	1.9
6	2.4	152	6.7	2.2	156.7	6.5
9	2.7	156	10.3	2.2	197.5	9.9
20	2.7	210	18.5	2.2	223.4	17.2
24	2.7	201	18.5	2.2	402.8	30.2

Table 8-14: Leaching results of cut PCBs in 0.25M and 0.5M CN, respectively.

Time	***mg/PCB in in 0.25 M CN***			***mg/PCB in 0.5 M CN***		
(Hours)	***Au***	***Cu***	***Ni***	***Au***	***Cu***	***Ni***
0	0.00	0.0	0.0	0	0	0
1	0.63	11.7	0.4	1.15	32.5	0.375
2	1.18	34.0	0.9	1.43	31.5	0.85
4	1.43	57.0	3.2	1.53	106	2.85
6	1.63	118	7.9	1.43	173	6.3
9	1.73	192	20.0	1.43	370	15.3
20	1.73	352	30.0	1.43	1270	60
24	1.80	1340	84.5	0	0	0

8.6 pH

The average values obtained for each set of tests from section 8.1 to 8.5 are represented by the pH values in Table 8-15 through Table 8-18. As indicated previously, each figure represents an average of three repetitions. Figure 8-1 shows the pH plot obtained in Table 8-17.

Table 8-15:The average pH recorded in during each simulation test.

Time	**pH**			
(Hours)	***0.5 M*** $S_2O_3^{2-}$	***0.5 M*** CN^-	***0.5 M*** $S_2O_3^{2-}$ ***+ Cu + Ni***	***0.5 M*** CN^- ***+ Cu + Ni***
0	10.4	10.9	10.1	11
0.5	10.4	10.9	10.2	11
2	10.3	10.9	10.2	12.4
2.5	10.3	11	10.2	12.6
4	10.3	11	10.2	12.7
5	10.3	11	10.2	12.8
8	10.3	11	10.2	12.9
24	10.2	11	10.2	12.9

Table 8-16: The pH average recorded during each sequence test.

Time (Hours)	**pH**			
	Sequence A	***Sequence B***	***Sequence C***	***Sequence D***
0	10.1	10.4	10.0	10.5
0.5	10.1	10.3	10.1	10.4
2	10.1	10.3	10.1	10.4
2.5	10.1	10.3	10.1	10.3
4	10.0	10.3	10.1	10.3
5	10.2	10.3	10.1	10.3
8	10.2	10.3	10.1	10.3
24	10.3	10.3	10.1	10.3

Table 8-17: The pH average recorded in each trial.

Time (Hours)	**pH**							
	Trial 1	***Trial 2***	***Trial 3***	***Trial 4***	***Trial 5***	***Trial 6***	***Trial 7***	***Trial 8***
0	10.3	10.3	9.9	9.87	10.4	10.4	10.1	10.3
0.5	10.2	10.4	9.91	9.92	10.4	10.4	10.1	10.3
1.5	10.2	10.3	9.95	9.92	10.4	10.4	10.1	10.3
2.5	10.2	10.3	9.89	9.91	10.4	10.4	10.1	10.2
3	10.2	10.3	9.9	9.91	10.4	10.4	10.0	10.2
6	10.1	10.3	9.89	9.90	10.3	10.4	10.2	10.2
8	10.1	10.3	9.94	9.90	10.4	10.4	10.2	10.2
9	10.1	10.3	9.89	9.90	10.4	10.4	10.2	10.2
24	10.0	10.1	9.89	9.88	10.4	10.4	10.3	10.2

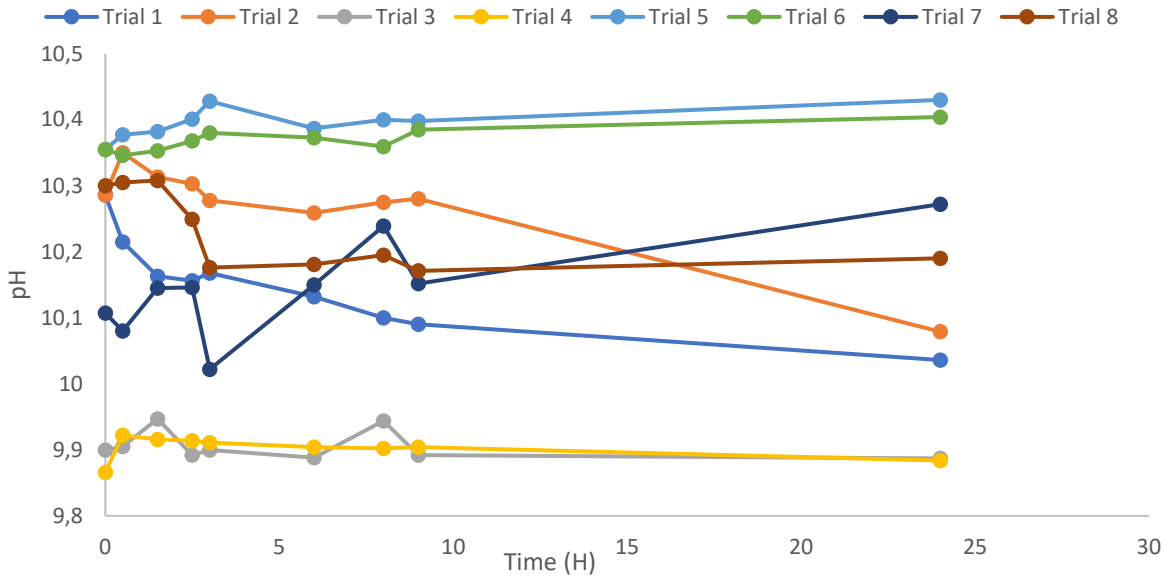

Figure 8-1:The pH average recorded in each trial.

Table 8-18: The pH average recorded during CN benchmarking tests.

Time (Hours)	**pH**			
	0.025 M CN^-	***0.05 M CN^-***	***0.25 M CN^-***	***0.5 M CN^-***
0	10.8	10.9	11.0	11.1
0.5	10.7	10.9	11.1	11.1
1.5	10.8	10.9	11.0	11.1
2.5	10.8	11.0	11.1	11.2
3	10.8	11.0	11.0	11.2
6	10.9	11.0	11.1	11.2
8	10.9	11.0	11.2	11.2
9	10.9	10.9	11.2	11.3
24	10.9	10.9	12	11.3

8.7 Mass balances

Table 8-19 to Table 8-21 shows the mass of Au, Cu, and Ni in each stage of PCB leach residue from each specified test. Equation A3 is the formula used to calculate the mass of each PCB, which weighed approximately 45g each. Table 8-23 to Table 8-24 show the total mass balance computed from Table 8-19 to Table 8-21.

Table 8-19: mass (mg) calculated from the aqua regia digestion tests of the PCB leached residue from the sequencing tests

Test	**Reverse Aqua regia Tests**		
	Au	**Cu**	**Ni**
	mg/PCB	***mg/PCB***	***mg/PCB***
Sequence A- $S_2O_3^{2-}$ **leached residue**	0.00093	5723.12	1.19
Sequence B- $S_2O_3^{2-}$ **leached residue**	0.18	5850.22	1.16
Sequence C- $S_2O_3^{2-}$ **leached residue**	0.10	6293.81	0.64
Sequence D- $S_2O_3^{2-}$ **leached residue**	0.00	1248.63	0.58
0.5 M CN leached residue	2.18	7724.63	29.73

Table 8-20: mass (mg) calculated from the aqua regia digestion tests of the PCB leached residue from the sequencing tests

Test	**Aqua regia Tests**		
	Au	**Cu**	**Ni**
	mg/PCB	***mg/PCB***	***mg/PCB***
Sequence A- $S_2O_3^{2-}$ **leached residue**	0.00	12.75	0.27
Sequence B- $S_2O_3^{2-}$ **leached residue**	0.00	21.19	0.26
Sequence C- $S_2O_3^{2-}$ **leached residue**	0.00	30.53	0.20
Sequence D- $S_2O_3^{2-}$ **leached residue**	0.00	12.10	0.024
0.5 M CN leached residue	0.017	38.96	0.68

Table 8-21: mass (mg) calculated from the microwave assisted digestion tests of the PCB leached residue from the sequencing tests

Test	**Microwave assisted digestion**		
	Au	**Cu**	**Ni**
	mg/PCB	***mg/PCB***	***mg/PCB***
Sequence A- $S_2O_3^{2-}$ **leached residue**	0.00	74.60	0.23
Sequence B- $S_2O_3^{2-}$ **leached residue**	0.00	2.024	0.27
Sequence C- $S_2O_3^{2-}$ **leached residue**	0.64	24.10	0.17
Sequence D- $S_2O_3^{2-}$ **leached residue**	0.0011	1.86	0.18
0.5 M CN leached residue	0.00	20.51	0.53

Table 8-22: Closing the total mass balance (%) of the 0.5M CN leaching tests

Total Mass balance for 0.5M CN leaching of PCBs			
	Cut PCBs		
	Au	**Cu**	**Ni**
Au Leaching	1.52	1352	84.68
Residue after leaching	2.18	7784.1	30.94
total %	3.72	9136	115.62
lost %	0.29	1240	30.38

Table 8-23:Closing the total mass balance of the sequencing tests C and D

Total Mass balance for the leaching of PCBs (includes a Cu leaching stage) (mg)						
	Sequence C (Cut)			**Sequence D (Shred)**		
	Au	**Cu**	**Ni**	**Au**	**Cu**	**Ni**
Cu leaching	0	2390.25	117.25	0	4601.97	103.84
Au Leaching	2.45	971.65	0.02	1.87	645.66	0.01
Sub-total	**2.45**	**3361.9**	**117.27**	**1.87**	**5247.63**	**103.85**
reverse Aqua regia leached residue	0.1	6293.81	0.64	0	1248.63	0.58
Aqua regia leached residue	0	0.53	0.2	0	12.1	0.024
Microwave assisted digestion	0.64	24.1	0.17	0.0011	1.86	0.18
total (mg)	**3.19**	**9680.34**	**118.28**	**1.8711**	**6510.22**	**104.634**
lost (mg)	0.82	695.05	27.49	2.1389	3865.17	41.136

Table 8-24:Closing the total mass balance of the sequencing tests A and B.

Total Mass balance for the leaching of PCBs (no Cu leaching stage involved) (mg)						
	Sequence A (Cut)			**Sequence B (Shred)**		
	Au	**Cu**	**Ni**	**Au**	**Cu**	**Ni**
Cu leaching	0	0	0	0	0	0
Au Leaching	3.89	4362.9	141.5	2.75	2500	121
Sub-total	**3.89**	**4362.9**	**141.5**	**2.75**	**2500**	**121**
reverse Aqua regia leached residue	0	5723.12	1.19	0.18	5850.22	1.16
Aqua regia leached residue	0	12.75	0.27	0	21.19	0.26
Microwave assisted digestion	0	74.6	0.23	0	2.024	0.27
total (mg)	**3.89**	**10173.37**	**143.19**	**2.93**	**8373.434**	**122.69**
lost (mg)	0.12	202.02	2.58	1.08	2001.956	23.08

Table 8-25: New head grade calculated after Cu Leach for sequence C and D

Recalculated head grade	**Au** (mg/PCB)	**Cu** (mg/PCB)	**Ni** (mg/PCB)
Original	4.01	10375.39	145.77
After Cu leaching (Sequence C)	4.01	7985.14	28.52
After Cu leaching (Sequence D)	4.01	5773.42	41.93

These values presented in Table 8-25 were obtained after deducting the extracted Cu and Ni masses in Table 8-23 and Table 8-24.

8.8 Fitted surface plots

The fitted surface plots generated by the central composite design are illustrated from Figure 8-2 to Figure 8-10. Each plot shows the response function as Au extraction as the y-axis. The range of from 0 to 1 represents the % Au extraction from 0 to 100%. Each plot also shows the response

function plotted against two specified variables within a specified range. with the third variable held constant.

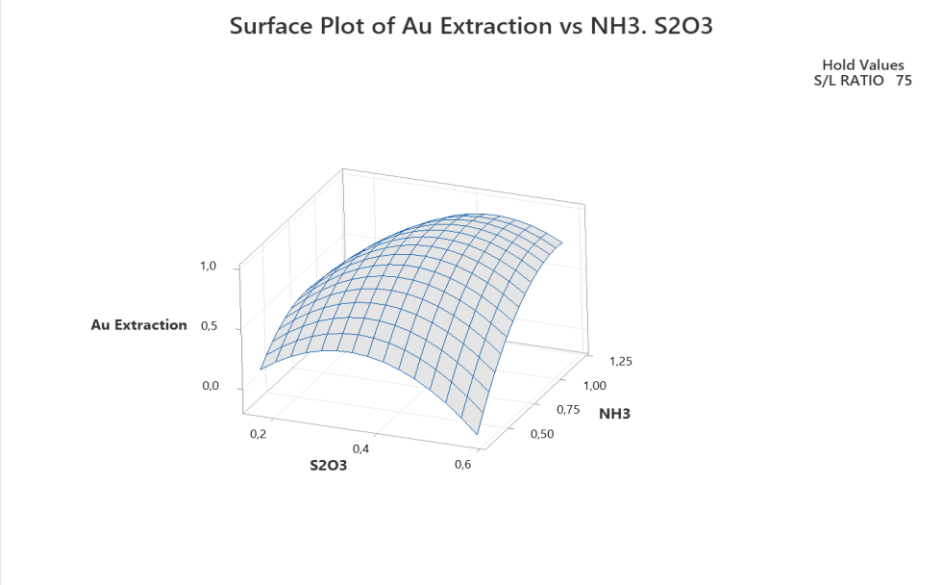

Figure 8-2: Fitted surface plot of Au Extraction against NH_3 and $S_2O_3^{2-}$,concentration with S/L ratio kept at 75g/L.

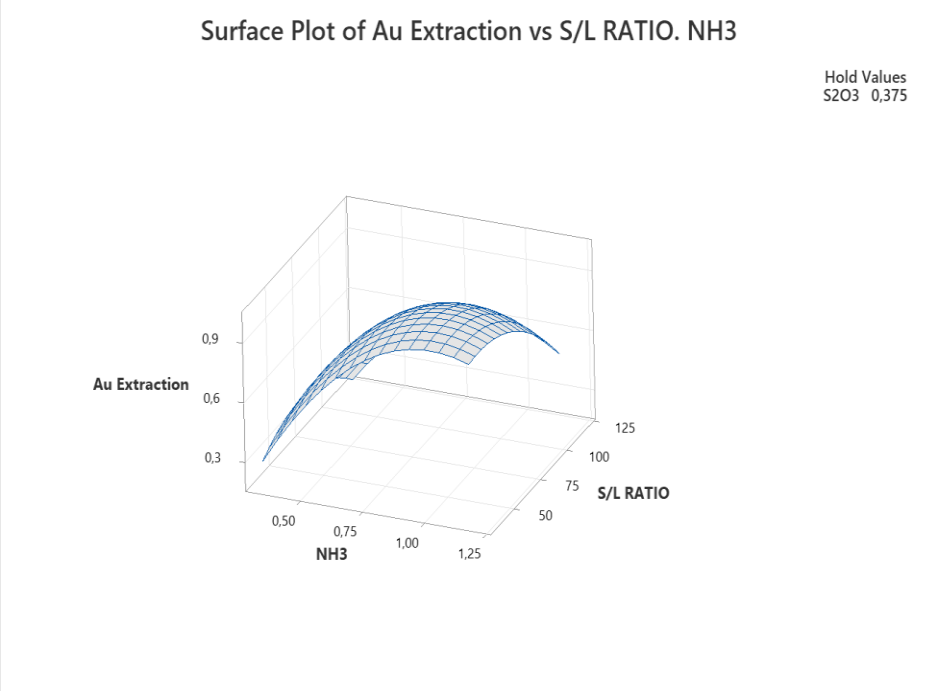

Figure 8-3: Fitted surface plot of Au Extraction against NH_3 concentration and S/L ratio, with $S_2O_3^{2-}$ concentration kept at 0.375 M.

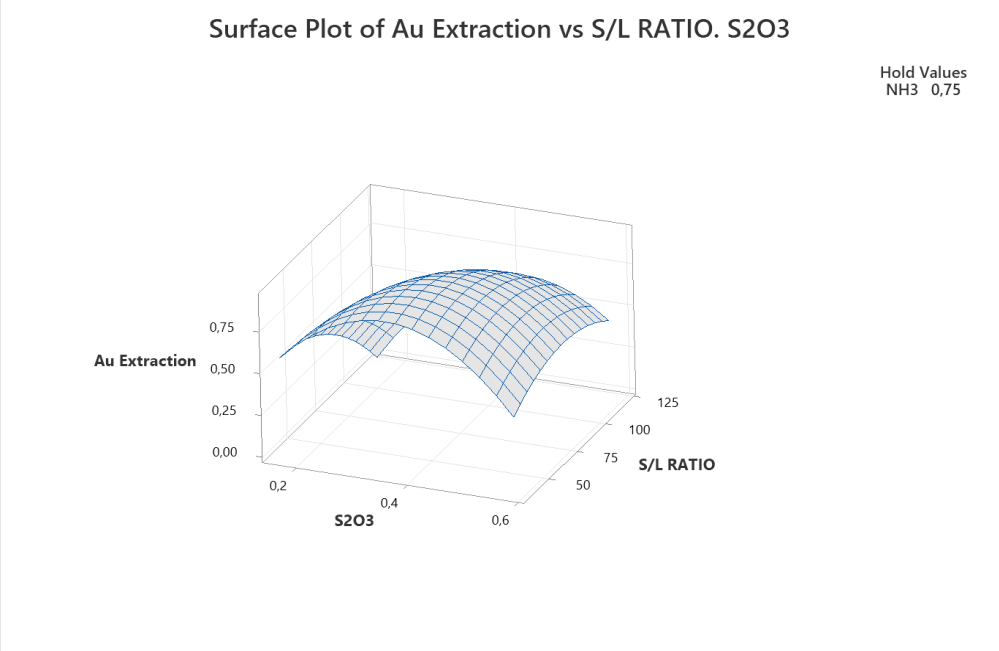

Figure 8-4: Fitted surface plot of Au Extraction against $S_2O_3^{2-}$ concentration and S/L ratio, with NH_3 kept at 0.75 M.

Next

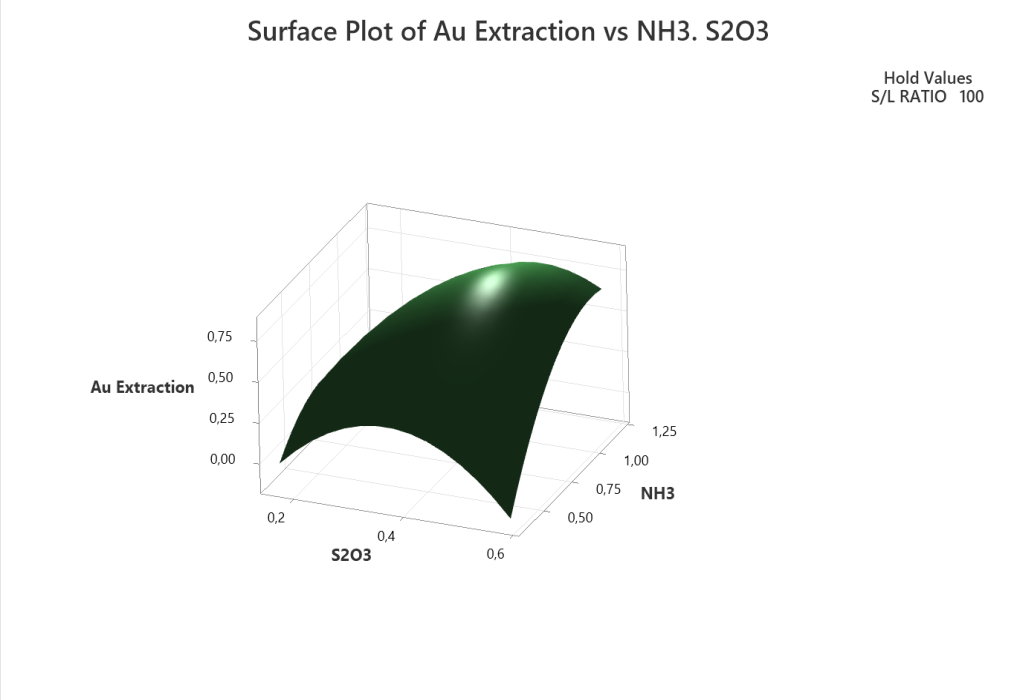

Figure 8-5: Fitted surface plot of Au Extraction against NH_3 and $S_2O_3^{2-}$ concentration, with S/L ratio kept at 100 g/L.

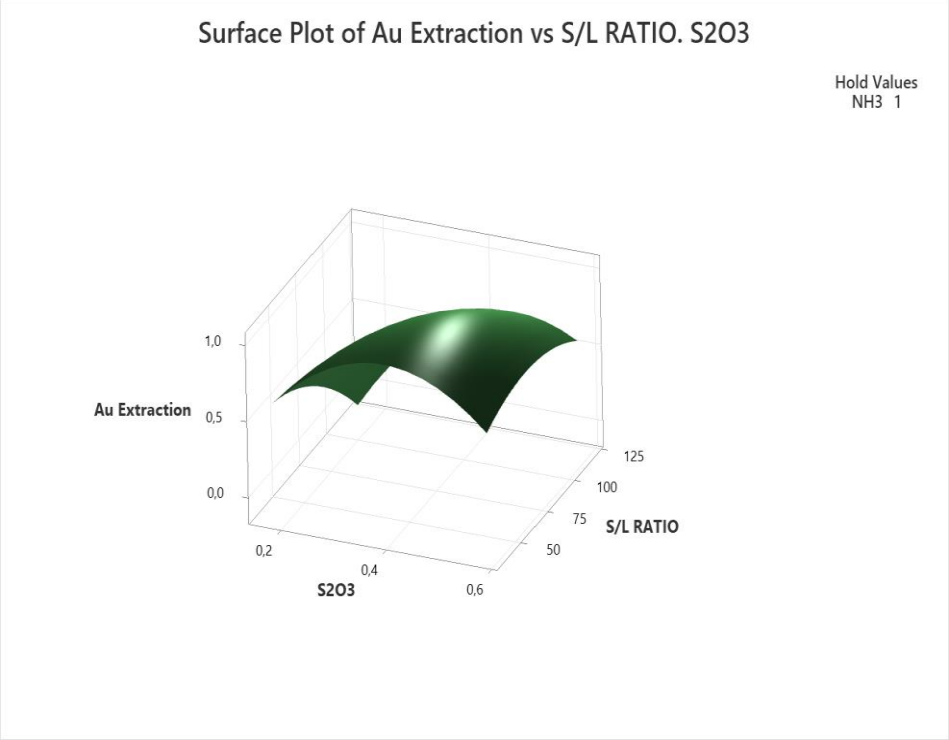

Figure 8-6:Fitted surface plot of Au Extraction against $S_2O_3^{2-}$ concentration and S/L ratio, with NH_3 concentration kept at 1 M.

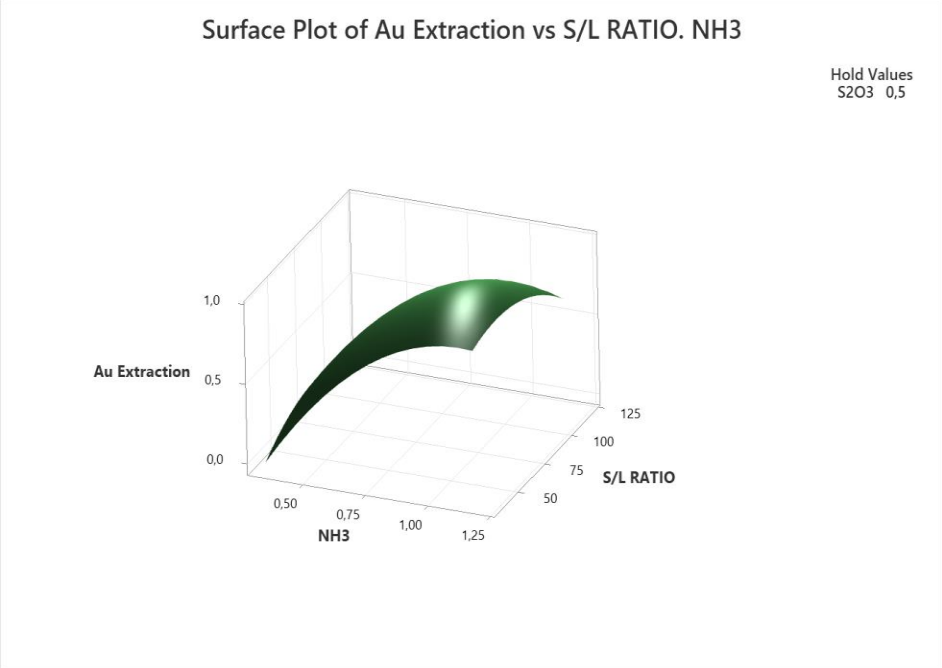

Figure 8-7:Fitted surface plot of Au Extraction against NH_3 concentration and S/L ratio, with $S_2O_3^{2-}$ concentration kept at 0.5M.

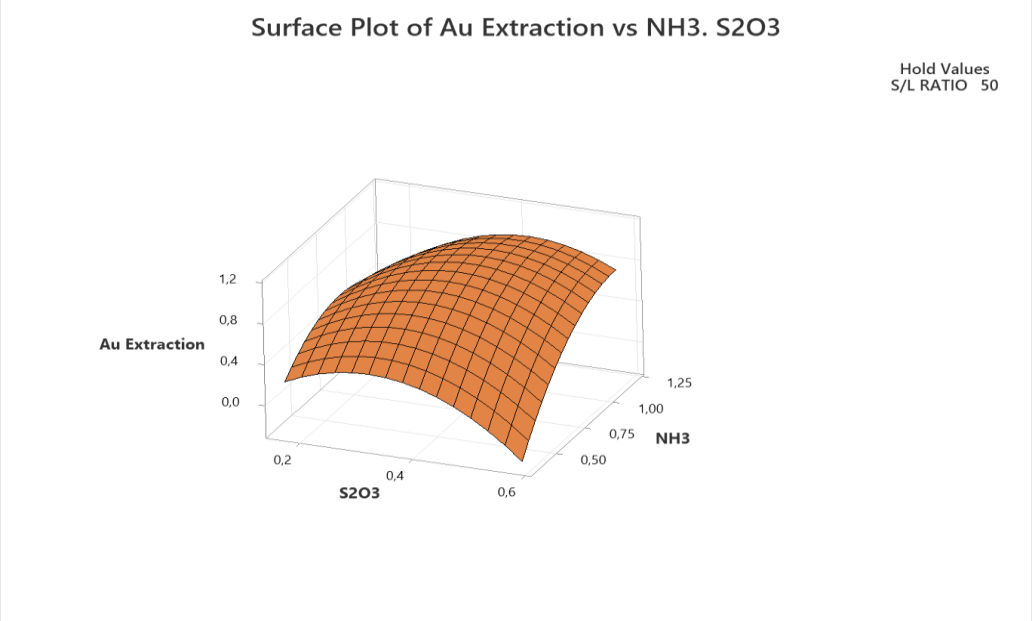

Figure 8-8:Fitted surface plot of Au Extraction against NH_3 and $S_2O_3^{2-}$ concentration, with S/L ratio kept at 50 g/L.

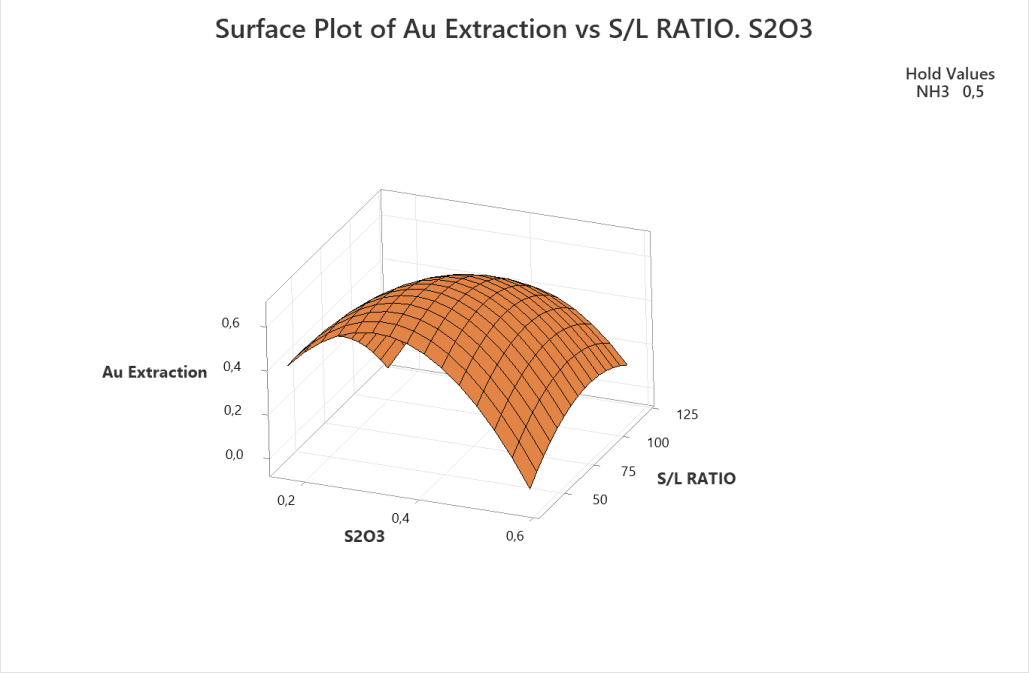

Figure 8-9::Fitted surface plot of Au Extraction against $S_2O_3^{2-}$ concentration and S/L ratio, with NH_3 concentration kept at 0.5 M.

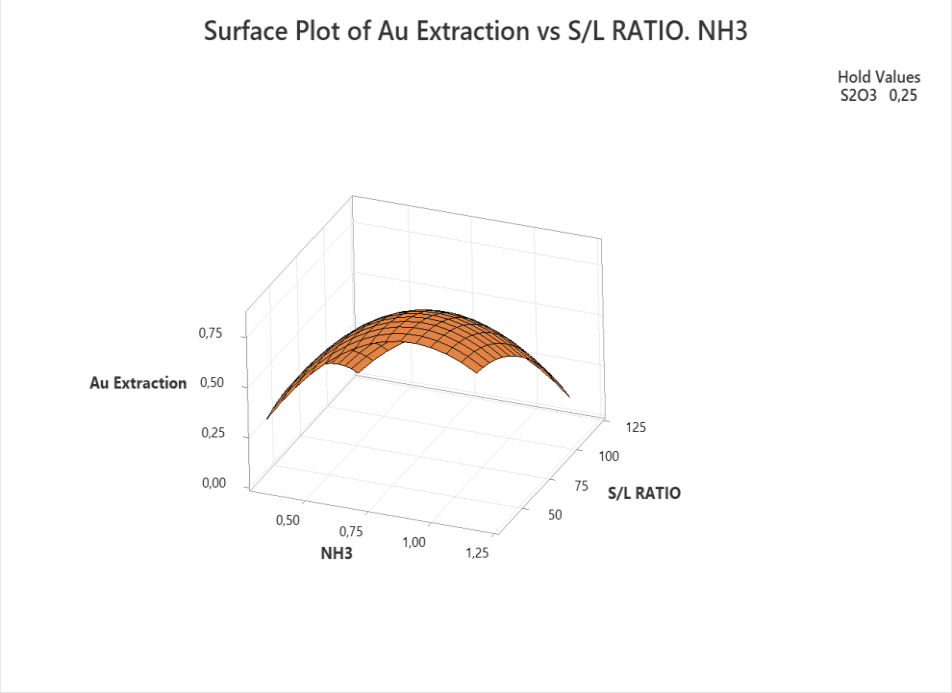

Figure 8-10:Fitted surface plot of Au Extraction against NH_3 concentration and S/L ratio, with $S_2O_3^{2-}$ concentration kept at 0.25M.

8.9 Rate limiting step plot

Figure 8-11 shows the outcome of the trial values obtained from equation 11-A given in section 2.7.4The values used were taken from each trial at 8 hours and plotted against time and linear trendlines were fitted in.

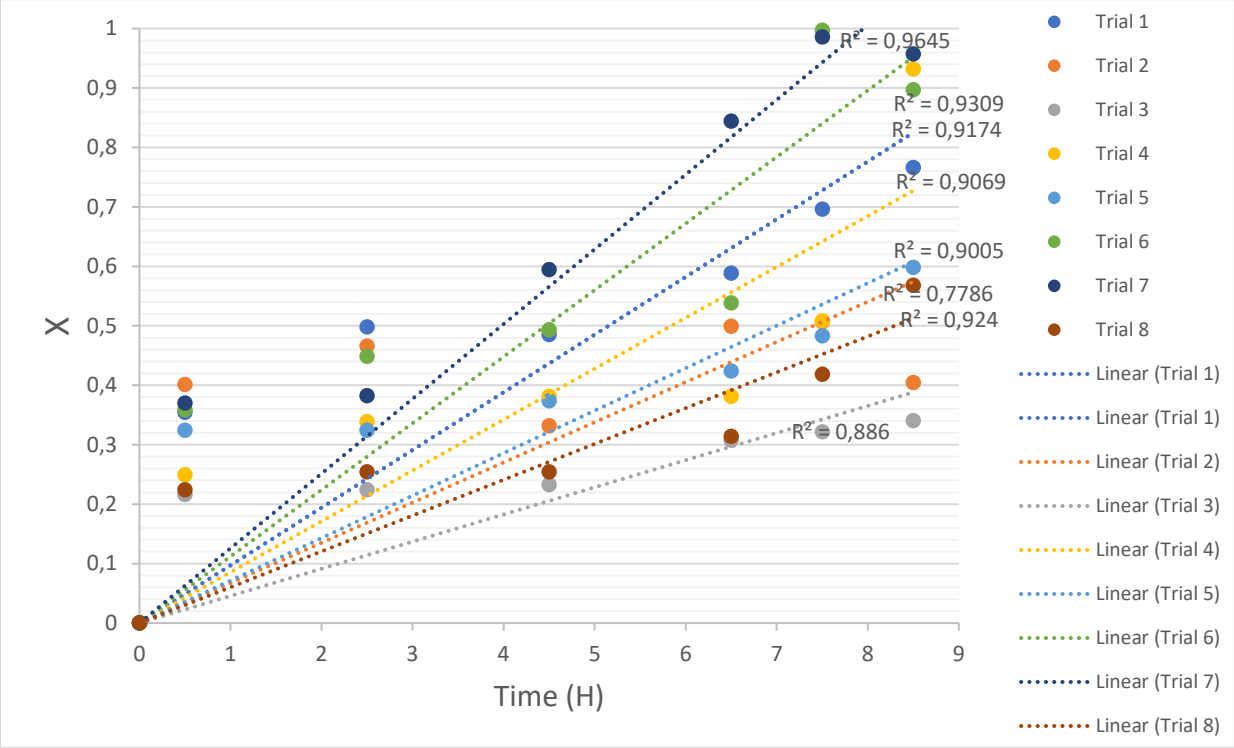

Figure 8-11:Rate controlled by film diffusion and chemical reaction.